

TECHNOLOGY UTILIZATION OFFICE  
GEORGE C. MARSHALL SPACE FLIGHT CENTER  
HUNTSVILLE, ALABAMA

*Texas A & M University*

space

OCEANOGRAPHY AND METEOROLOGY

Research Conducted through the

*Texas A & M Research Foundation*

COLLEGE STATION, TEXAS



GPO PRICE \$

OTS PRICE(S) \$

Hard copy (HC) 4.00

Microfiche (MF) .75

AN INVESTIGATION TO ESTABLISH LOW-LEVEL  
TURBULENT WIND DEFINITION IN TERMS OF MEAN  
MICROMETEOROLOGICAL PARAMETERS

Summary Report

for Period

30 April 1962—30 September 1963

George C. Marshall Space Flight Center  
Contract NAS8-2652 Request Nos. TP2-81065(1F)  
TP3-81063(1F)

A&M Project 314  
Ref. 63-23F  
October 1963

FACILITY FORM 602

N 65 12439  
(ACCESSION NUMBER)

103  
(PAGES)

CR 59719  
(NASA CR OR TMX OR AD NUMBER)

(THRU)

(CODE)

20  
(CATEGORY)

The research reported in this document was sponsored by the National Aeronautics and Space Administration, George C. Marshall Space Flight Center, Huntsville, Alabama.

TEXAS A & M RESEARCH FOUNDATION  
and the  
Department of Oceanography and Meteorology  
of the  
TEXAS A&M UNIVERSITY  
College Station, Texas

AN INVESTIGATION TO ESTABLISH LOW-LEVEL TURBULENT  
WIND DEFINITION IN TERMS OF MEAN  
MICROMETEOROLOGICAL PARAMETERS

30 April 1962 - 30 September 1963

Prepared by

William H. Clayton and B. Jesse Eckelkamp

SUMMARY REPORT

NAS8-2652 Request Nos.: TP2-81065(1F)  
TP3-81063(1F)

31 October 1963

Prepared for

George C. Marshall Space Flight Center  
Huntsville, Alabama

## PURPOSE

The purpose of this study is to develop a mathematical (meteorological) model relating the turbulent characteristics of atmospheric wind flow to the mean parameter determinations of such flow, from the surface to a minimal elevation of 200 feet, through analyses of measurements in both scales of motion. The research for accomplishment of this purpose will be performed in four phases as listed below:

Phase 1. A survey of instrumentation capability and availability for turbulent and mean motion scales sufficient to permit functional correlation without loss of physical reality—completed.

Phase 2. Acquisition and installation of measurement facilities selected in Phase 1 in a field measurement complex—completed for mean scale and wind determination in turbulent scale.

Phase 3. Conduction of joint measurement and analysis studies to establish inter-scale functional definition. The analyses will include:

- a) the relationship between mean velocities and turbulent velocities
  - 1) without regard to any other parameters,
  - 2) as a function of temperature,
  - 3) as a function of ground roughness,
  - 4) as a function of atmospheric stability, and
  - 5) as a function of vertical gradients of mean wind and mean temperature;
- b) spectra of turbulence;
- c) gust characteristics:
  - 1) gust amplitudes as functions of stability, roughness and temperature;
  - 2) gust genesis and decay.
- d) cross spectra of turbulence between different altitudes—begun.

Phase 4. Development of mathematical models for simulation solution based on the analyses of Phase 3—not yet begun.

ABSTRACT

1439  
12349

A summary of activities on phases 1 and 2 (selection and installation of measurement capabilities) of a four-phase research program designed to afford definition of the instantaneous or gust-wind profile as a function of mean flow definition. Included are a review of sonic anemometer theory pertinent to the research goals of the study, schematic description of the sonic anemometry employed, and outlines of analytical procedures and techniques to be followed, as well as details of a comparative field measurement test covering various types of wind measurement instrumentation in current use.

*Quatro*

## TABLE OF CONTENTS

	Page
Objectives . . . . .	ii
Abstract . . . . .	iii
List of Figures . . . . .	v
List of Tables . . . . .	vi

### CONTRACTUAL ACTIVITIES

I. General . . . . .	1
II. Sonic Theory . . . . .	7
III. Instrumentation . . . . .	17
a. Sonic System . . . . .	17
b. Analog Systems . . . . .	19
c. Cedar Hill Wind Speed Comparison Tests . . . . .	44
IV. Data Processing and Analysis . . . . .	53
V. Experimental Data . . . . .	56

CONCLUSIONS AND RECOMMENDATIONS . . . . .	79
---	----

Personnel . . . . .	83
References . . . . .	84

# LIST OF FIGURES

No.		Page
1	Front Panel Layout . . . . .	20
2	Logic Module Location Guide . . . . .	21
3	Relay Control and Switch Connections . . . . .	22
4	System Start Logic . . . . .	23
5	Channel Sequencing-Recorder Turn-off Logic . . . . .	24
6	Channel Control Logic . . . . .	25
7	Gate Control Logic . . . . .	26
8	Counting Register Logic . . . . .	27
9	Cycle Counter Logic . . . . .	28
10	DVM Output Buffer and Control Logic . . . . .	29
11	Assembly Register . . . . .	30
12	Write Register . . . . .	31
13	DI-20 Modification for DVM Output Buffer . . . . .	32
14	DVM Interconnection Cabling . . . . .	33
15a	TR-21 Crystal Position . . . . .	34
15b	Sonic Transducer Mount . . . . .	34
16	Sonic Anemometer Assembly . . . . .	35
17	Preamplifier . . . . .	36
18	Preamplifier Circuit Board . . . . .	37
19	Preamplifier Housing . . . . .	38
20	Receiver . . . . .	39
21	Transmitter Amplifier and Cable Identification . . . . .	40
22	Automatic Record Gap Control . . . . .	41
23	AN/GMQ-12 Schematic Diagram . . . . .	43
24a	Wind Aspirated Dry-Bulb Thermal Shelter . . . . .	44
24b	Wind Aspirated Wet-Bulb Thermal Shelter . . . . .	45
25	Temperature Difference Amplifier . . . . .	46
25a	Power Supply for Temperature Difference Amplifier . . . . .	47
26	Cedar Hill Wind Sensor Comparison Test, Instrument Location . . . . .	51
27	Instrumentation - Cedar Hill Comparison Test . . . . .	52
28	Sonic Sensor Installation (Close-up View) . . . . .	52
29	Sonic Sensor Installation at Station A . . . . .	54

# LIST OF TABLES

Table		Page
1	Upper Vertical Zero Test - Run 1A . . . . .	58
2	Upper Horizontal Zero Test - Run 1B . . . . .	61
3	Lower Vertical Zero Test - Run 1C . . . . .	62
4	Lower Horizontal Zero Test - Run 1E . . . . .	63
5	First Two Seconds of Raw Data - Run 1F . . . . .	64
6	Velocity Anomalies for First Two Seconds of Run 1F . . .	66
7	Average Wind Components and Flux of Momentum - Run 1F . .	67
8	First Two Seconds of Raw Data - Run 1L . . . . .	68
9	Velocity Anomalies for First Two Seconds of Run 1L . . .	73
10	Average Wind Components and Flux of Momentum - Run 1L . .	74
11	Et Comparative Summary . . . . .	75
12	Mean Horizontal Wind Summary . . . . .	76

## CONTRACTUAL ACTIVITIES

### I. General

Research effort under way on the subject contract to determine meteorological description of turbulent and mean flow regimes as a means of evaluating missile response is based on the concept that the turbulent characteristics of atmospheric flow are functionally related to and therefore definable from mean flow characteristics. The concept is, of course, classical but the method of attack is not and fully recognizes that direct measurements of the turbulent and mean fields must be made simultaneously in order to determine realistic interdependence, rather than mean flow measurements alone with theoretical extrapolation to the turbulent field based on classical premises that such extrapolation must necessarily follow in order that observed gross mean phenomena can be realized. Of course, earlier studies in this vein were not so conducted as a matter of choice but of practical necessity inasmuch as reliable instrumentation of response suitable to define the turbulent field has not heretofore been available and even now is largely of an experimental nature.

It is pertinent to review briefly some earlier theoretical studies since they illustrate the reasoning behind activities and procedures that are being pursued in the current research program. One of the earliest and best-known works is that of Osborne Reynolds in the late nineteenth century which demonstrated that the mean form of the equation of motion for fluid flow could not be applied to a turbulent regime without the addition of terms which are independent of viscosity and which have since that time been referred to as "Reynolds stresses." Thus Reynolds' work leads immediately to the definition of the flux of momentum (shearing stress), the convective heat flux, and the evaporative heat flux in terms of instantaneous values of flow parameters, i.e., wind, temperature, and vapor pressure,



and anomalies to the mean values of these same parameters. In a practical sense, of course, "instantaneous" has no meaning and should be replaced by frequency or response considerations based on significant energy considerations. Meteorologically, we can consider instantaneous to represent frequency response of the order of 10-15 cycles per second, probably, as an upper limit. That is, frequencies in excess of this value are assumed to contain only a relatively minor portion of the available energy.

Assuming that this definition of instantaneous is adequate, the question arises as to how one measures instantaneous values. The classicists, lacking instrumentation of sufficient response characteristics, were forced to fall back on the concept previously noted, specifically that somehow or other the turbulent regime was related to the mean flow regime, and many equating attempts can be found in literature, the best-known being that of Wilhelm Schmidt in 1917 through postulation of the exchange coefficients based on an analogy of turbulent and laminar flow. This analogy was furthered by Prandtl in 1934 with the introduction of a mixing length which in a limited sense corresponds to the mean free path of kinetic theory.

In more recent years, statistical theories of turbulence have achieved eminence and some of these will be referred to later. For the moment, however, the works of Reynolds, Schmidt, and Prandtl are sufficient to provide the mathematical and physical groundwork for our purposes, which is shown in equations (1) through (7) below:

$$\tau = -\rho \overline{u'w'} \equiv \rho K_m \frac{d\bar{u}}{dz} \quad (1)$$

$$\frac{q_h}{C_p} = -\rho \overline{T'w'} = \rho K_h \frac{d\bar{T}}{dz} \quad (2)$$

$$\frac{q_c}{L} = -\rho \overline{q'w'} = \rho K_e \frac{\partial \bar{q}}{\partial z} \quad (3)$$

$$u = \bar{u} + u' \quad (4)$$

$$w = w' \quad (5)$$

$$\rho = \bar{\rho} \quad (6)$$

$$K_m = l \sqrt{w'^2} \quad (7)$$

where

$u'$  and  $w'$  represent the anomalies to the mean flow in the horizontal and vertical directions respectively;

$T'$  and  $q'$  represent the anomalies of temperature and specific humidity;

$K_m$ ,  $K_h$ , and  $K_e$  are the eddy (exchange) coefficients for momentum, heat, and vapor;

$l$  is the mixing length and it is shown here only to relate it to the exchange coefficients and it will not be used henceforth inasmuch as such definition can always be found through equation (7) or corresponding relationships for  $K_h$  and  $K_e$  with respect to  $K_m$ ;

$\tau$ ,  $q_h$ , and  $q_e$  are the vertical fluxes of momentum, sensible heat, and latent heat;

$\rho$  is air density;

$C_p$  is the specific heat (at constant pressure) for air; and

$L$  is the latent heat of vaporization for water.

The format employed in equations (1) through (7) is more or less standard and is based on the usual meteorological coordinates and assumptions. That is, the prevailing wind for the time interval considered flows along the  $u$  axis,  $\bar{v}$  and  $\bar{w}$  are zero,  $\rho'$  is zero, laminar contributions are negligible and temperature may be regarded as the actual temperature rather than the potential temperature, since the two will be practically equivalent for the near-surface atmospheric layers which we will consider.

From these background equations one can "derive" the so-called well-known relationships expressed in equations (8), (9), and (10):

$$\tau = \rho u_*^2 = \rho \epsilon^2 u^2 = \tau_0 \quad (8)$$

$$u = \frac{u_*}{k} \ln \frac{z}{z_0} \quad (9)$$

$$\bar{T} = \frac{T_*}{k} \ln \frac{z}{z_0} + T_0 \quad (10)$$

where

$u_*$  is the "friction" (shear) velocity;

$T_*$  is the "friction" temperature (so called because of its analogy to  $u_*$ );

$z_0$  is the "roughness height" (length);

$\epsilon^2$  is the "roughness parameter";

$k$  is von Karman's constant ( $.38 \pm .02$ ); and

the subscript zero refers to the surface.

The equations have their basic origin in empiricism and are limited in application to specific mean environmental conditions with regard to stability and the underlying surface over which the flow occurs. In these relationships, and henceforth in all others, we shall omit the bar to indicate averages, and it should be understood that any quantity which is not primed represents a mean value based on a time-interval of not less than 30 minutes to an hour (unless completely determinable by primed quantities).

The profile relationships of equations (9) and (10) (and a corresponding one for vapor pressure) can be extended to other stability situations and other surface conditions through various empirical and/or theoretical arguments, and considerable work has been done on this subject, e.g., Clayton and Merryman,<sup>1</sup> Deacon,<sup>2</sup> Elliott,<sup>3</sup> Ellison,<sup>4</sup> Halstead,<sup>5</sup> Monin and Obukhov,<sup>6</sup> Panofsky, Blackadar and McVehil,<sup>7</sup> and others.

The question is, how does the groundwork cited prepare for an understanding of turbulent flow and satisfaction of research aims of the subject contract. The answer is, not at all except to demonstrate the necessity of instantaneous data usage since two of the most important characteristics of turbulence, specifically  $\tau$  and  $q_h$  or  $q_h/\rho C_p$ , though defined by equations (1) and (2), are still unknown quantities because functional definitions of  $K_m$ ,  $K_h$ , and  $K_e$  are as yet unavailable. As to what are the remaining important characteristics of turbulent flow, this is also an open question, but would certainly include gravitation, acceleration, a stability parameter, such as the Richardson number  $Ri$  or the Monin-Obukhov universal

function  $Z/L$ , friction temperature  $T_*$ , and friction velocity  $u_*$ . Thus, the right-hand forms of equations (1) and (2) are not useful for the particular research goals under consideration, and it follows that the only procedure open is to seek definition of the fluxes of momentum and heat through the Reynolds stress definition, that is, through  $u'$ ,  $T'$ , and  $w'$ . Considerations of the evaporative heat flux are being avoided here because mean values of humidity are not routinely measured with reliability, much less instantaneous values.

Let us postulate, for the moment, that  $u'$  is a function of  $\bar{u}$ ,  $\bar{T}$ ,  $z_0$ , and  $Ri$ , and that we can measure the instantaneous values of  $u'$ ,  $w'$ , and  $T'$  and hence deduce the nature of this functional dependence from simultaneous measurements of the necessary mean parameters. Of course, it should be recognized that the functional dependence for  $u'$  as indicated is not necessarily complete but only a first approximation. Further, we will postulate that there exists, for all stability cases, mean profile relationships for  $u$  and  $T$  as shown in equations (11) and (12):

$$u = \frac{u_*}{k} \left[ \ln \frac{z}{z_0} + \alpha(z - z_0)^{1/2} \right] \quad (11)$$

$$T - T_0 = \frac{T_*}{k} \left[ \ln \frac{z}{z_0} + \alpha(z - z_0)^{1/2} \right] \quad (12)$$

where

$\alpha$  is a stability parameter.

These particular profile relationships, proposed by Clayton and Merryman<sup>1</sup> and based on analyses of the data of projects Great Plains (1952), Prairie Grass (1956), and Green Glow (1959), need not be considered inviolate and may be replaced by other generalized profile laws, for example, those of Monin and Obukhov.<sup>6</sup> From differentiation of (11) and (12) the friction temperature  $T_*$  can be written as

$$T_* = \frac{u_* \frac{\partial T}{\partial z}}{\frac{\partial u}{\partial z}} = \frac{u_* T Ri}{g} \frac{\partial u}{\partial z} = - \frac{q_h K_m}{\rho C_p K_h u_*} \quad (13)$$

It is interesting to note that  $T_*$  here agrees exactly with the  $T_*$  value advanced by Monin<sup>8</sup> by similarity theory except for a factor equal to the reciprocal of the von Karman constant which, quoting Monin,<sup>8</sup> was introduced to simplify calculations.

From equations (11), (12), and (13), it follows that  $\alpha$  may be written as

$$\alpha = \frac{CT_*}{u_*^2} = \frac{CTR_1}{8u_*} \frac{\partial u}{\partial z} \quad (14)$$

where

$C$  is a constant of the order of  $300 \text{ cm}^3/2/\text{deg C/sec}^2$ . Thus, from the preceding, it may be seen that from measurements of  $u^0$ ,  $w^0$ ,  $T'$ ,  $z_0$ , the vertical gradients of mean wind and temperature, and mean wind speed:  $\alpha$ ,  $u_*$ , and  $T_*$  can be evaluated and the functional definition of  $u^0$  as postulated can be studied, as well as functional definition of the exchange coefficients for momentum and heat, though only on a limited basis. Also, of course, if the basic profile equations (11) and (12), or replacements therefor, can be solved as a function of time, mean measurements (which may be made routinely with standard instrumentation) can yield definition of the instantaneous or gust profile on a forecast basis.

Let us assume the existence of capabilities for mean measurements and the existence of a model for time solution of equations (11) and (12) as well as the necessary input data and computational facilities required for model solution (this is the situation that exists due to parallel research efforts\* at Texas A&M University), thus pinpointing the basic deficiency with regard to turbulent definition potential—specifically, measurement of  $u^0$ ,  $w^0$ , and  $T'$ , or instantaneous values of  $u$ ,  $w$ , and  $T$  within the definition of instantaneous as previously given, since the latter measurements would yield the anomalous values. Therefore, it follows that these

---

\* Sponsored by the U. S. Army Electronics Research and Development Laboratory, Fort Monmouth, New Jersey, Contract DA 36-039 AMC-02195(E), and by National Science Foundation, Washington, D. C., Grant GP-1902.

measurements are not only the necessary first step in the execution of the research tasks of the subject contract, but without such measurements the objectives of the research cannot be realized.

Thus, with the basic question of what needs to be done resolved, the question arises as to how such measurements should be made. On the surface there seem to be several possible measurement modes that would be suitable for usage; however, a more careful investigation which takes into account not only reliability but availability, cost, maintenance, and operation requirements narrows the field down considerably, and it was found that sonic anemometry offered the most potential for the instantaneous measurement of wind and possibly T although thermocouples or thermistors would seem more directly applicable for the latter.

The preceding discussion summarizes the activities during phases 1 and 2 of the subject contract but without details of instrumentation selection or why particular sonic anemometers were chosen. This will be discussed in a subsequent section following presentation of some basic principles of sonic anemometry with general application.

## II. Sonic Theory

Sonic anemometry is largely in an experimental stage and not widely employed. This state of affairs, however, is not due to lack of understanding of the principles that are involved in sonic measurements but rather to engineering limitations in application of these principles.

In the engineering sense there are two basic types of sonic anemometers: the pulse-type sonic and the continuous-wave sonic, and progress on both basic types runs about evenly with preference between them primarily a factor of engineering-design considerations and planned usage of collected data. Within the two basic types there are several subtypes, classified according to head (sensor) characteristics and spacing, and again choice is largely dictated by engineering considerations and planned application.

Whatever the type and configuration, the basic principles of sonic anemometry theory, which are presented below, will apply. The material presented herein is in no sense a comprehensive representation but rather a summary in the practical sense of usage, and consequently omits many of the theoretical considerations that are involved. While no single paper completely encompasses the field of sonic anemometry, a comprehensive picture can be had by combined referencing of such authors as Armstrong,<sup>9</sup> Kaimal,<sup>10</sup> Suomi and Businger,<sup>11</sup> and Stewart and Post.<sup>12</sup>

It can be shown that if acoustic energy, propagated as a spherical wave front, is emitted at some point in a rectangular coordinate system that is moving at the exact speed of the enveloping air mass, such air mass motion being purely translational, the shape and speed of the wave front at any position with respect to the moving axes will be identical with respect to a like situation involving fixed axes in motionless air. The significance of the preceding statement is twofold: It fixes the quality of the assumptions employed in the derivation of the basic equations of sonic anemometry, and it sets the limitations in the employment of sonic anemometry used in atmospheric measurements. For example, the path over which the sonic energy is transmitted must necessarily be limited to an extent consistent with the response characteristics of the components employed in measuring the transfer of sonic energy. That is, assuming that ten cycles per second constitutes the upper limit of significant atmospheric frequencies, and one has engineering capabilities as well as research requirements for this frequency limit, then measurements over a path-length of, say, 100 feet will obviously be useless.

Consider a point source of acoustic energy, located at  $x = 0$ ,  $y = 0$ , and  $z = 0$ , which emits energy at time  $t = 0$ . The position of any point on a constant phase surface at some later time,  $t_1$  (necessarily a very short time later), is given by:

$$(x - ut_1)^2 + (y - vt_1)^2 + (z - wt_1)^2 = (St_1)^2 \quad (15)$$

where  $S$  is the speed of sound in motionless air, and  $u$ ,  $v$ , and  $w$  are

the  $x, y, z$  components of the velocity,  $V$ , of the air. Solving for  $t_1$  in (15),

$$t_1 = \frac{2(ux + vy + wz) - [4(ux + vy + wz)^2 - 4L^2(V^2 - S^2)]^{1/2}}{2(V^2 - S^2)} \quad (16)$$

where  $L^2 = x^2 + y^2 + z^2$  and  $V^2 = u^2 + v^2 + w^2$ . Now let us replace the reception point by two points on a coordinate axis, say the  $x$ -axis, and at equal distances from the transmitter at the origin, that is, at the points,  $x, 0, 0$  and  $-x, 0, 0$ . From (16) the transmission times to  $x$  and  $-x$  are, respectively,

$$t_x = \frac{ux - x(S^2 - v^2 - w^2)^{1/2}}{v^2 - S^2} \quad (17)$$

and

$$t_{-x} = \frac{-ux - x(S^2 - v^2 - w^2)^{1/2}}{v^2 - S^2} \quad (18)$$

The difference between these times ( $t_x$  with the air motion,  $t_{-x}$ , against) and the sum of these times are given in equations (19) and (20), assuming that  $S^2$  is much greater than  $V^2$ .

$$t_{-x} - t_x = \Delta t_x = \frac{2ux}{S^2} \quad (19)$$

$$t_{-x} + t_x = \Sigma t_x = \frac{2x}{S} \quad (20)$$

Equations (19) and (20) are immediately extendable, of course, to the other coordinate axes and to any position along the axes, such that we may consider three two-point systems, where each point (sensor) is simultaneously a receiver and transmitter (though not in a practical sense), and if the separation  $D$  between points is the same for all coordinate axes, (19) and (20) may be replaced by

$$\Delta t_x = \frac{2uD}{S^2} \quad (21)$$

$$\Delta t_y = \frac{2vD}{S^2} \quad (22)$$

$$\Delta t_z = \frac{2wD}{S^2} \quad (23)$$



$$q' = b_1 T' (\Sigma t)^2 \quad (41)$$

and

$$\frac{q_h}{C_p} = - \overline{\rho T' w'} \quad (42)$$

and

$$\frac{q_e}{L} = - \overline{\rho q' w'} \quad (43)$$

where L is the latent heat of vaporization.\* It should be recognized that possible over-simplification is involved here. That is, the variation of T and e is not independent, hence (42) and (43) are less "instantaneous" in nature than is (26) since in essence the former two equations call for a non-significant variation of e over short intervals.

Of course, if this information (that is, the fluxes of heat and vapor) are determinable in this fashion, then, of course, through equations (2) and (3) information concerning the functional definition of exchange coefficients is forthcoming, assuming the existence of mean gradient measurements. While the study of exchange coefficients is not a part of the fundamental research requirements of this contract, it is certainly a basic meteorological requirement and if obtainable through temperature measurements that are comparable with wind measurements employing sonic anemometry, should not be ignored.

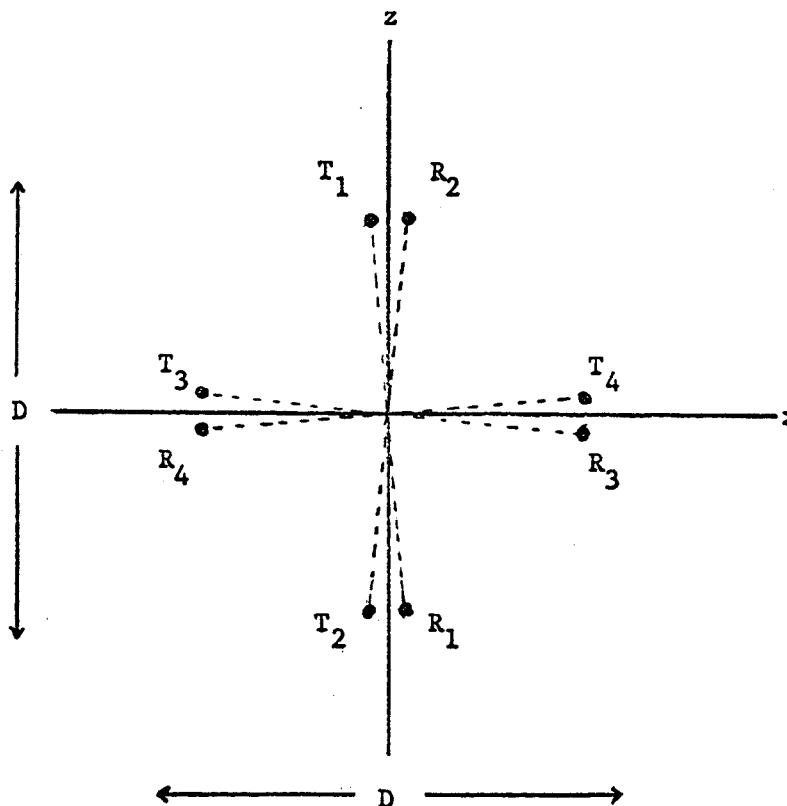
As noted previously, the above is not intended to be a comprehensive review of sonic theory but only that part pertinent to the contractual effort. Additionally, it is necessary to look into the practical limitations in the application of this theory with regard to significance of measurements made with sonics and, again, this will be confined to the particular problems at hand. That is, the discussion will be restricted to the sonic anemometers which have been developed

---

\* It is important to note that the sonic anemometers themselves do not yield T but  $T_v$  or  $T_s$ , hence independent measurements must be made of T (or e, which is not readily done) in order to get the energy fluxes for heat and vapor.

on the contract by Dr. R. M. Stewart, Jr. and Dr. R. E. Post of Iowa State University.

Consider two four-head sonic systems, as shown below,



where one system measures the horizontal wind component and the other measures the vertical.  $T_1, T_2, T_3$  and  $T_4$  are transmitter heads whereas the receiver heads are indicated by  $R_1, R_2, R_3$  and  $R_4$  (two-head systems, that is, where each head is alternatively a transmitter and receiver, are not unknown but introduce engineering difficulties not easily resolved). In order to fit this illustration in with the symbology employed, the transit time from  $T_1$  to  $R_1$  would be  $t_{-z}$  and the time from  $T_2$  to  $R_2$  would be  $t_z$ , the difference  $\Delta t_z$ , etc. The transit times are sequentially determined along each axis and for both axes, that is, the transit times in the  $x$  and  $z$  directions cannot be measured simultaneously. The error introduced by sequential operation need not be large, provided that the sequencing is done at a rapid rate.

However, this is only a necessary condition and does not constitute sufficiency, and it is more informative to consider the sequential error from another point of view.

Ideally, all transit times, which are line averages, should be for the same air path. Another way of saying this, with only a slight departure from the ideal, is to assume that if the atmosphere is of eddy structure, the transit times in the plus and minus directions will be measured in the same eddy. Thus not only is rapid sequencing a requirement but also minimum separation of transmitter and receiver heads must be sought. Or, referring again to the preceding illustration,  $T_1$  and  $R_1$  should be as close together as practicality permits as should  $T_1$  and  $R_2$ , etc. The latter requirement is obvious and the former can be shown by example. Let us assume a head spacing,  $D$  ( $T_1$  to  $R_1$ ) of one meter, a repetitious sampling rate of 25 times per second, a parallelepiped eddy structure that is several meters in extent in the  $x$  and  $y$  plane and one meter thick, and a vertical velocity component of five meters per second. For such a highly ideal and physically unreal situation, and neglecting the fact that  $T_1 - R_2$  and  $T_2 - R_1$  are not on one path, five measurements of  $u$  and  $v$  and only one of  $w$  (almost) can be made. We can improve our structure assumption by reducing the head spacing to a half-meter; however, the sampling rate will then have to be doubled in order to yield the same number of measurements.

A further complication is also present in the simple existence of the measuring heads and their supporting structure in the measuring field in which the measurements are to be made, since such impediments to the flow create turbulence. Thus it may be seen that head size and spacing, as well as the nature of the supporting structure, associated bracing, etc. are all factors in the useful employment of sonic anemometry and about the only design criterion that can be established is to seek idealness within the limitations of practicality. A roughly equivalent way of saying this is that if an ideal sonic anemometer existed it would be a requirement for the generation of design-characteristics for the practical sonic which, of course, would not be needed if one had an ideal sonic.

To return to more tangible considerations, it will suffice to say that the Principal Investigator, the Contracting Officer's technical representatives, Dr. Stewart, and Dr. Post, after due consideration of project requirements and design practicality, agreed that four four-head anemometers with the following capabilities and specifications would be utilized:

1. Each sonic anemometer could be operated independently of every other such that one, two, or three component measurements could be made.
2. Head-spacing would be adjustable within the approximate limits of 25 to 70 cm and 75 to 125 cm.
3. Sampling rate would be 50 cycles per second for head-spacings below 70 cm and 25 cycles per second above 75 cm.
4. The cable length that could be driven on the sonic system would be no less than 200 feet, thus permitting operation at elevations of approximately 200 feet as a maximum condition.
5. The system would be completely of solid-state components with readout in digital format on magnetic tape and the readout would include not only the eight sonic time words but also identification and timing words, with the option of replacement of the identification word with a digital conversion of any one of several possible analog inputs.
6. The transducers as well as associated electronic components, cables and connectors would be so designed as to be weather-proof.
7. System resolution would be .2 of a microsecond\* for any

---

\* Resolution to .1 or even .01 of a microsecond is not an impossible engineering requirement but without merit inasmuch as a head-spacing error of 1% will introduce an error in transit-time determination (individual, not differential) on the order of ten microseconds, and head-spacing errors of less than .1%, remembering that mounting structures vibrate, closely approaches physical impossibility.

individual transit time [the equivalent—for a one-half meter head-spacing—of three cm per second in wind speed by equation (25)].

This completes the discussion of sonic anemometry as applied on the subject contract although further discussion as to implementation of the principles and specifications will be found in the next two sections of the report.

### III. Instrumentation

The discussion of this section is largely descriptive although schematic diagrams are presented. The reason for this rests in the fact that a detailed operational explanation will provide little more than academic interest except to the engineer and those operating the sonics, and for these a Maintenance and Operation Manual exists. However, the presented descriptive material and the schematics should suffice to provide thorough understanding of the operational characteristics though not the details of the total system.

#### a. Sonic System

Basically, the operation of this system is as follows. At a time,  $t$ , selected by the operator, the recording system is turned on and a fixed identification word controlled by panel switches and composed of 18 binary bits is transferred to magnetic tape within  $(t + 2)$  milliseconds. In the interval  $(t + 2)$  to  $(t + 4)$  ms, a second 18-bit word consisting of the contents of a cycle counter (which is automatically reset at the beginning of a run and is augmented by one on each complete data-sequence) is transferred to the tape.

Two milliseconds after turn-on or initiation of the data sequence, the following occurs: Transmitter  $T_1$  emits a 20-kc pulse of sonic energy; receiver  $R_1$  is turned on and all other receivers are blocked, and a counting register begins counting of five-megacycle pulses. This register continues to count until the sonic pulse is received at receiver  $R_1$ . This reception cuts the counting register off, and the contents of the counting register (word 3) are then

transferred to the tape before  $(t + 6)$  ms. At  $(t + 4)$ -ms the same pattern of events occurs for sonic path  $T_2$  to  $R_2$ , etc. Words 5 through 10 are generated in the same fashion. Thus words 3 through 10 (18 bits) are transit times for each of the eight sonic paths and consist of the number of five-megacycle pulses (or the number of .2 microseconds of time) registered in the counting register during the respective transmit-receive intervals.

In general the transit times for a head separation of one-half meter will be on the order of 1.5 milliseconds; however, the system permits approximately 1.95 milliseconds for the transit to occur, thus permitting the variability in head-spacing previously noted.

At the completion of the ten-word sequence which takes 20 milliseconds, the sequence is repeated as many times as the operator, through setting of a preset STOP control, may have chosen. Of course, provision is automatically made that a sequence will always start with word 1 and always end following word 10.

The ident word (word 1) may be replaced by a digitized form of any one of several analog inputs, although within a given run<sup>\*</sup> the type of analog input may not be varied, and the analog-to-digital conversion is performed through a commercial digital voltmeter (DANA DVM Model 4000).

Four basic operational modes of the sonic system are available. The first of these is described above, that is, a sampling rate of 50 samples per second. The second mode replaces the ident by an analog input and may also operate at 50 samples per second but inasmuch as the digital voltmeter requires some 30 milliseconds to make a reading, the analog readings would not be valid. Thus the normal operation of this second mode is 50 samples per second for all basic sonic system information and a nominal readout rate on the A-D channel of 50 samples per second but with every other analog word being blocked (alternate zero readout, actual A-D rate of 25 samples per second) in order to permit

---

\* As used here, a run is any prechosen time interval during which the measuring system is operating under control of internal program logic. A "sonic run" is any number of runs made during a specific field trip, usually covering one or two days.

the DVM ample time to settle.

The third mode permits a sequence sampling rate of 25 per second (both the sonic and the A-D channels) and is necessary for head spacings in excess of approximately 60 cm. The fourth mode is the same as the third except that analog readings (if used), though nominally at 25 readings per second, are zero for every other reading. That is, the actual analog sampling rate would be 12.5 per second.

As can be seen from examination of the following schematic diagrams (Fig. 1-22), considerable liberty has been taken in explanation of the operation, but the principles are correct. It may also be seen that numerous "foolproof" controls have been incorporated in the system such as: a time-delay for the tape recorder to come up to speed before the data sequence actually begins; preset record gaps at fixed intervals for simplicity of computer processing and analyses of data; automatic or manual operation of record-length, and so on.

b. Analog Systems

In order to seek information concerning the functional definition of the anomalous wind values with mean values, as well as flux definition beyond momentum flux, additional data are required. The majority of these data are furnished through a cooperative research program sponsored by the U. S. Army Signal Corps under Contract DA 36-039 AMC-02195(E) and consist of mean wind speed, measured at logarithmic intervals beginning at one-half meter and ending at 32 meters; air temperature at the same logarithmic levels for both dry- and wet-bulb readings; soil temperatures at seven depths; wind direction; insolation; reflected insolation; net radiation, and soil heat flux. All of these parameters are measured at two locations<sup>\*</sup> in digital format, and the methods of measurement, readout, processing, and analyses have been fully described by Clayton and Eckelkamp.<sup>13</sup>

---

\* Stations A and B of the Dallas Tower Network. The sonic instrumentation is self-contained in its own trailer housing and is presently located at Station A.

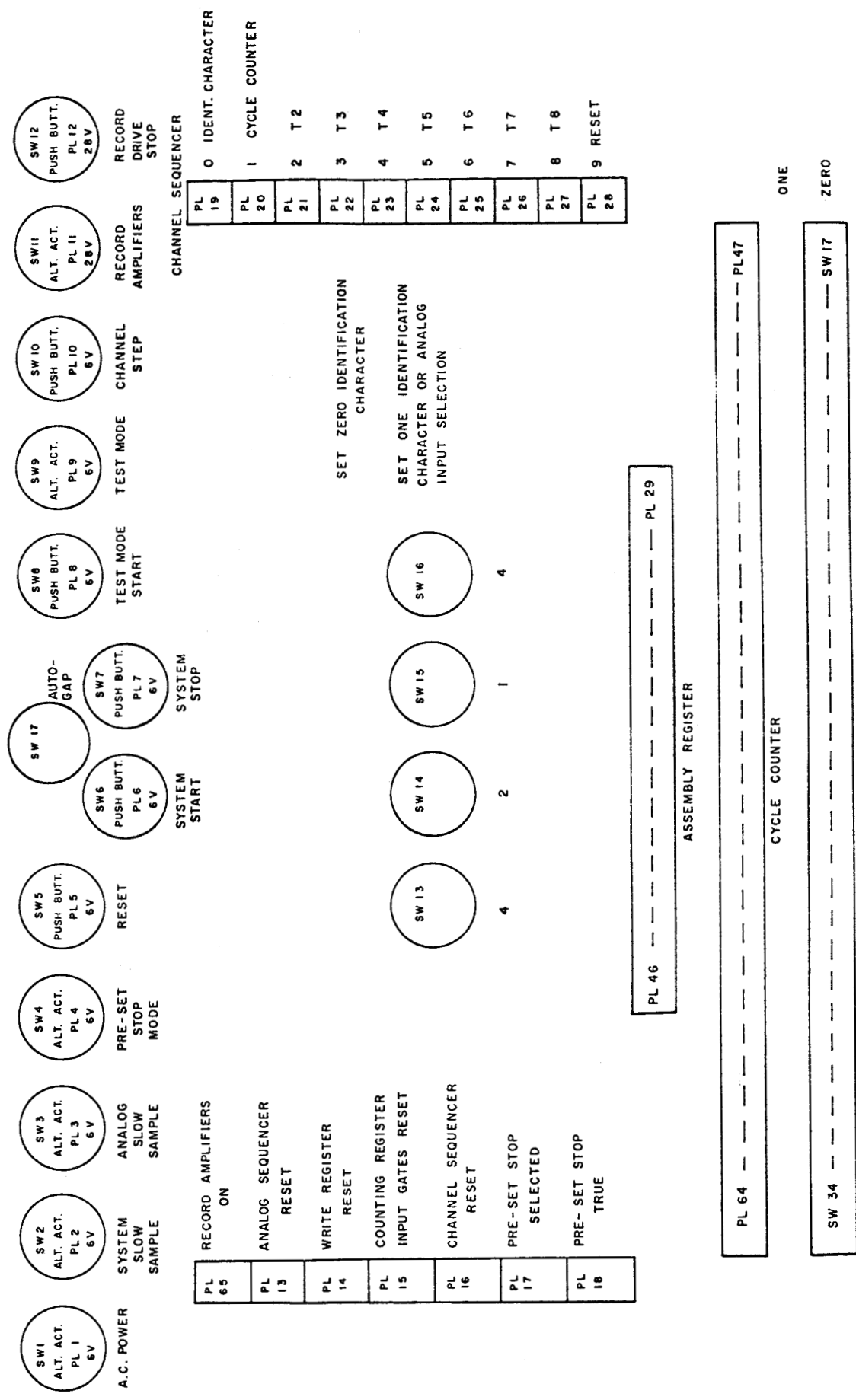


FIGURE 1. FRONT PANEL LAYOUT



1	2	3	4	5	6	7	8	9	10	11	12	13	14	15	16	17	18	19	20	21	22	23	24	25	26	27
ST-30	BC-20	UF-35	MC-35	BC-35	DI-20	BC-30	BC-20	DI-20	BC-20	DM-20A	DN-20	DM-20A	DI-20	DM-20A	DM-20A	DI-20	DM-20A	DM-20A	DN-30	DM-20A	TIE PTS.	d, b AVAIL.				SD-30
											DIODE CLUSTER AVAIL.		h AVAIL.						DIODE CLUSTER AVAIL.	DM-20A						c, d AVAIL.

A

<div></div>																										
<div></div>																										
1	2	3	4	5	6	7	8	9	10	11	12	13	14	15	16	17	18	19	20	21	22	23	24	25	26	
DN-20	DN-20	DI-20	LD-30	FF-20	DI-20	FF-20	FF-20	DI-20	LD-30	FF-20	FF-20	DL-20	DL-20	DL-20	DN-20	DI-20	BC-20	BC-20	LD-30	DI-20	DI-20	DI-20		UT-30	TIE PTS.	
<div>DIODE CLUSTER AVAIL.</div>																										
<div>b AVAIL.</div>																										
<div>N.P. AVAIL.</div>																										
<div>m, n, p AVAIL.</div>																										
<div>b, c, e, f, g, h AVAIL.</div>																										
<div>DI-20 SPEC.</div>																										
<div>DI-20 SPEC.</div>																										
<div></div>																										
<div></div>																										
<div></div>																										
<div></div>																										
<div></div>																										
<div></div>																										
<div></div>																										
<div></div>																										
<div></div>																										
<div></div>																										
<div></div>																										
<div></div>																										
<div></div>																										
<div></div>																										
<div></div>																										
<div></div>																										
<div></div>																										
<div></div>																										
<div></div>																										
<div></div>																										
<div></div>																										
<div></div>																										
<div></div>																										
<div></div>																										
<div></div>																										
<div></div>																										
<div></div>																										
<div></div>																										
<div></div>																										
<div></div>																										
<div></div>																										
<div></div>																										
<div></div>																										
<div></div>																										
<div></div>																										
<div></div>																										
<div></div>																										
<div></div>																										
<div></div>																										
<div></div>																										
<div></div>																										
<div></div>																										
<div></div>																										
<div></div>																										
<div></div>																										
<div></div>																										
<div></div>																										
<div></div>																										
<div></div>																										
<div></div>																										
<div></div>																										
<div></div>																										
<div></div>																										
<div></div>																										
<div></div>																										
<div></div>																										
<div></div>																										
<div></div>																										
<div></div>																										
<div></div>																										
<div></div>																										
<div></div>																										
<div></div>																										
<div></div>																										
<div></div>																										
<div></div>																										
<div></div>																										
<div></div>																										
<div></div>																										
<div></div>																										
<div></div>																										
<div></div>																										
<div></div>																										
<div></div>																										
<div></div>																										
<div></div>																										
<div></div>																										
<div></div>																										
<div></div>																										
<div></div>																										
<div></div>																										
<div></div>																										
<div></div>																										
<div></div>																										
<div></div>																										
<div></div>																										
<div></div>																										
<div></div>																										
<div></div>																										
<div></div>																										
<div></div>																										
<div></div>																										
<div></div>																										
<div></div>																										
<div></div>																										
<div></div>																										
<div></div>																										
<div></div>																										
<div></div>																										
<div></div>																										
<div></div>																										
<div></div>																										
<div></div>																										
<div></div>																										
<div></div>																										
<div></div>																										
<div></div>																										
<div></div>																										
<div></div>																										
<div></div>																										
<div></div>																										
<div></div>																										
<div></div>																										
<div></div>																										
<div></div>																										
<div></div>																										
<div></div>																										
<div></div>																										
<div></div>																										
<div></div>																										
<div></div>																										
<div></div>																										
<div></div>																										
<div></div>																										
<div></div>																										
<div></div>																										
<div></div>																										
<div></div>																										
<div></div>																										
<div></div>																										
<div></div>																										
<div></div>																										
<div></div>																										
<div></div>																										
<div></div>																										
<div></div>																										
<div></div>																										
<div></div>																										
<div></div>																										
<div></div>																										
<div></div>																										
<div></div>																										
<div></div>																										
<div></div>																										
<div></div>																										
<div></div>																										
<div></div>																										
<div></div>																										
<div></div>																										
<div></div>																										
<div></div>																										
<div></div>																										
<div></div>																										
<div></div>																										
<div></div>																										
<div></div>																										
<div></div>																										
<div></div>																										
<div></div>																										
<div></div>																										
<div></div>																										
<div></div>																										
<div></div>																										
<div></div>																										
<div></div>																										
<div></div>																										
<div></div>																										
<div></div>																										
<div></div>																										
<div></div>																										
<div></div>																										
<div></div>																										
<div></div>																										
<div></div>																										
<div></div>																										
<div></div>																										
<div></div>																										
<div></div>																										
<div></div>																										
<div></div>																										
<div></div>																										
<div></div>																										
<div></div>																										
<div></div>																										
<div></div>																										
<div></div>																										
<div></div>																										
<div></div>																										
<div></div>																										
<div></div>																										
<div></div>																										
<div></div>																										
<div></div>																										
<div></div>																										
<div></div>																										
<div></div>																										
<div></div>																										
<div></div>																										
<div></div>																										
<div></div>																										
<div></div>																										
<div></div>																										
<div></div>																										
<div></div>																										
<div></div>																										
<div></div>																										
<div></div>																										
<div></div>																										
<div></div>																										
<div></div>																										
<div></div>																										
<div></div>																										
<div></div>																										
<div></div>																										
<div></div>																										
<div></div>																										
<div></div>																										
<div></div>																										
<div></div>																										
<div></div>																										
<div></div>																										
<div></div>																										
<div></div>																										
<div></div>																										
<div></div>																										
<div></div>																										
<div></div>																										
<div></div>																										
<div></div>																										
<div></div>																										
<div></div>																										
<div></div>																										
<div></div>																										
<div></div>																										
<div></div>																										
<div></div>																										
<div></div>																										
<div></div>																										
<div></div>																										
<div></div>																										
<div></div>																										
<div></div>																										
<div></div>																										
<div></div>																										
<div></div>																										
<div></div>																										
<div></div>																										
<div></div>																										
<div></div>																										
<div></div>																										
<div></div>																										
<div></div>																										
<div></div>																										
<div></div>																										
<div></div>																										
<div></div>																										
<div></div>																										
<div></div>																										
<div></div>																										
<div></div>																										
<div></div>																										
<div></div>																										
<div></div>																										
<div></div>																										
<div></div>																										
<div></div>																										
<div></div>																										
<div></div>																										
<div></div>																										
<div></div>																										
<div></div>																										
<div></div>																										
<div></div>																										
<div></div>																										
<div></div>																										
<div></div>																										
<div></div>																										
<div></div>																										
<div></div>																										
<div></div>																										
<div></div>																										
<div></div>																										
<div></div>																										
<div></div>																										
<div></div>																										
<div></div>																										
<div></div>																										
<div></div>																										
<div></div>																										
<div></div>																										
<div></div>																										
<div></div>																										
<div></div>																										
<div></div>																										
<div></div>																										
<div></div>																										
<div></div>																										
<div></div>																										
<div></div>																										
<div></div>																										
<div></div>																										
<div></div>																										
<div></div>																										
<div></div>																										
<div></div>																										
<div></div>																										
<div></div>																										
<div></div>																										
<div></div>																										
<div></div>																										
<div></div>																										
<div></div>																										
<div></div>																										
<div></div>																										
<div></div>																										
<div></div>																										
<div></div>																										
<div></div>																										
<div>&lt;/</div>																										

B

1	2	3	4	5	6	7	8	9	10	11	12	13	14	15	16	17	18	19	20	21	22	23	24	25	26	27
BC-20	DI-20	BC-20	BC-20	DI-20	BC-20	BC-20	LD-30	MC-30	BC-20	BC-20	DN-35	DM-20A	PN-20	BC-20	DI-20	OD-20	DI-20	DI-20	DC-20	DL-20	DL-20	DC-20	PA-20	DI-20 SPEC.	BP-30	PN-20
											DIODE CLUSTER AVAIL.								4 DIODE CLUSTER AVAIL. g,h AVAIL.	g,h AVAIL.	g,h AVAIL.	5 DIODE CLUSTER AVAIL.	d AVAIL.			

C

BLOWER

FIGURE 2: LOGIC MODULE LOCATION GUIDE

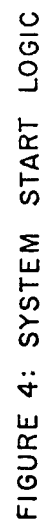


FIGURE 4: SYSTEM START LOGIC

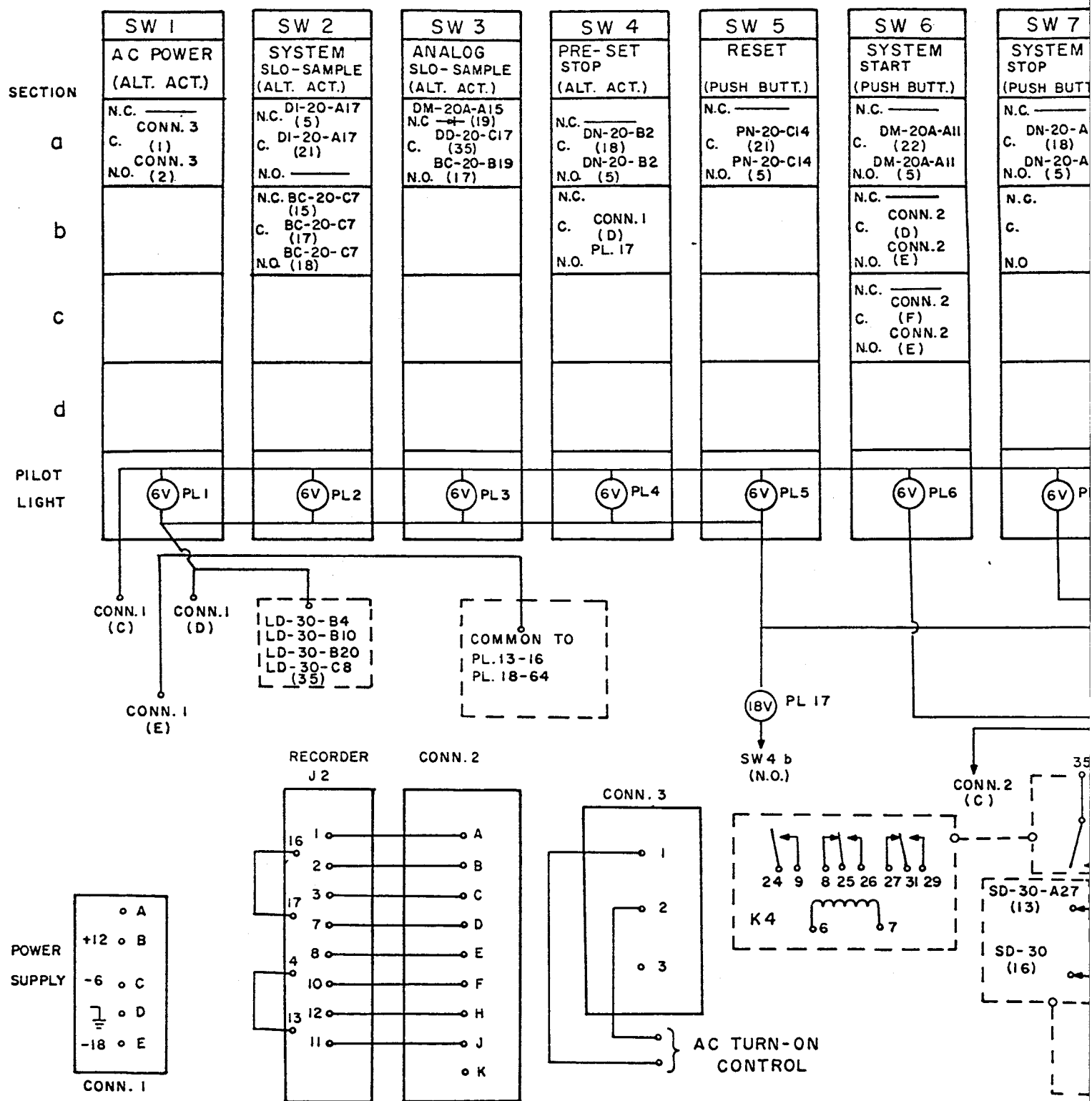
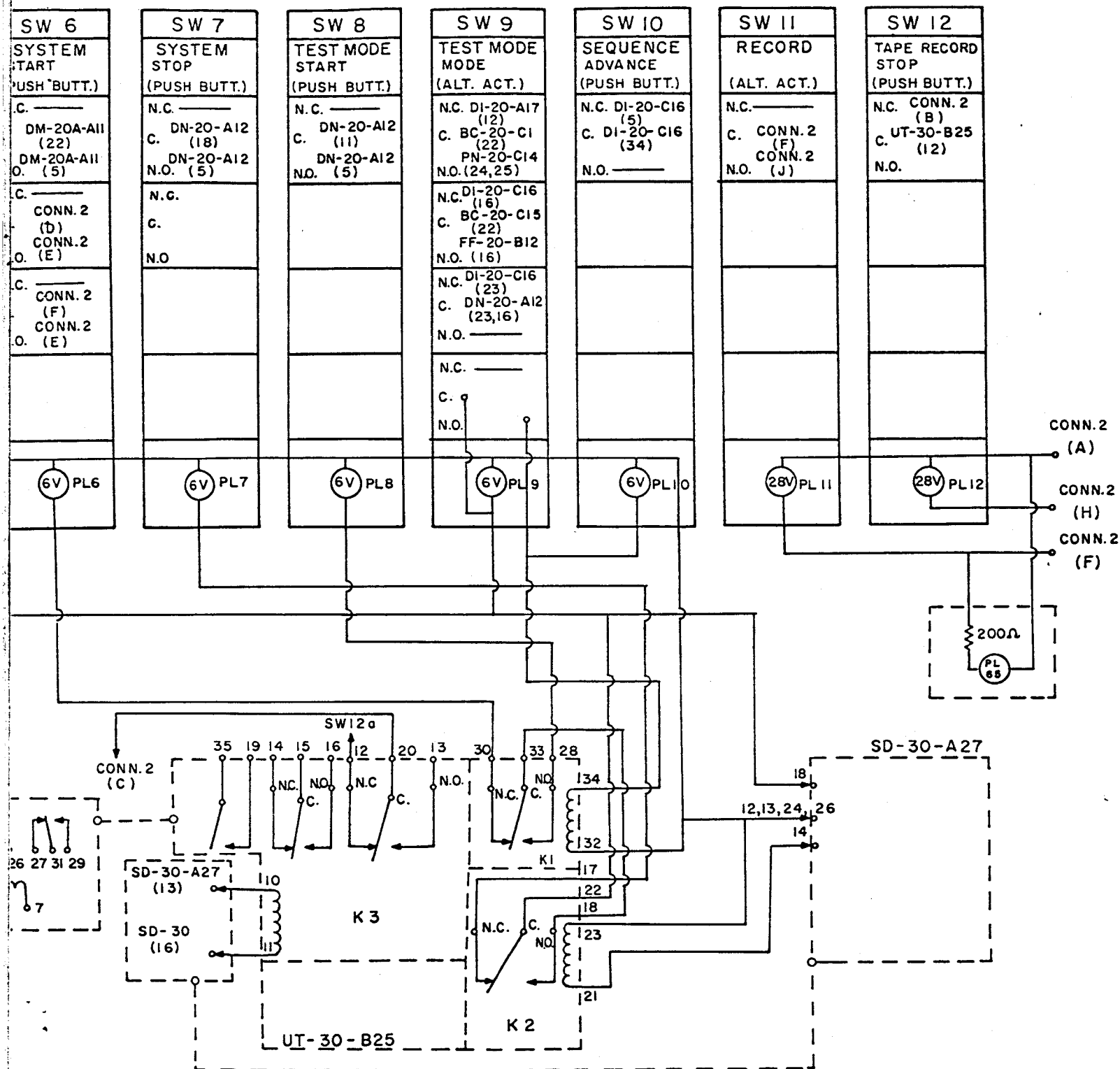


FIGURE 3: RELAY AND CONTROL SWITCH



CONTROL SWITCH CONNECTIONS

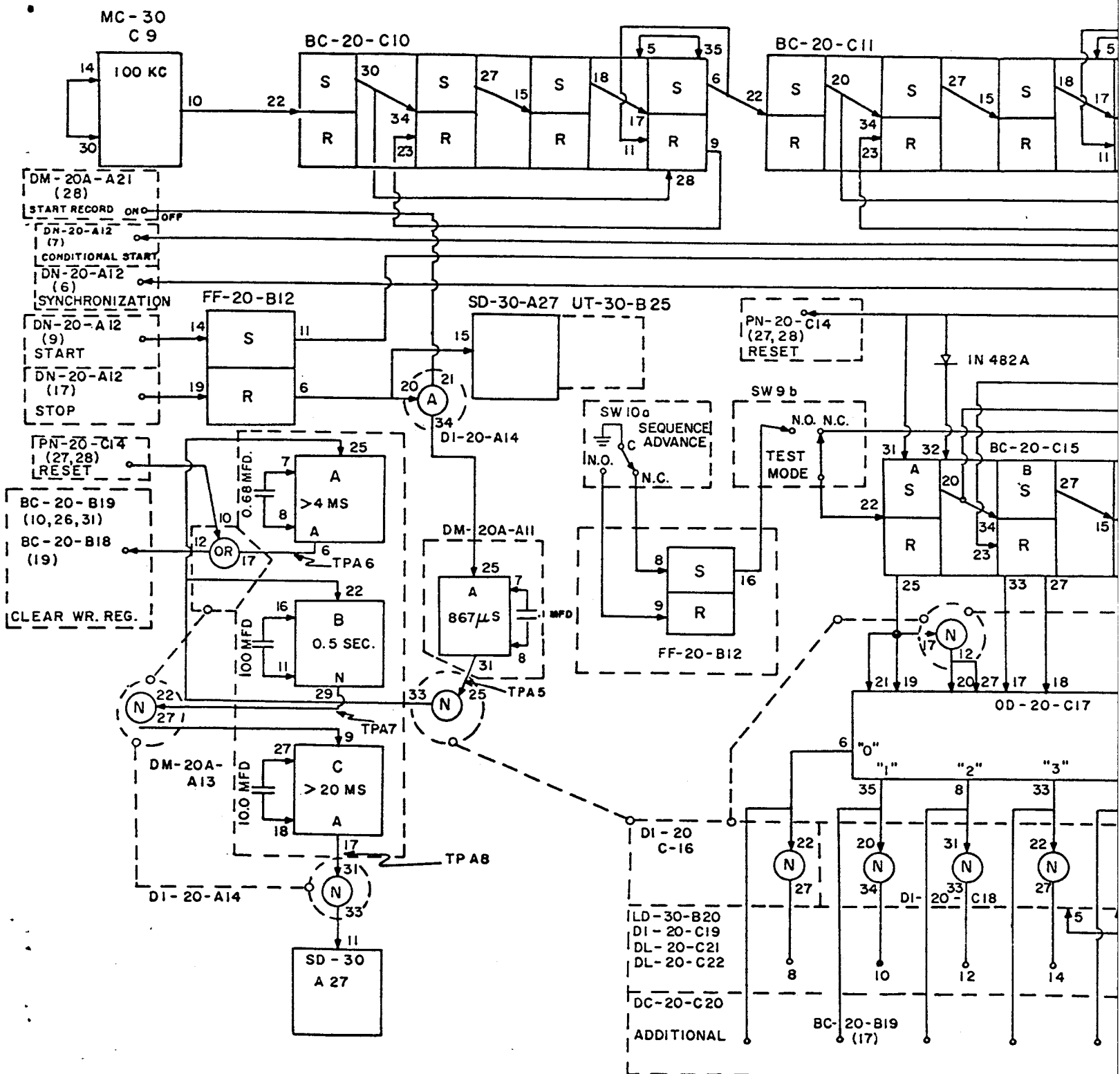
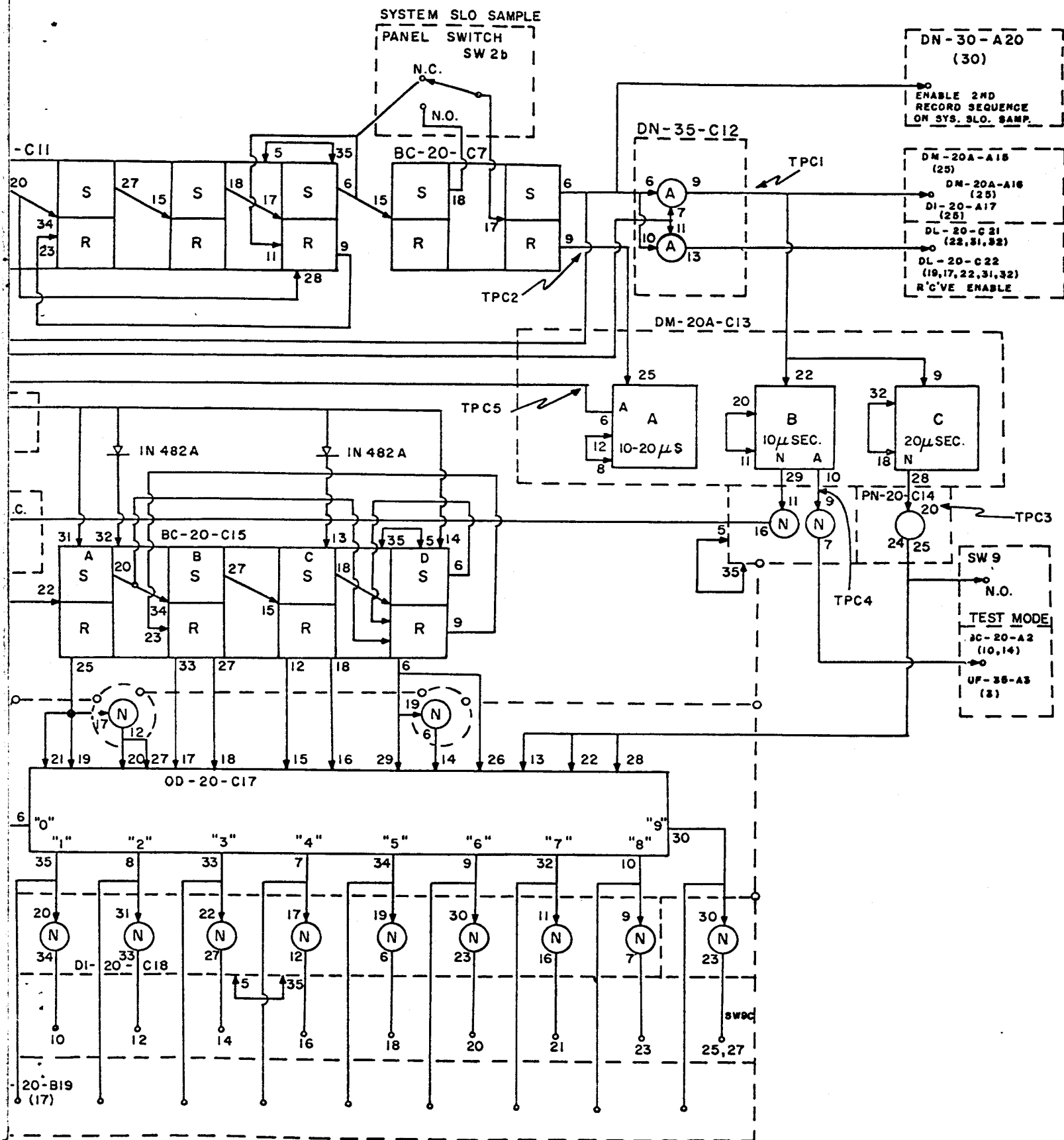


FIGURE 5: CHANNEL SEQUENCING — RECORDER



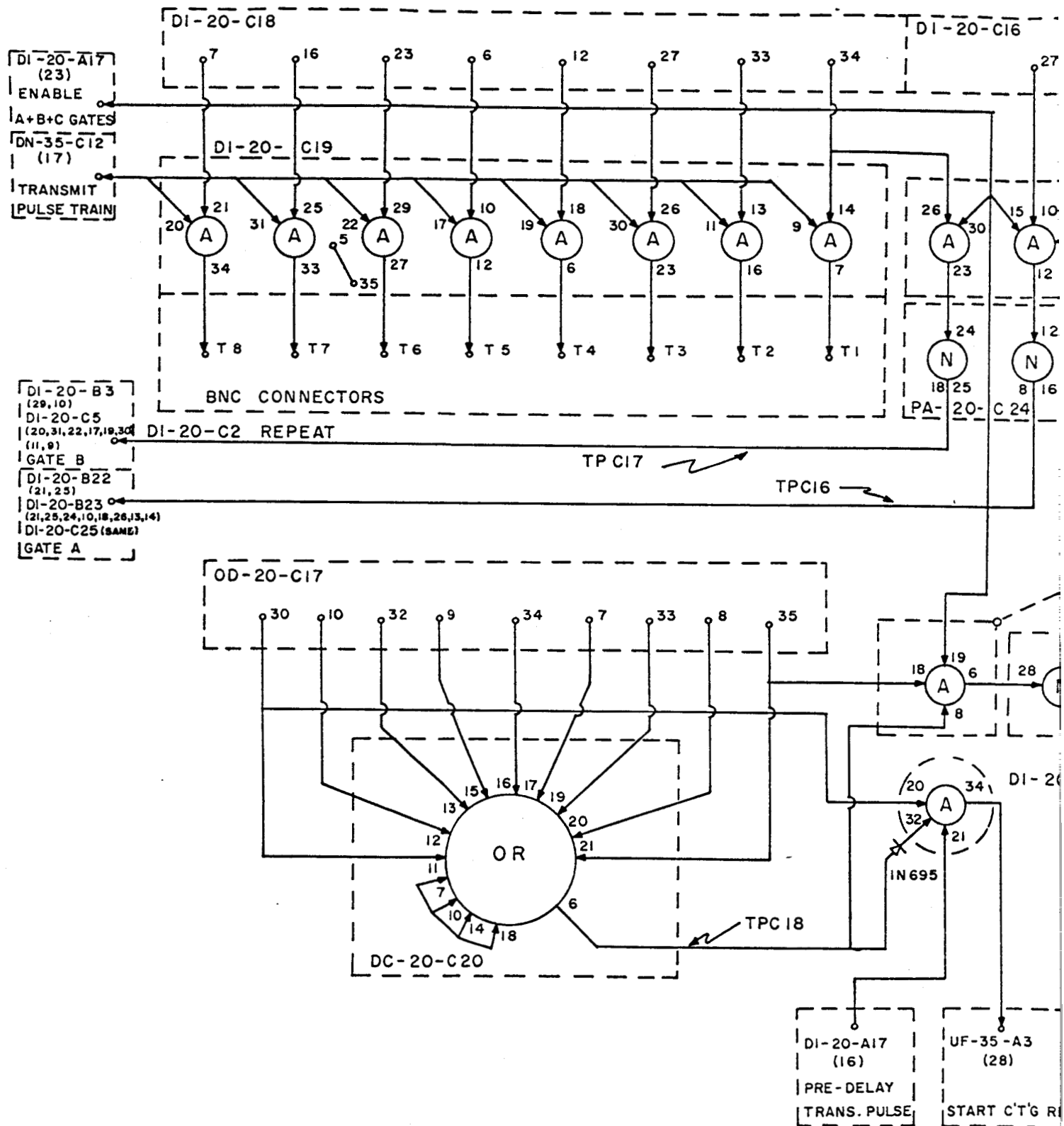


FIGURE 6: CHANNEL C

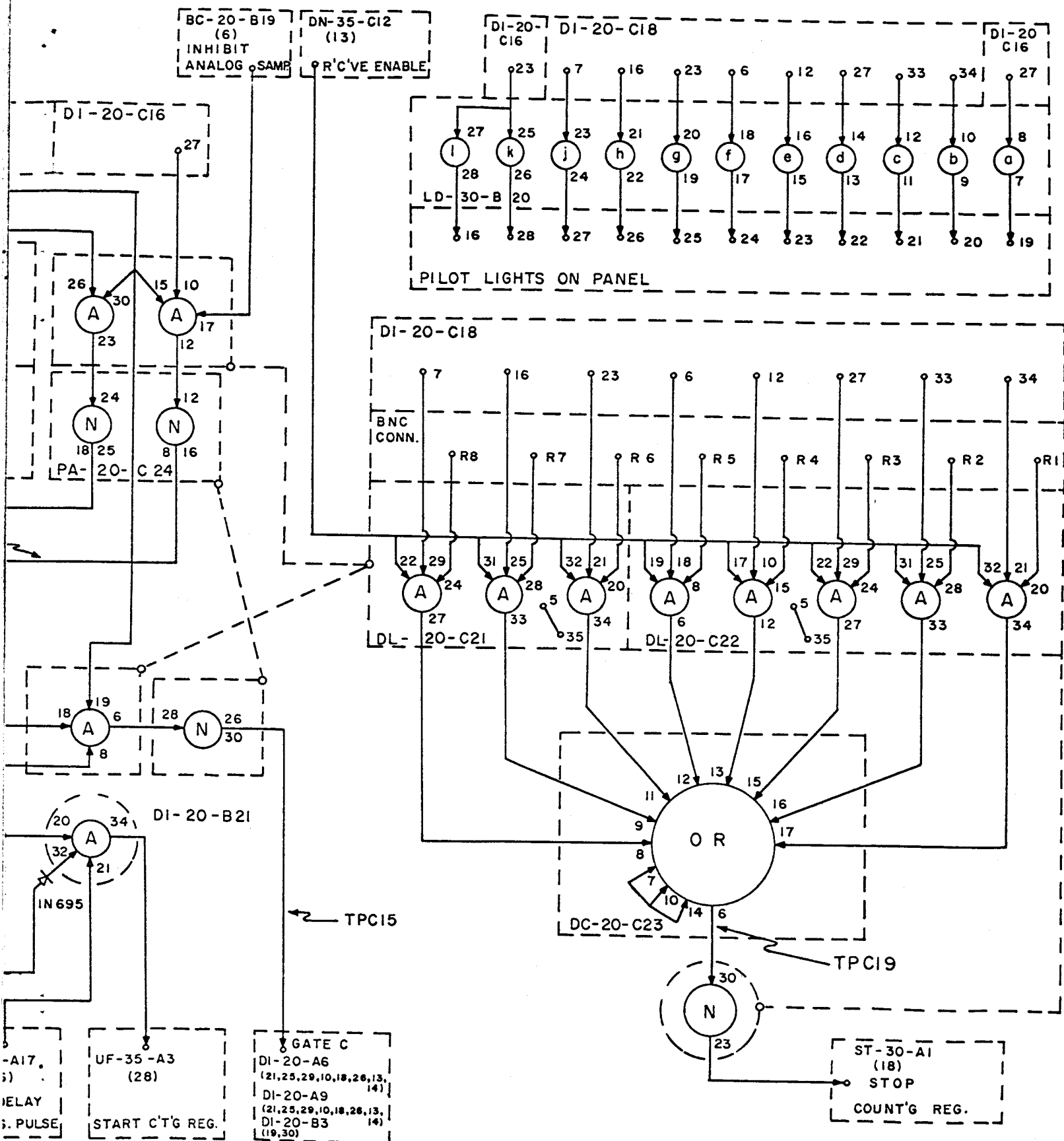


FIGURE 6: CHANNEL CONTROL LOGIC



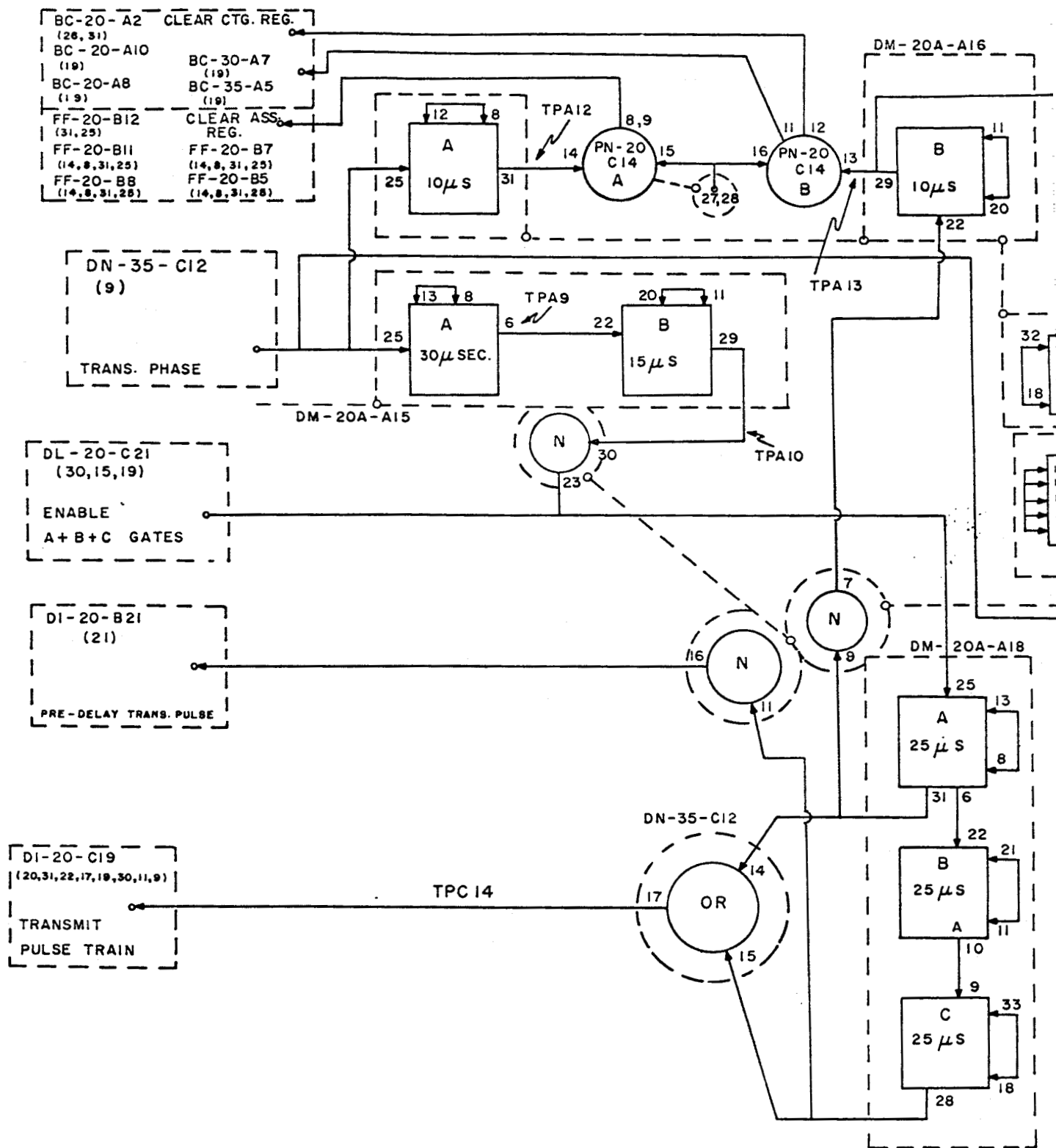
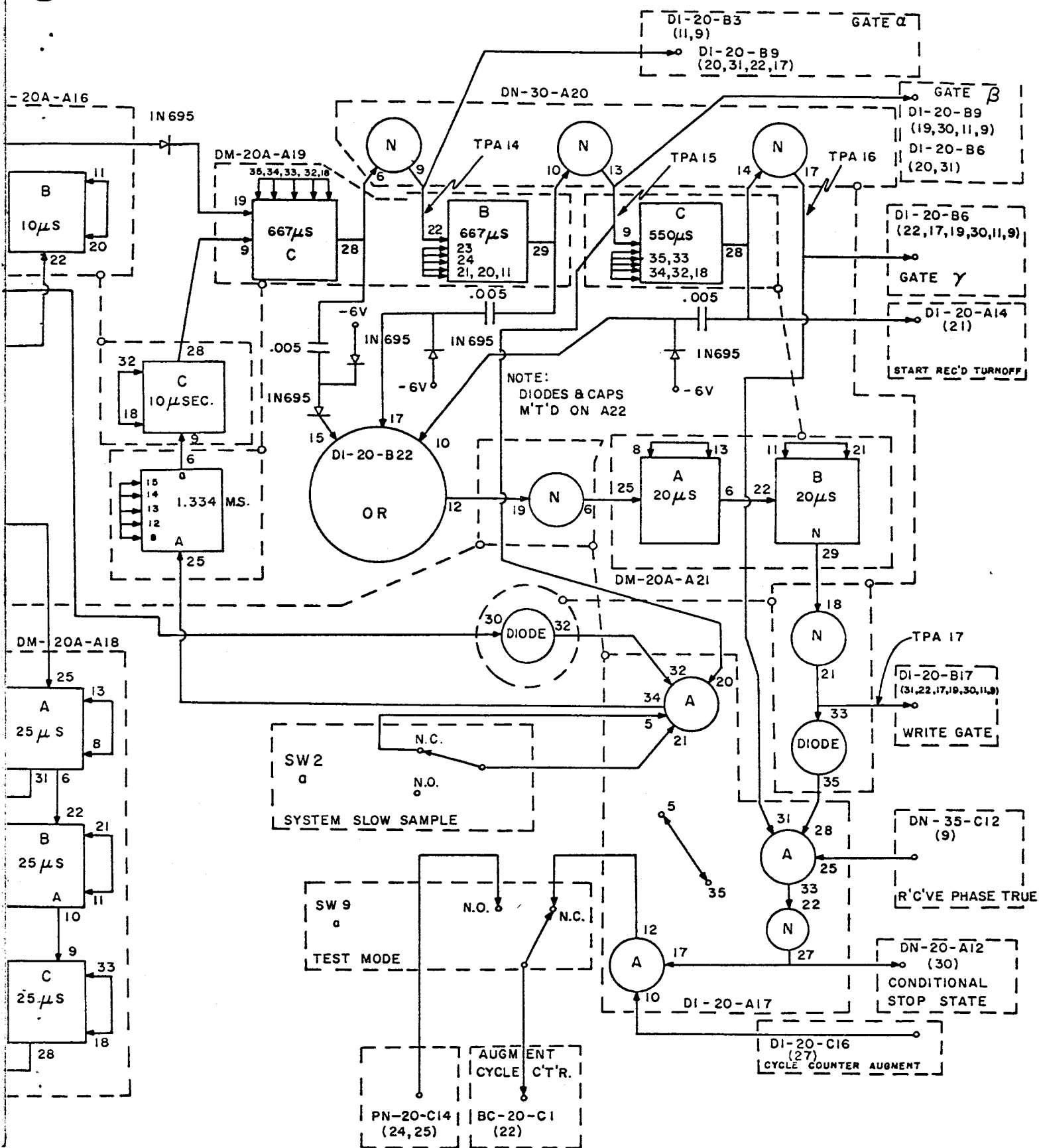


FIGURE 7: GATE CON

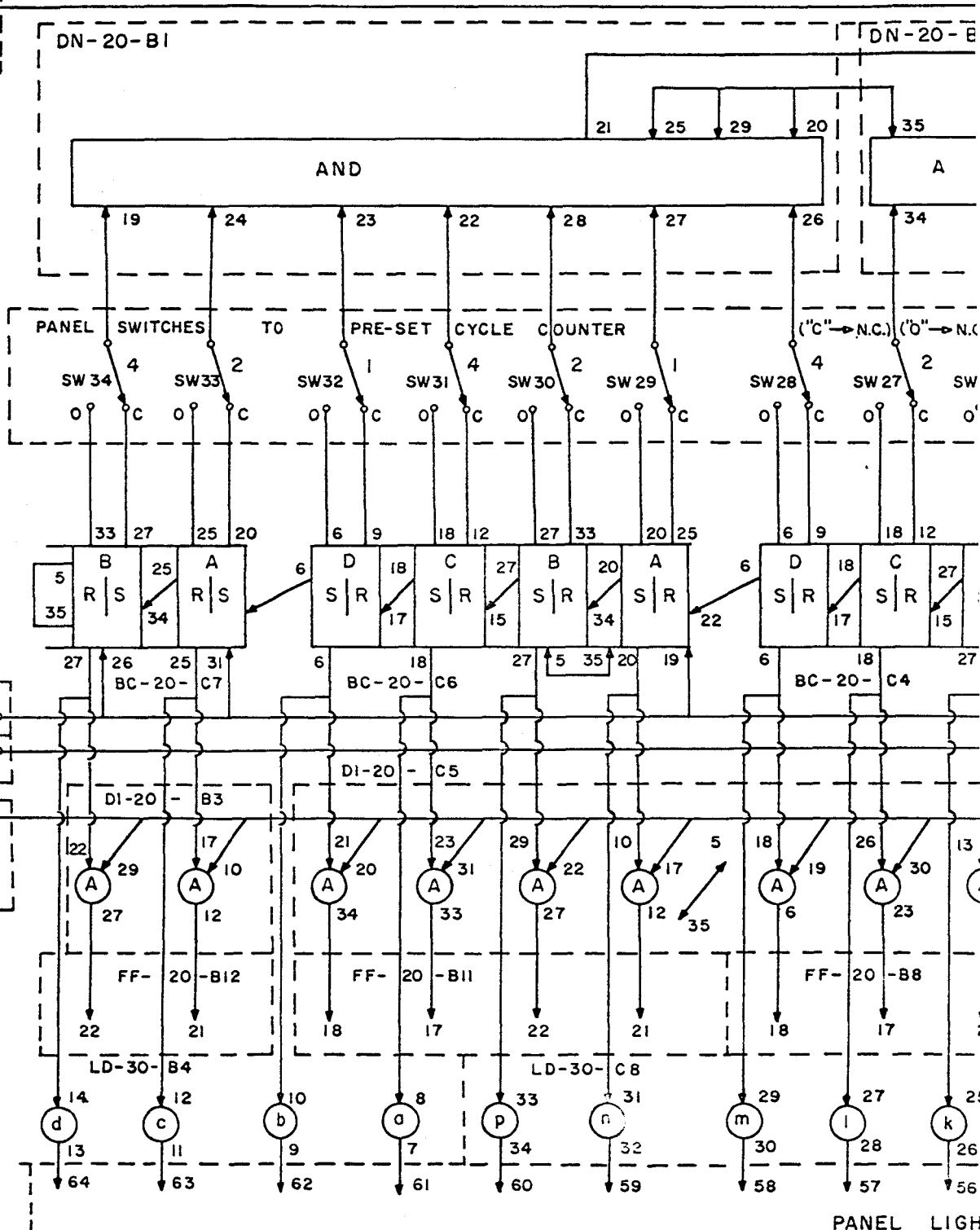


7: GATE CONTROL LOGIC

PL-1

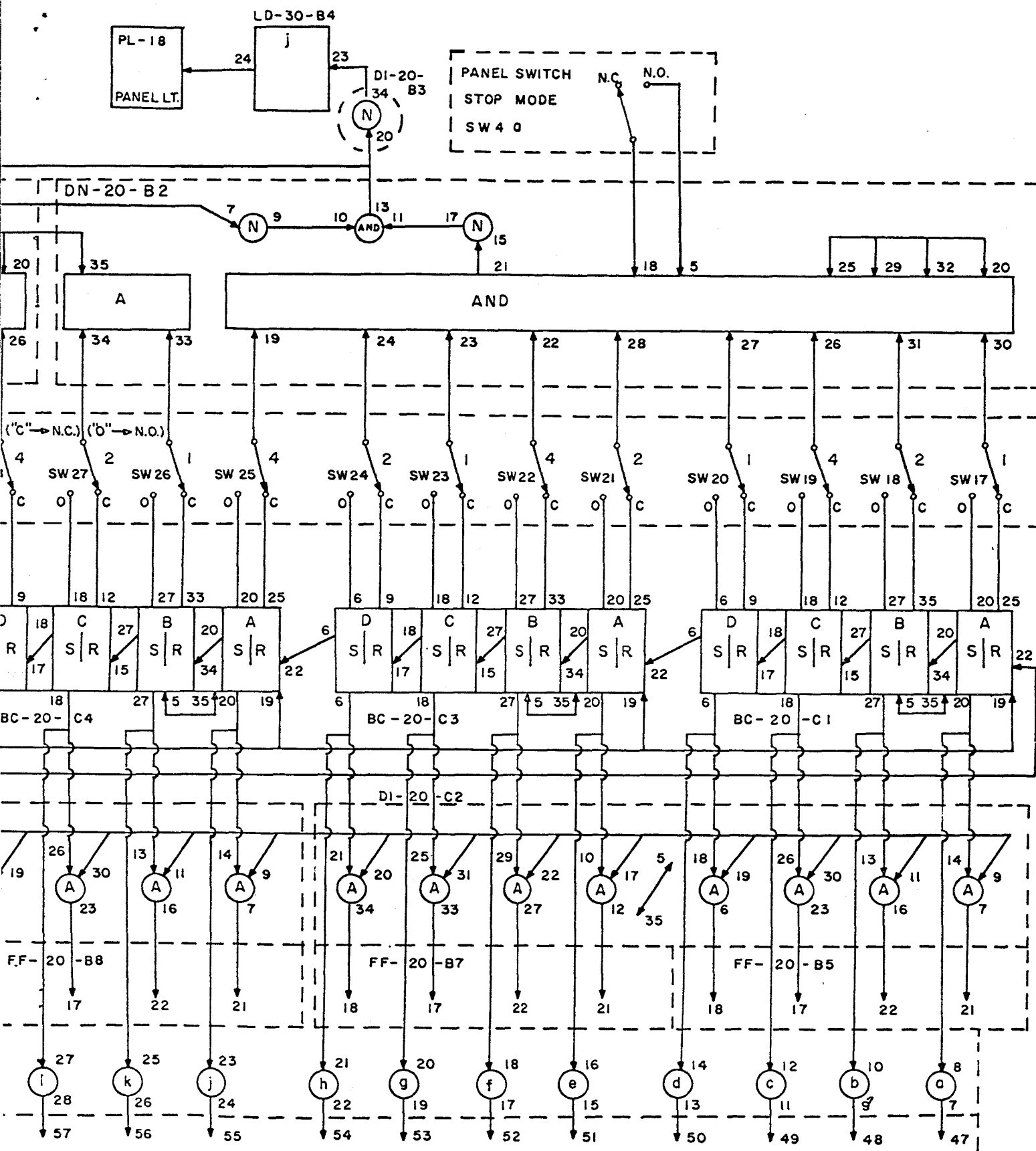
PANEL

DN-20-A12  
(19)  
  
PRE-SET STOP TRUE



PANEL LIGHT

FIGURE 9: CYCLE COUNTER



PANEL LIGHTS

CYCLE COUNTER LOGIC

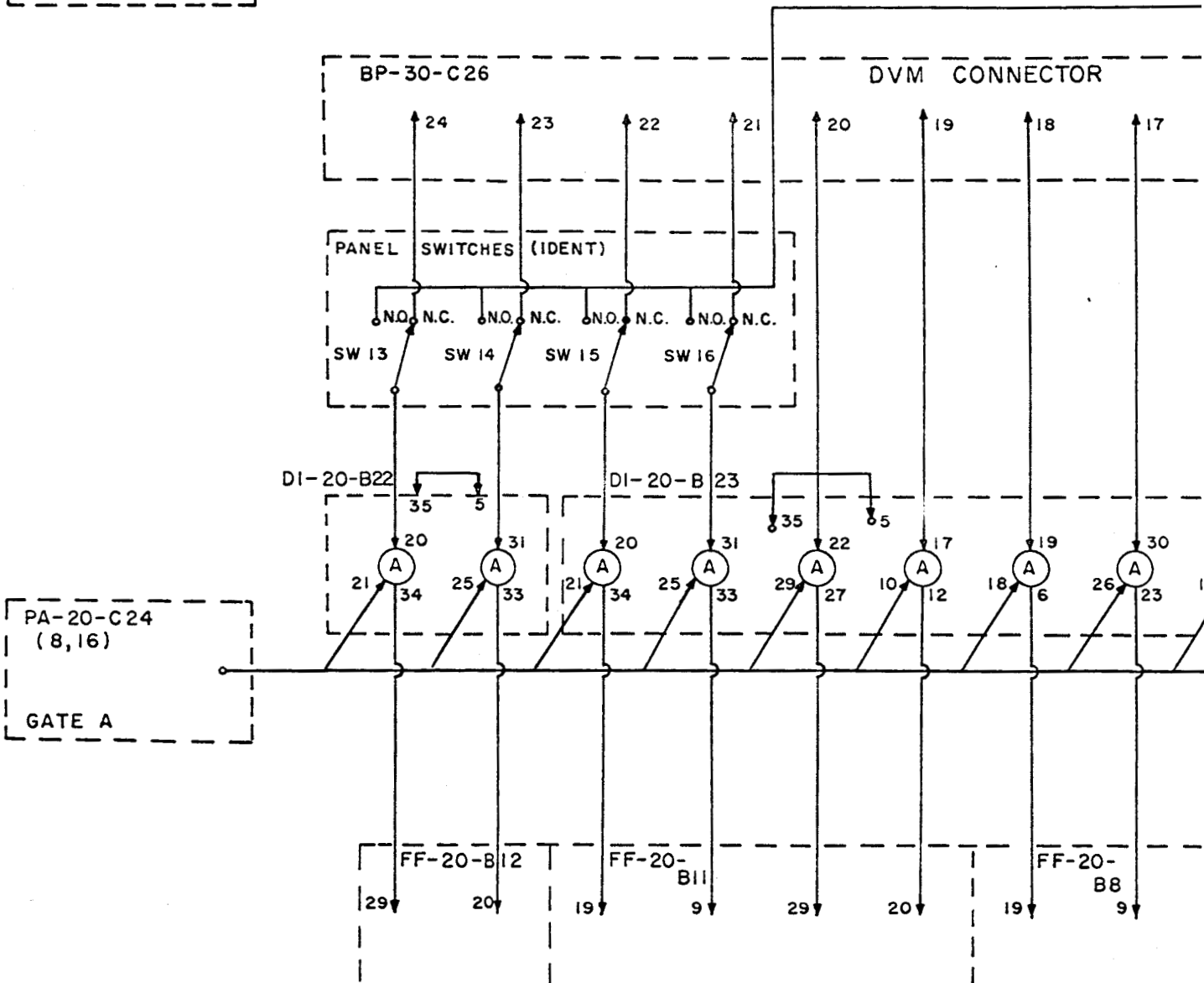
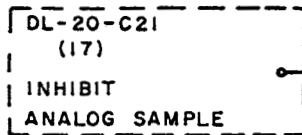
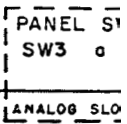
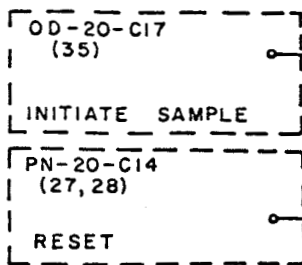
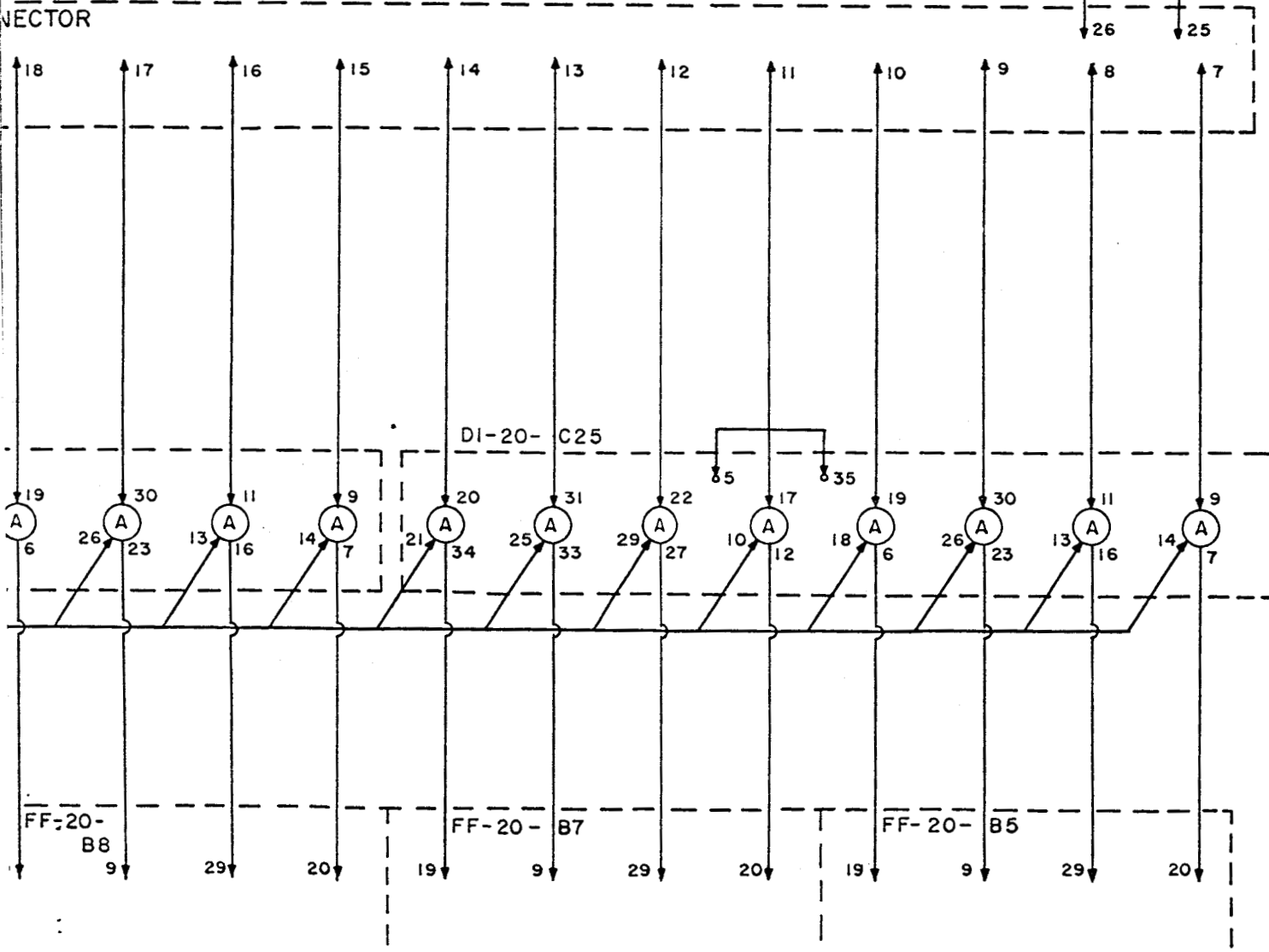
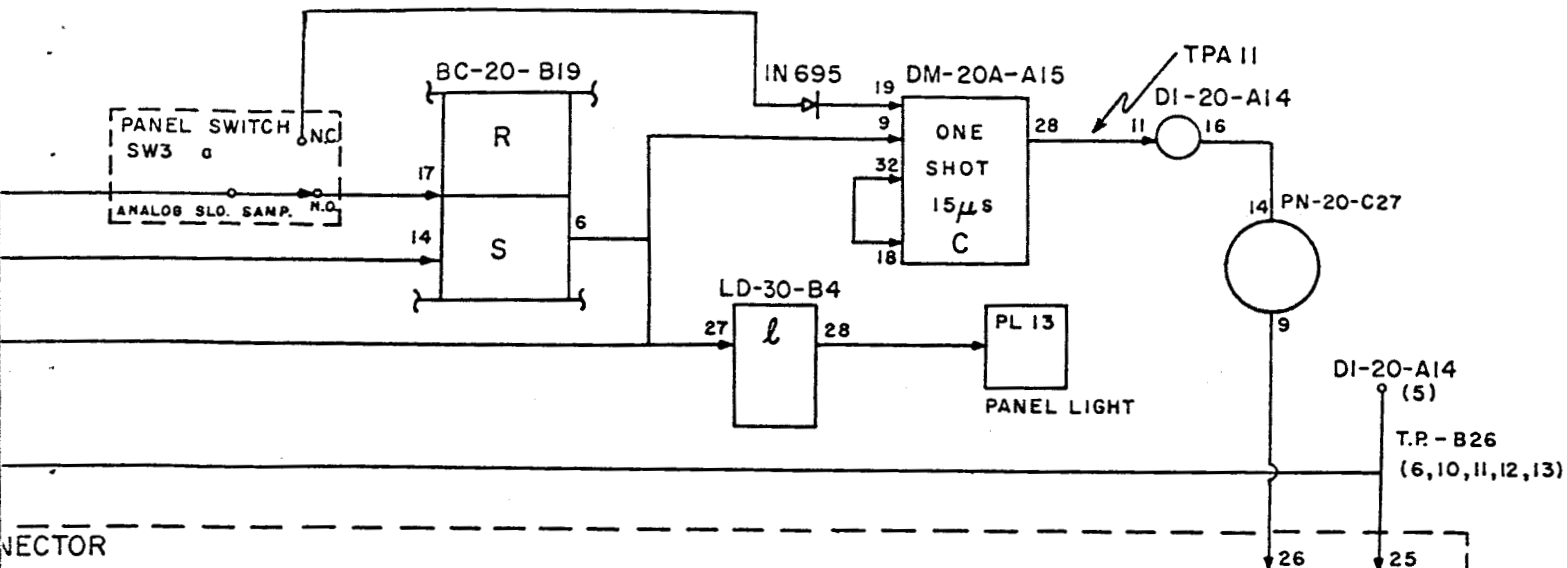


FIGURE 10: DVM OUTPUT BUFF



OUTPUT BUFFER & CONTROL LOGIC

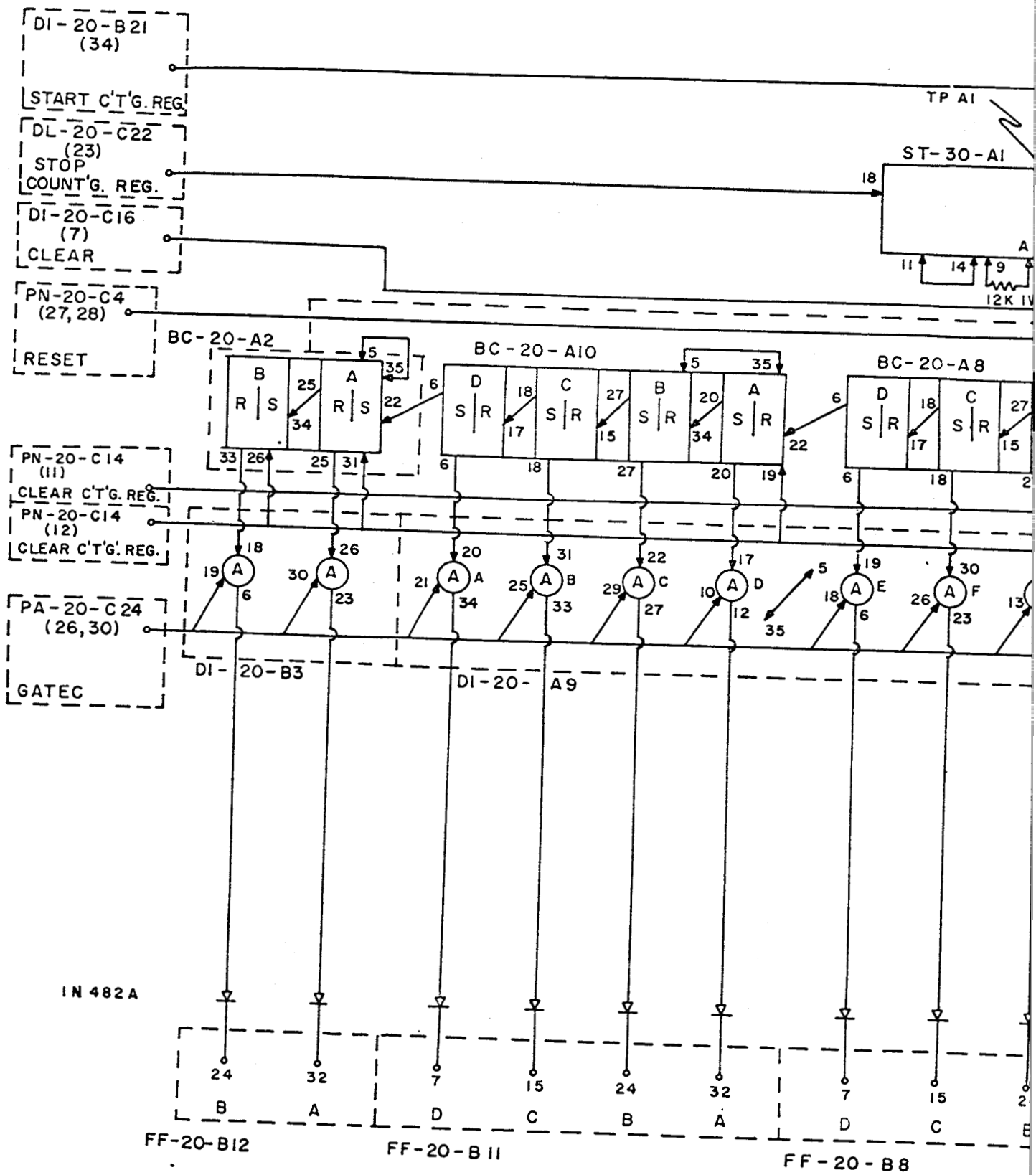
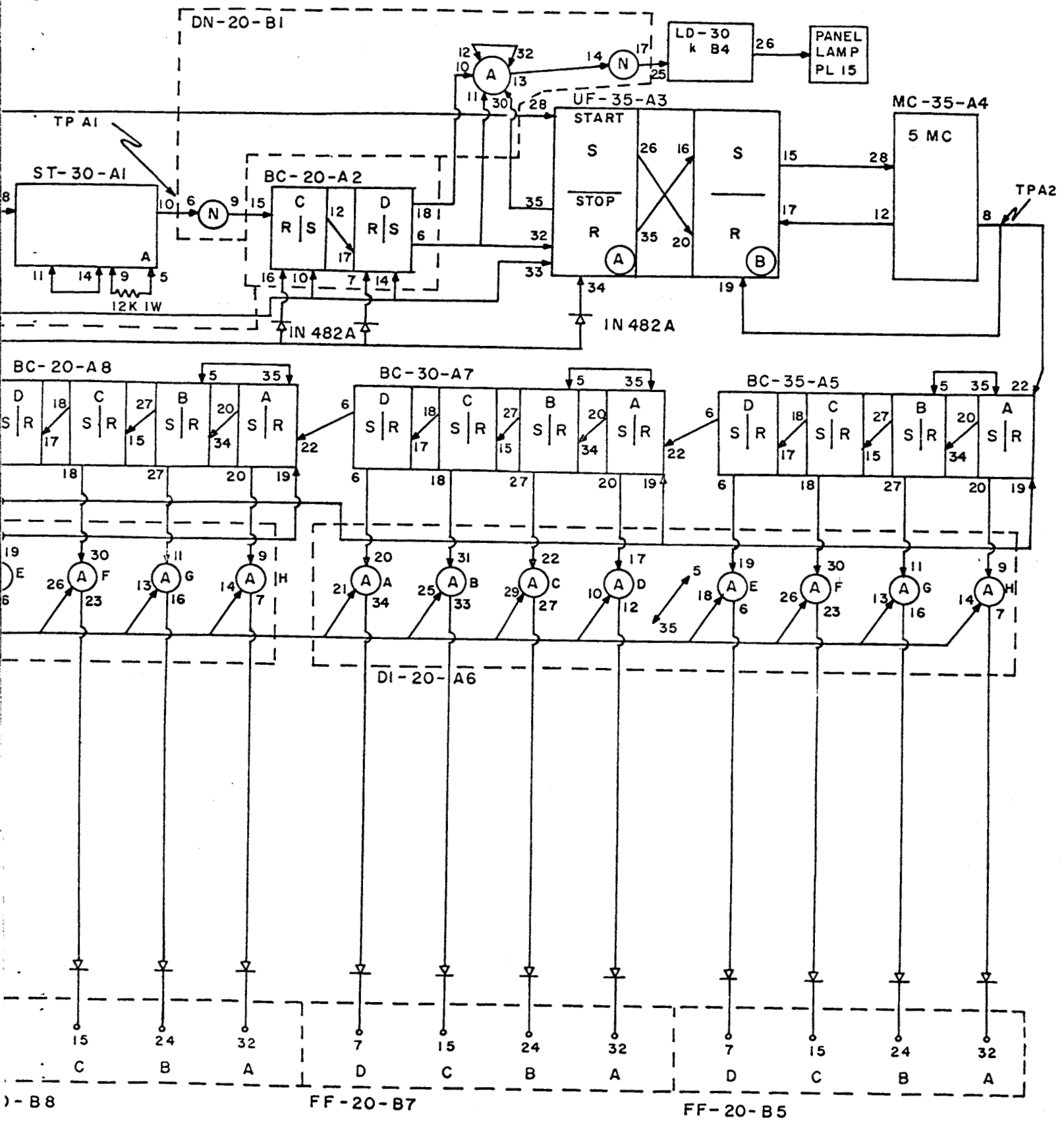


FIGURE 8: COUNTING R



COUNTING REGISTER LOGIC



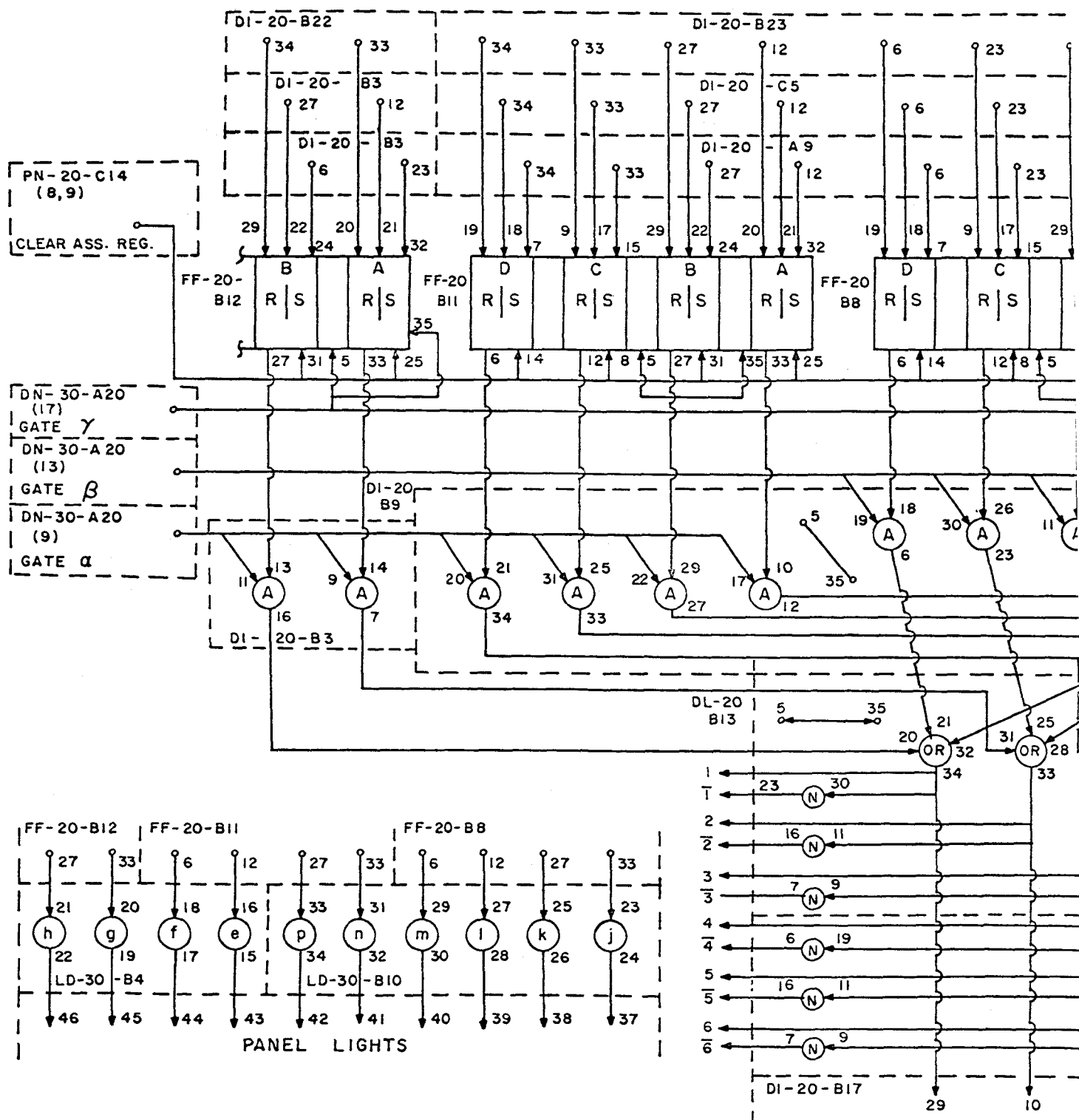
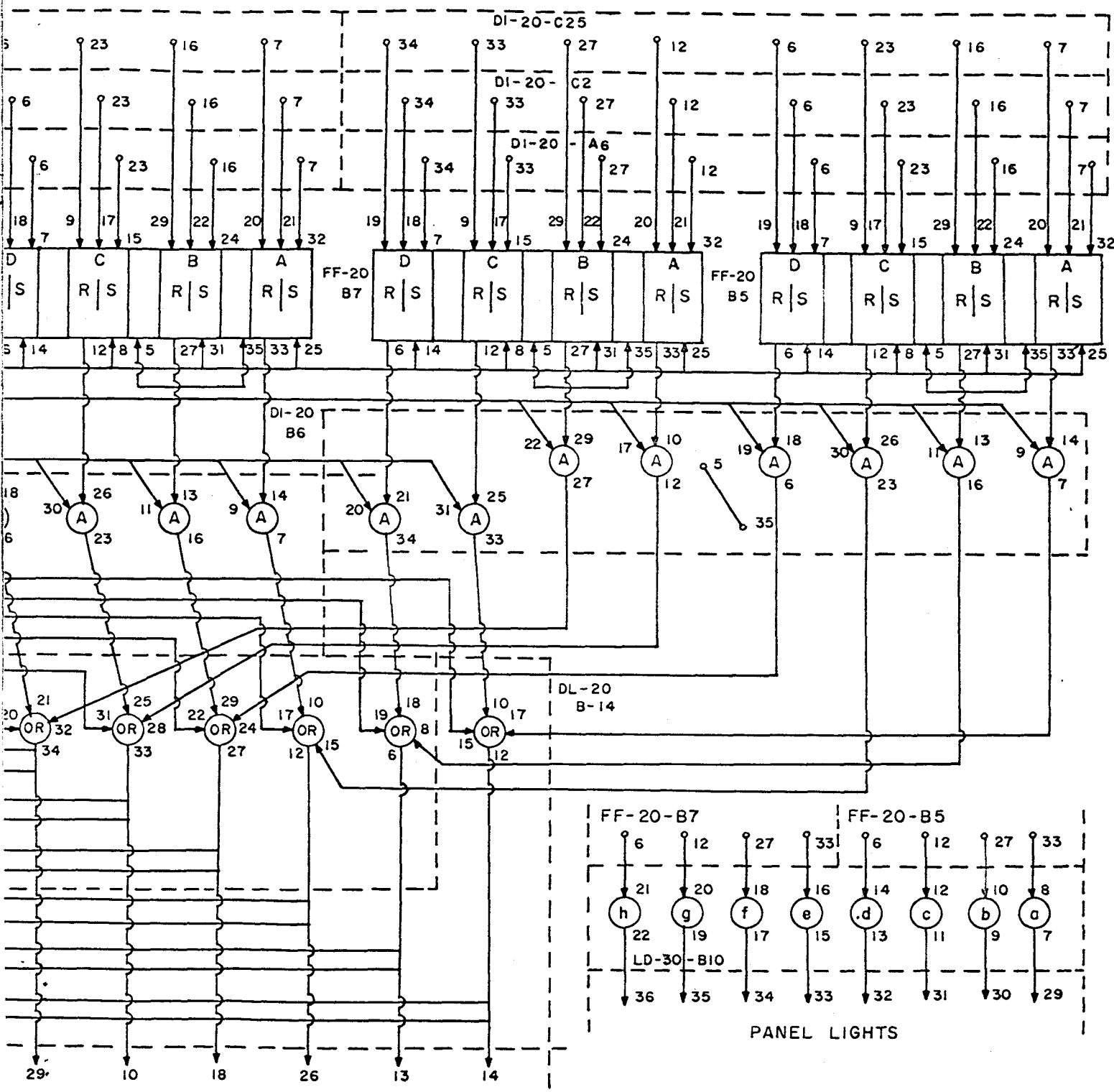


FIGURE II: ASSEMBLY



RE II: ASSEMBLY REGISTER

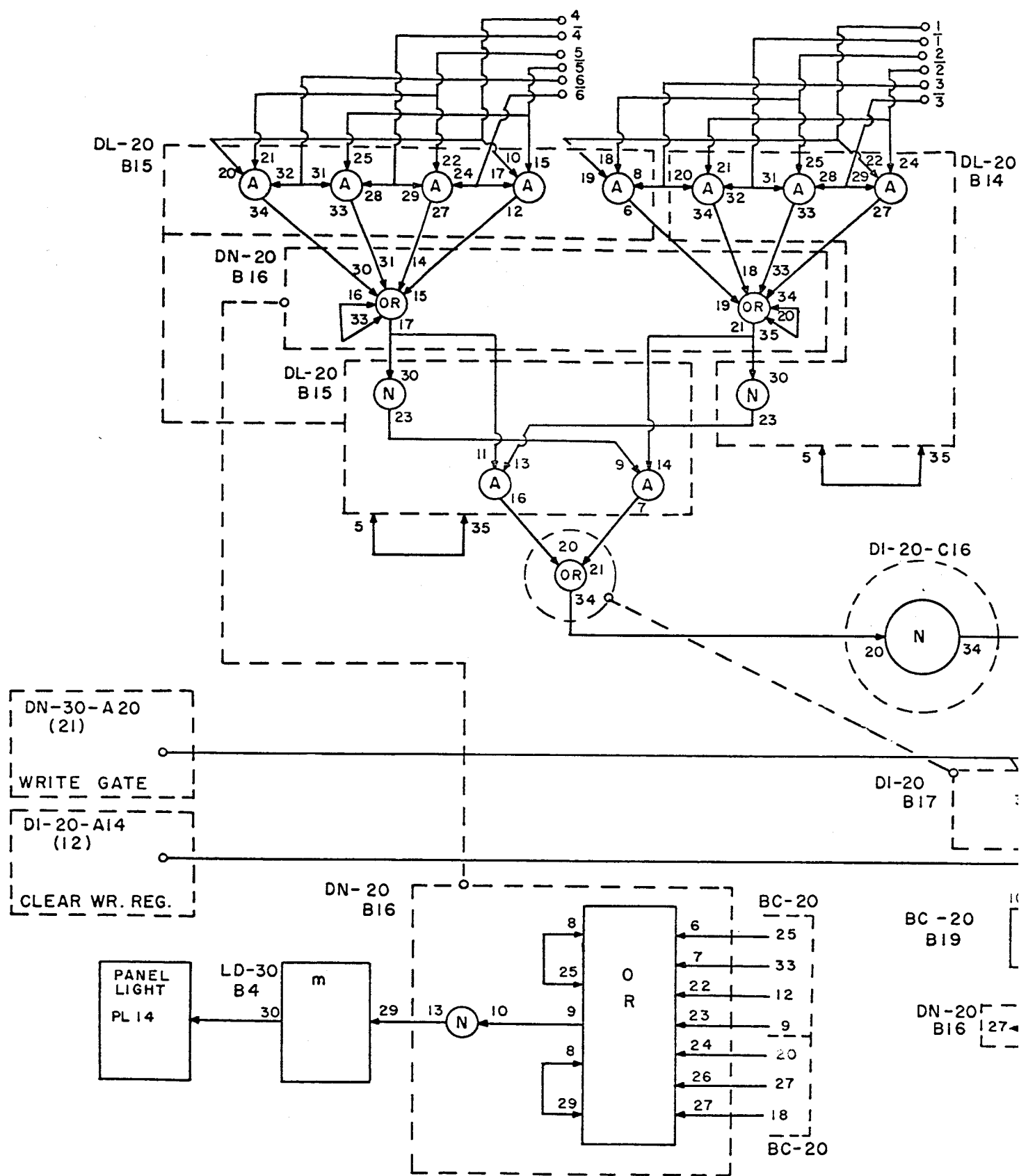


FIGURE 12: WRITING

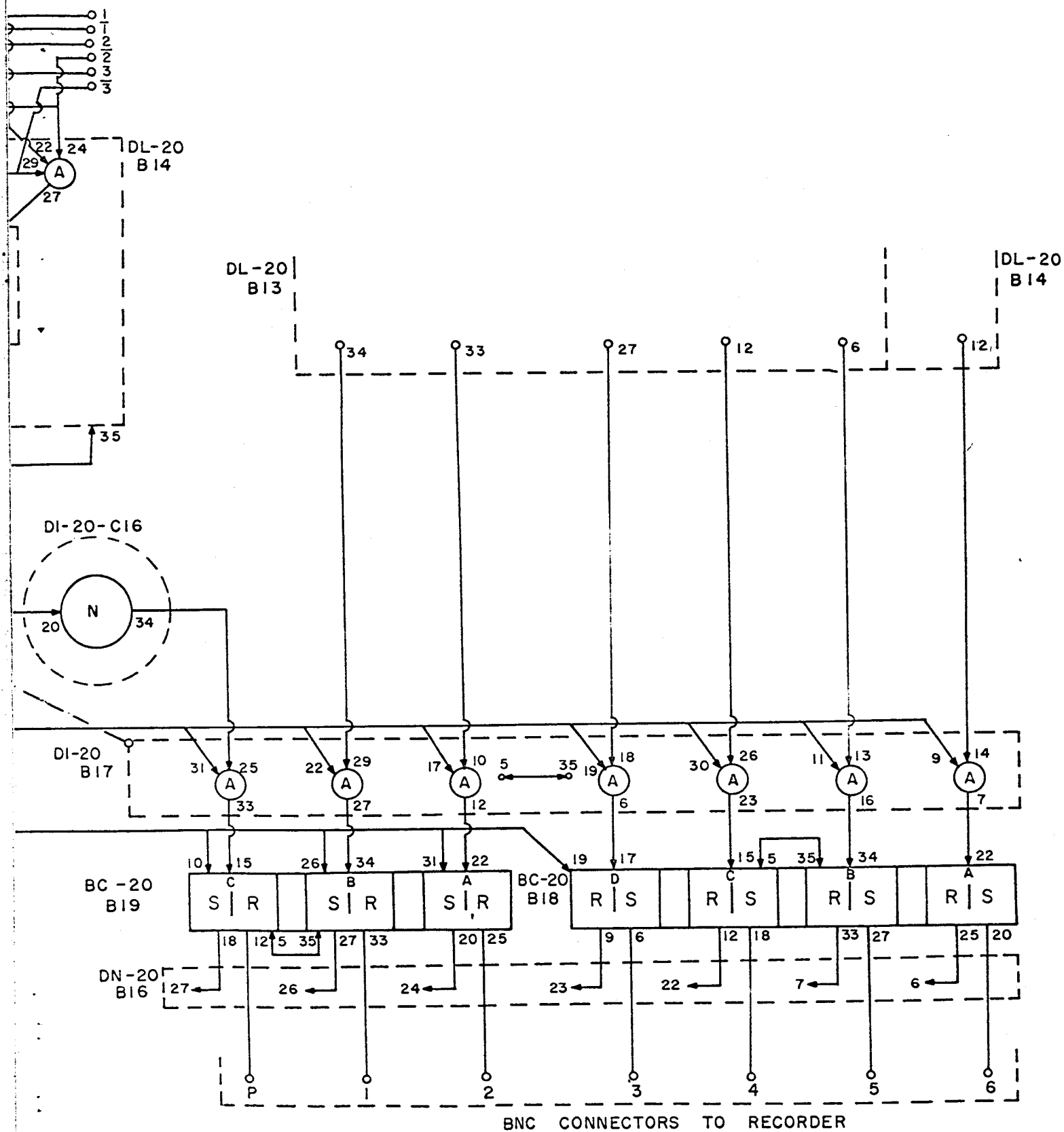


FIGURE 12: WRITE REGISTER

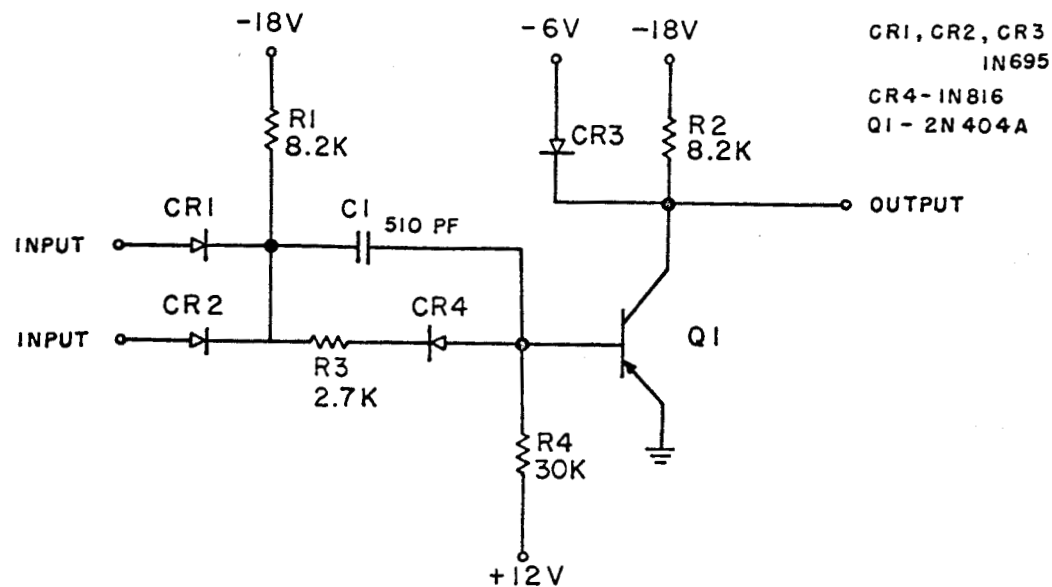
consists of a Solion transducer (manufactured by Texas Research Electronics—now Self-Organizing Systems—of Dallas, Texas) designed to measure  $1/2 C_D u_1^2$  with a frequency-response capability of about one-half cycle per second as an upper limit. The sensor output is fed simultaneously and directly to a TI Servowriter recorder and the A-D sonic channel. To date, however, no success has been realized in obtaining satisfactory operation of this transducer and it is probable though not certain that this device will have to be abandoned. The basic purpose in making such a measurement is to provide a gross back-up check on the sonic outputs and if subsequent efforts should continue to be unsuccessful in operation of this device, its loss will not be significant in the research sense.

4. Flow Corporation Dynamic Wind Force Indicator ("bouncing ball"). This transducer was available to the project for only a short period through sponsor-loan and was intended as a check-device on the sonics. Measurement location was near the surface (due to mass) and at a point some six feet from the sonic mounting pole. However, the operational characteristics and requirements for calibration and recording are such that it did not appear feasible to retain this transducer, and it was returned to the manufacturer through the sponsor's representatives. Following manufacturer's modifications it may be reinstalled and, if so, recording for any two of the three coordinate components will be by a Dual-Channel TI Servowriter, with simultaneous input to the A-D sonic channel.

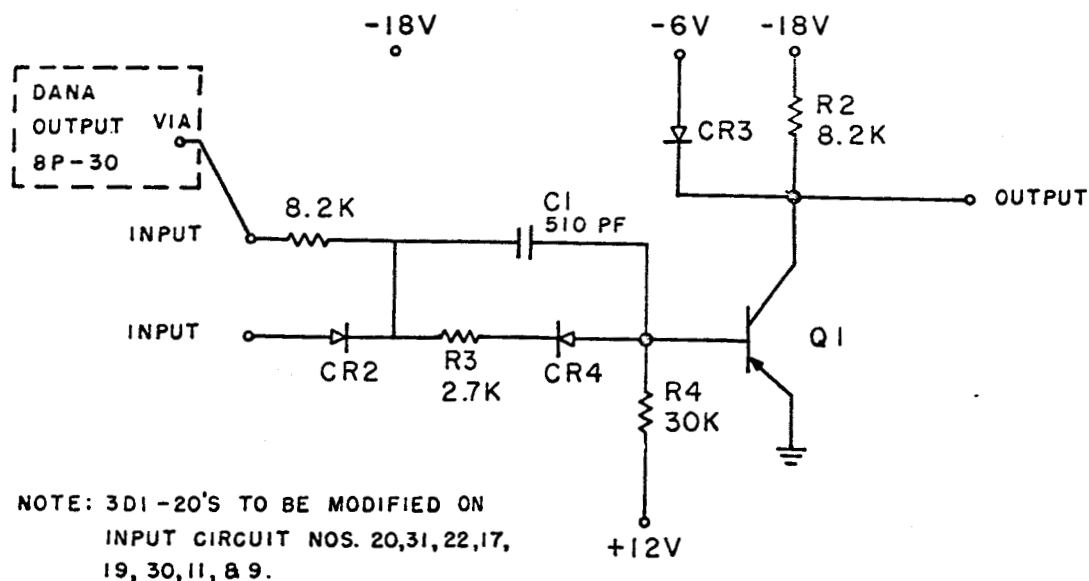
5. Instantaneous temperature. This system has yet to be designed and will not be so until further investigation as to necessity and feasibility is completed. If, however, such installation is made, two transducers will be employed, one at each of the sonic measuring levels, with recording on the dual-channel Servowriter and simultaneously on the A-D channel of the sonic system.

c. Cedar Hill Wind Speed Comparison Tests

In an attempt to provide answers to long-standing and significant questions concerning the relative capabilities of various wind-measuring devices in both the mean and instantaneous sense, to



STANDARD CIRCUIT



MODIFIED CIRCUIT

FIGURE 13: DI-20 MODIFICATION FOR DVM OUTPUT BUFFER

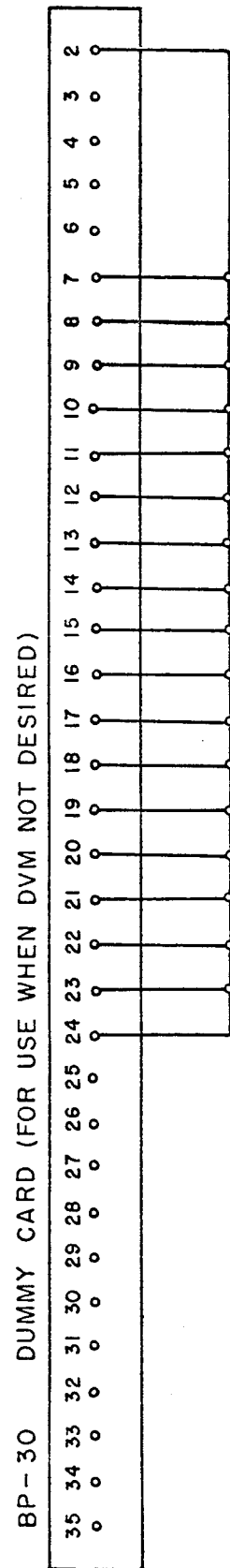
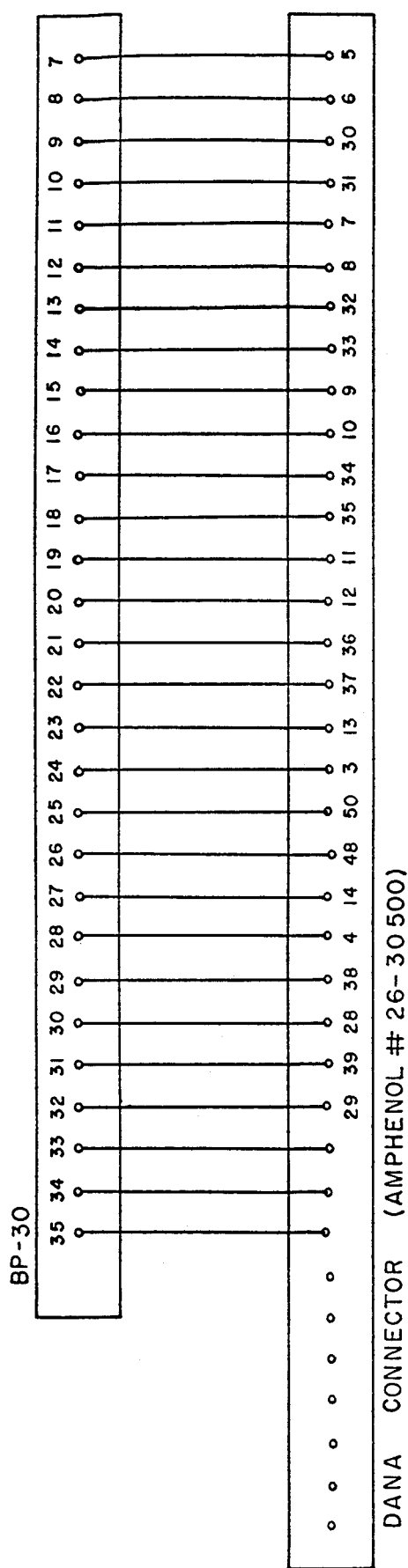


FIGURE 14: DVM INTERCONNECTION CABLING

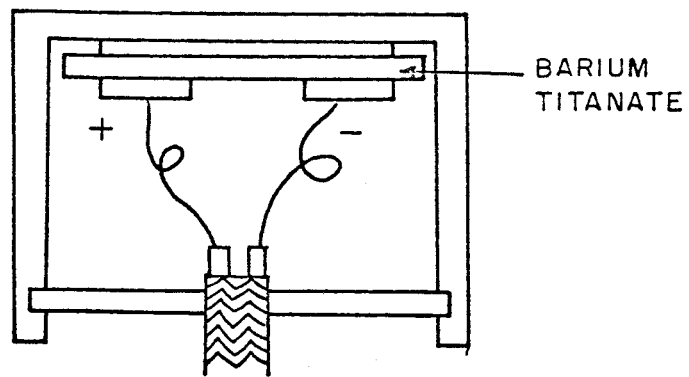


FIGURE 15a: TR-21 CRYSTAL POSITION

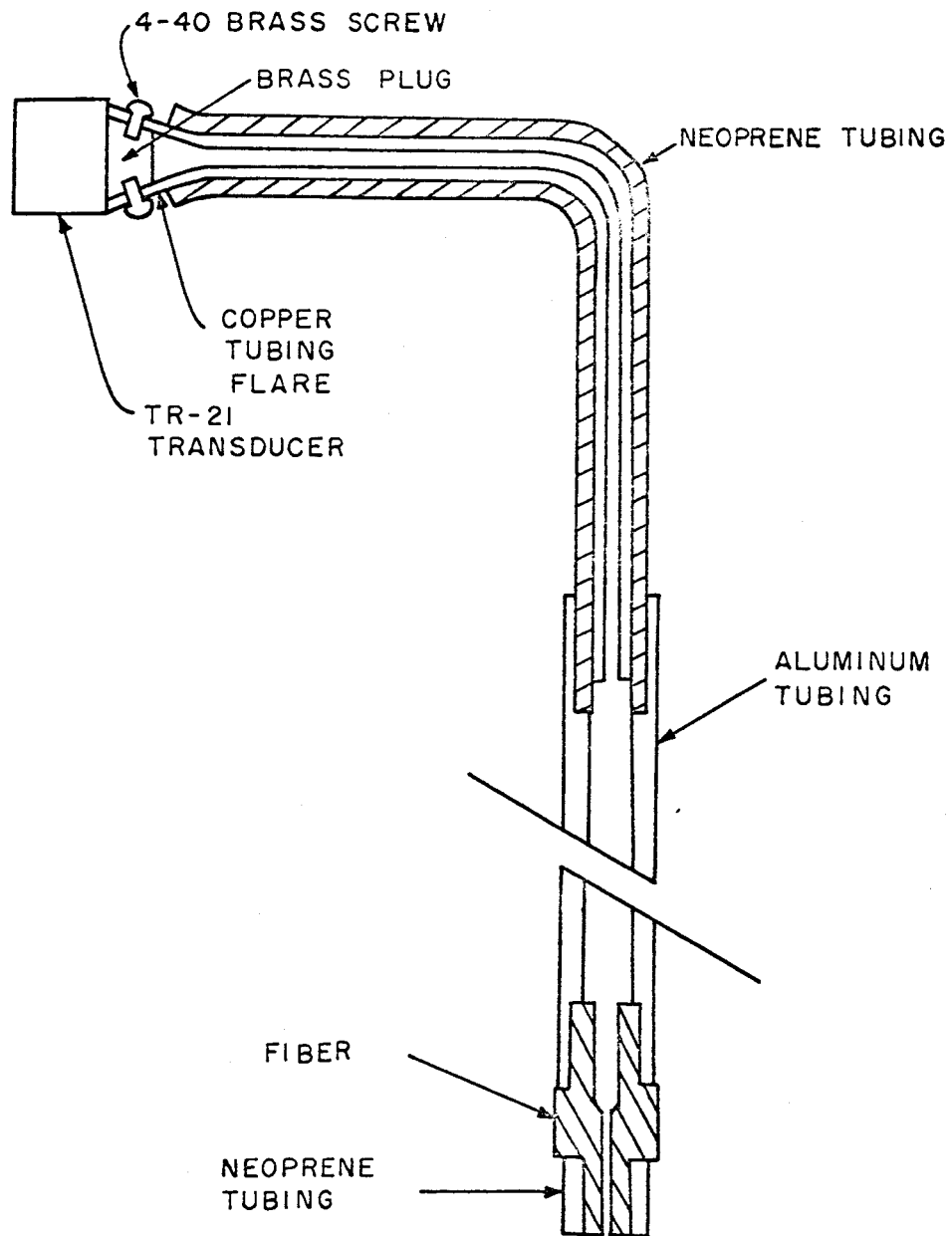


FIGURE 15b: SONIC TRANSDUCER MOUNT



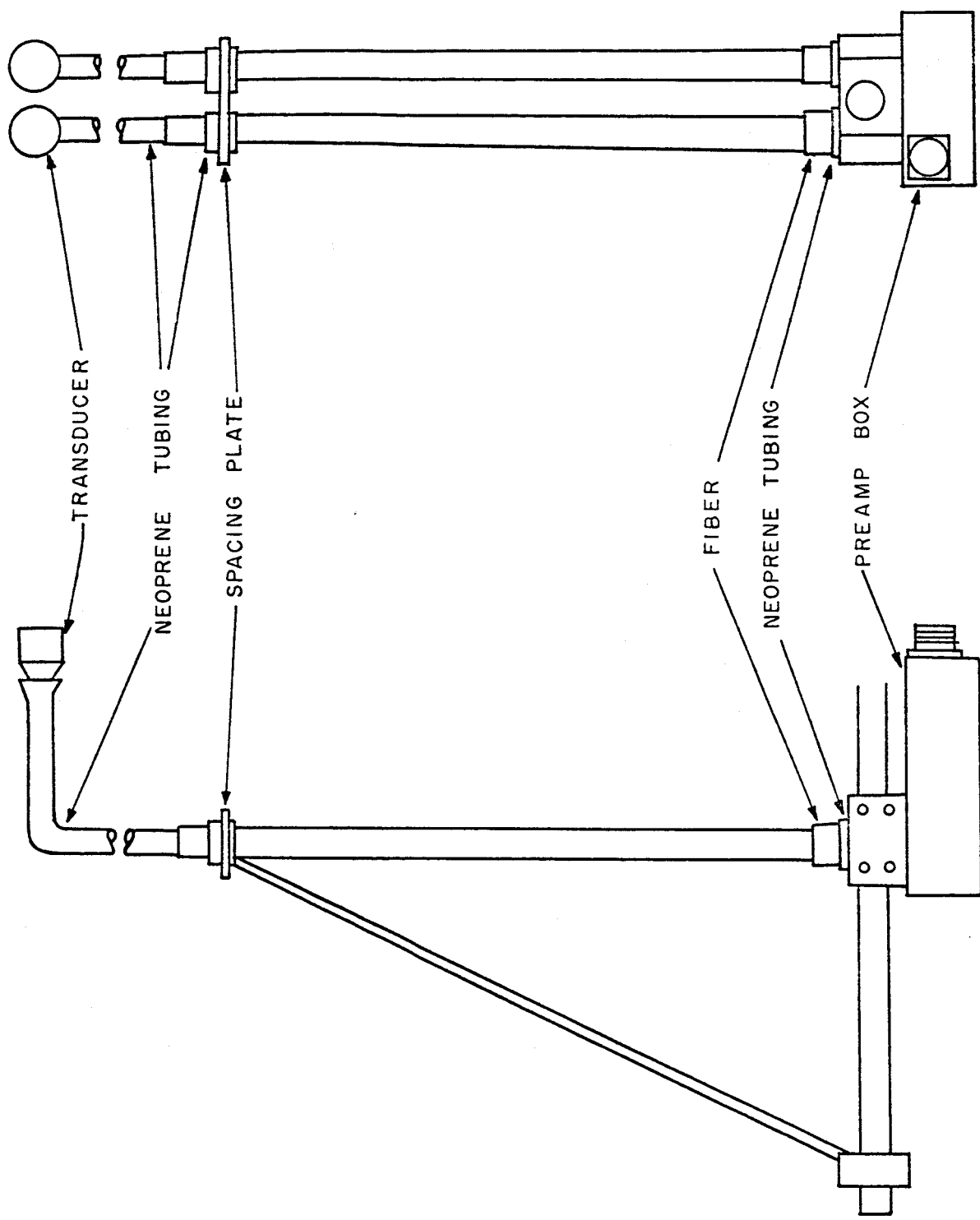
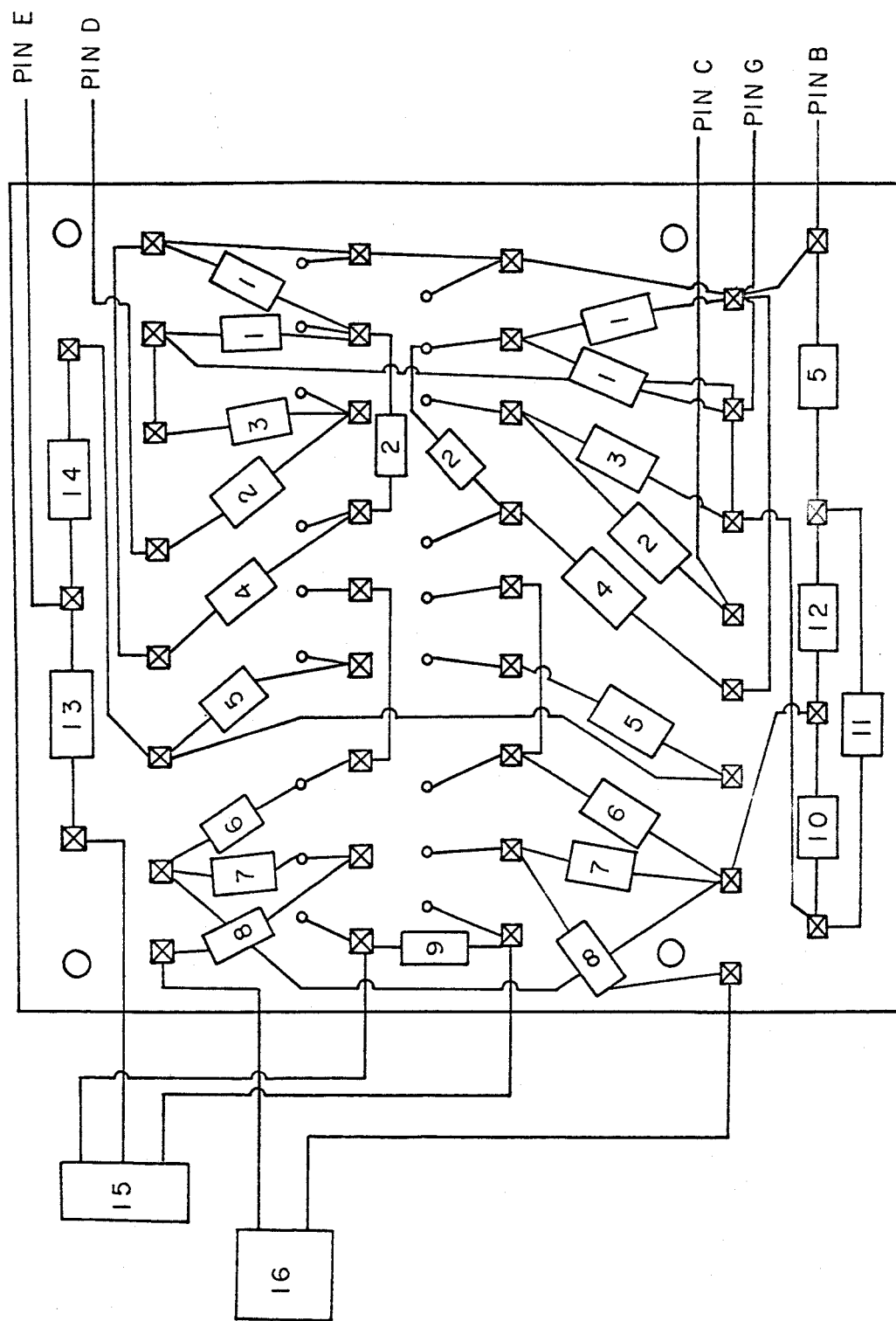


FIGURE 16: SONIC ANEMOMETER ASSEMBLY






- |                 |                  |  |               |
|-----------------|------------------|--|---------------|
| 1 - 470K        | 5 - 330 $\Omega$ | 9 - 2K   | 13 - 560K     |
| 2 - .03 $\mu$ f | 6 - 20K          | 10 - 100 $\Omega$  | 14 - 30K      |
| 3 - 4.7K        | 7 - 2.2M         | 11 -  | 15 - 2K POT   |
| 4 - 36K         | 8 - 10K          | 12 - 390 $\Omega$  | 16 - ARCO 306 |

FIGURE 18: PREAMPLIFIER CIRCUIT BOARD

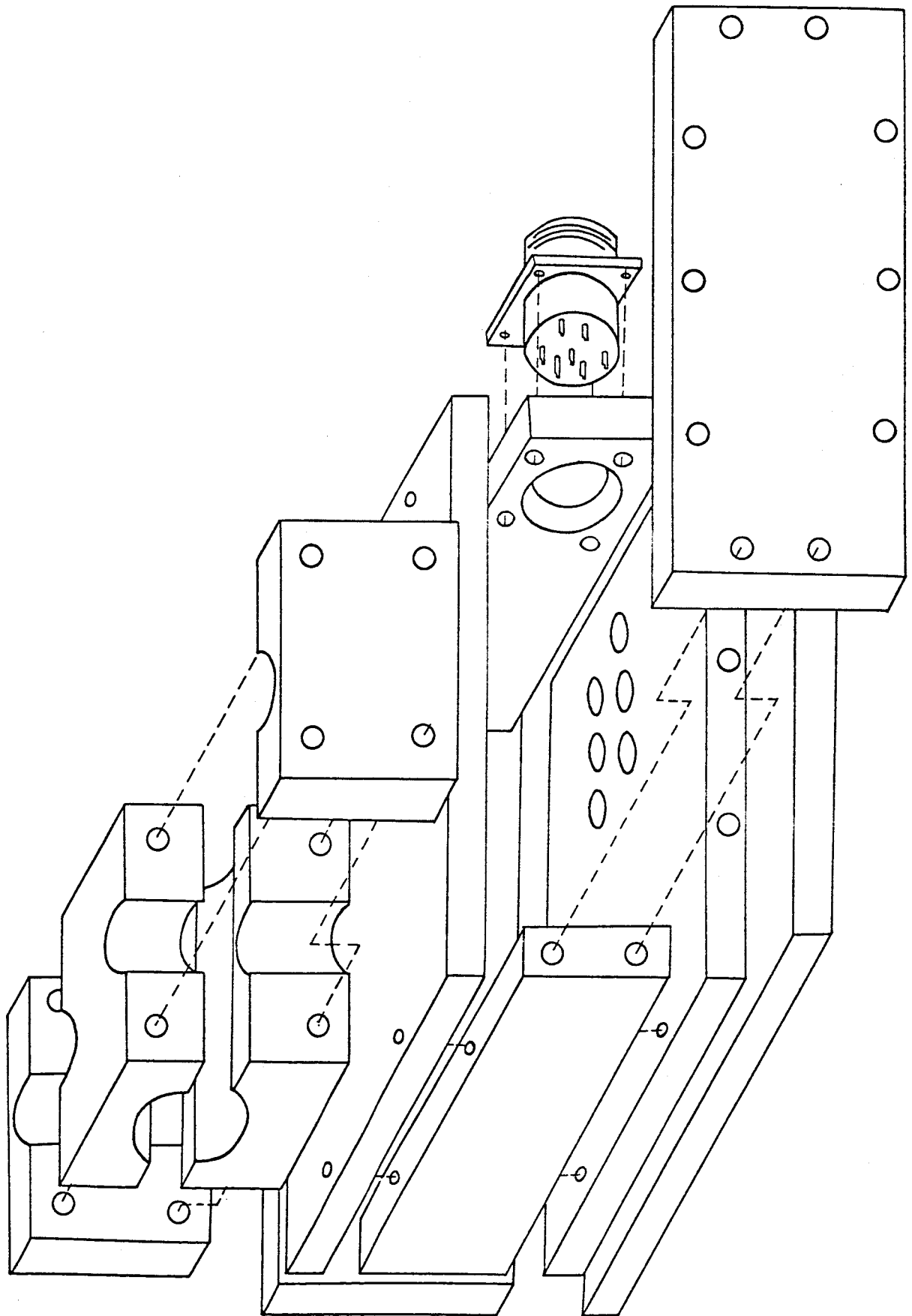


FIGURE 19: PREAMPLIFIER HOUSING

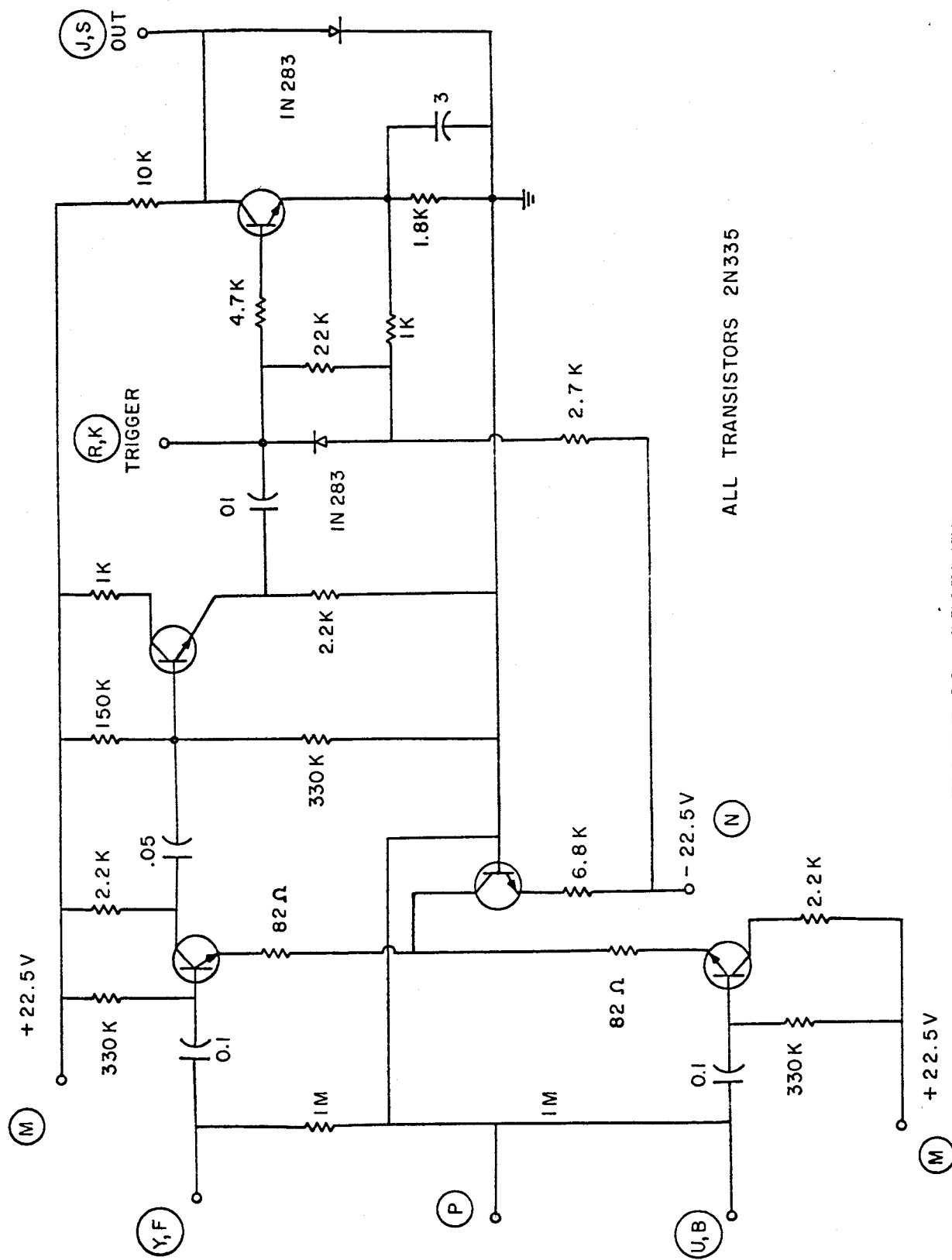
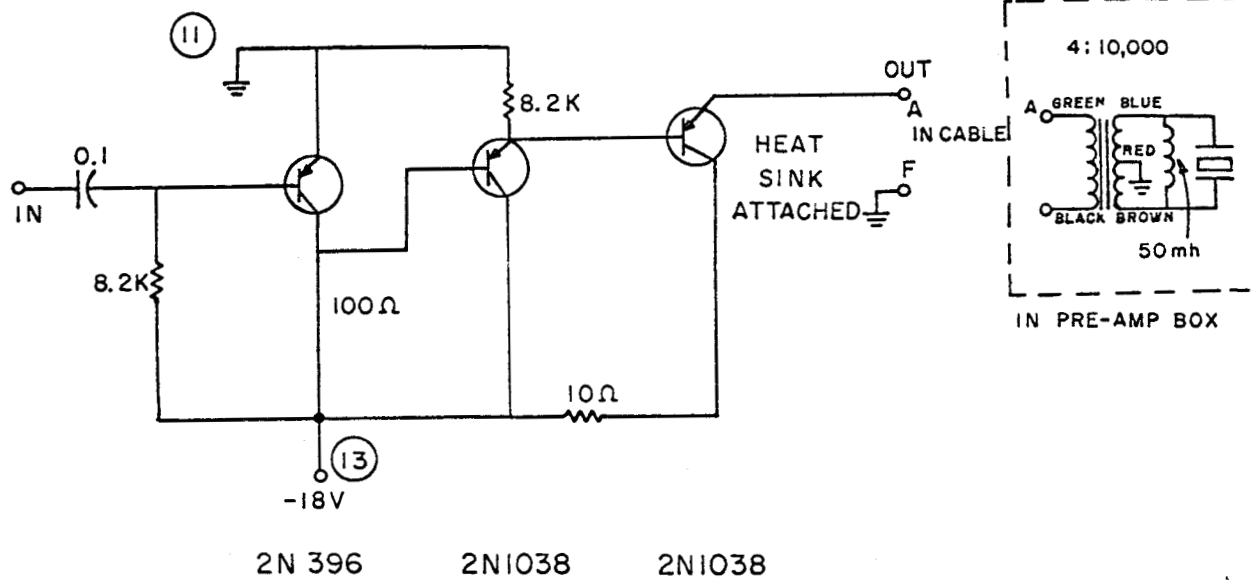


FIGURE 20: RECEIVER



INPUT-OUTPUT PAIRS ARE

[3, 2] [7, 8] [17, 16] [21, 22]

#### CABLE IDENTIFICATION

G - GROUND (SHIELD & POWER)

C & D - SIGNAL FROM PREAMPS TO RECEIVER

B - +22.5V

E - -22.5V

F - GROUND (TRANSMITTER ONLY)

A - PULSE FROM TRANSMITTER TO CIRCUIT BOX

FIGURE 21: TRANSMITTER AMPLIFIER & CABLE IDENTIFICATION

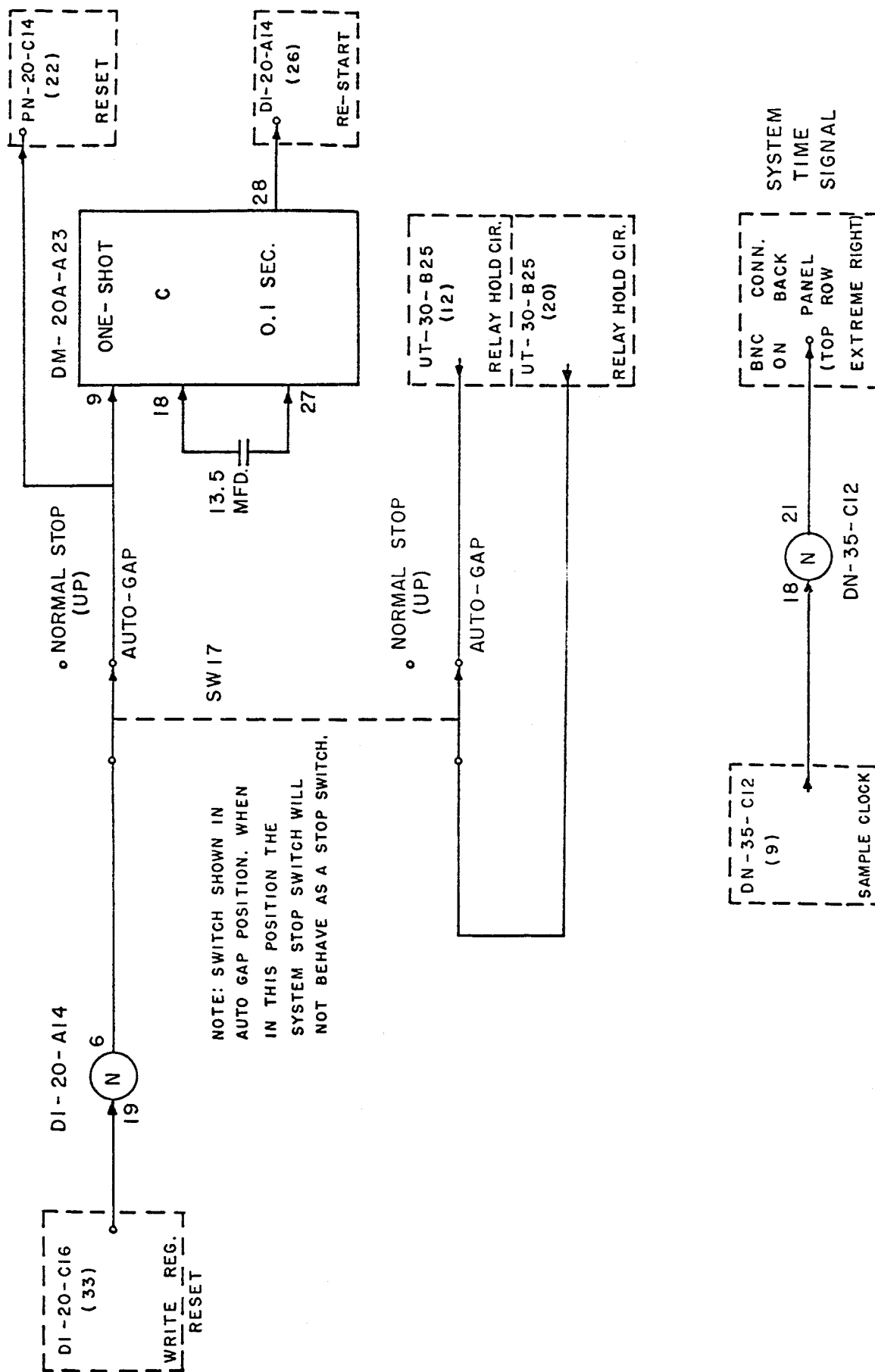


FIGURE 22: AUTOMATIC RECORD GAP CONTROL

The above-listed parameters do not completely satisfy the requirements for the current research nor can they be fed to the A-D channel of the sonic system as discussed previously. Consequently, additional measurements, as noted below, have been incorporated as a part of the sonic system complex.

1. Mean wind speed. The sensor for this parameter is located between the two levels employed for sonic instrumentation (currently 2, 4, 6 or 8 meters) and is a Rett anemometer normally incorporated in the Army AN/GMQ-12 Wind-Measuring Set and is a copy of the Beckman-Whitley 100-hole chopper anemometer. The signal from this transducer is led directly to the housing of the sonic system and fed into an L&N recorder as well as the A-D channel of the sonic readout sequence. (The mean wind speed measurements of Station A, which include all the levels listed above, are made with Beckman-Whitley single-hole chopper anemometers, which supply the same information capability as the Rett device over a four-minute period but are not at the same physical location--by some 20 feet--nor capable of the same resolution for intervals shorter than four minutes.) The necessary amplification and rectification is supplied by the standard translator of the aforementioned AN/GMQ-12 Wind-Measuring Set complement, which is schematically shown in Fig. 23.

2. Vertical temperature gradient. This parameter, normally measured between the two levels of sonic determination, is accomplished through bucked copper-constantan thermocouples housed in wind-aspirated thermoshields, and fed, following necessary amplification and scaling, to an L&N recorder (Speedomax) and simultaneously, as in the case of the mean wind, to the A-D channel. Details of the thermal shelters and amplification are shown in figures 24 and 25.

3. Horizontal and/or vertical wind force differential. This sensor which is normally mounted at either one of the sonic levels,



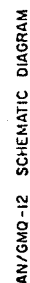
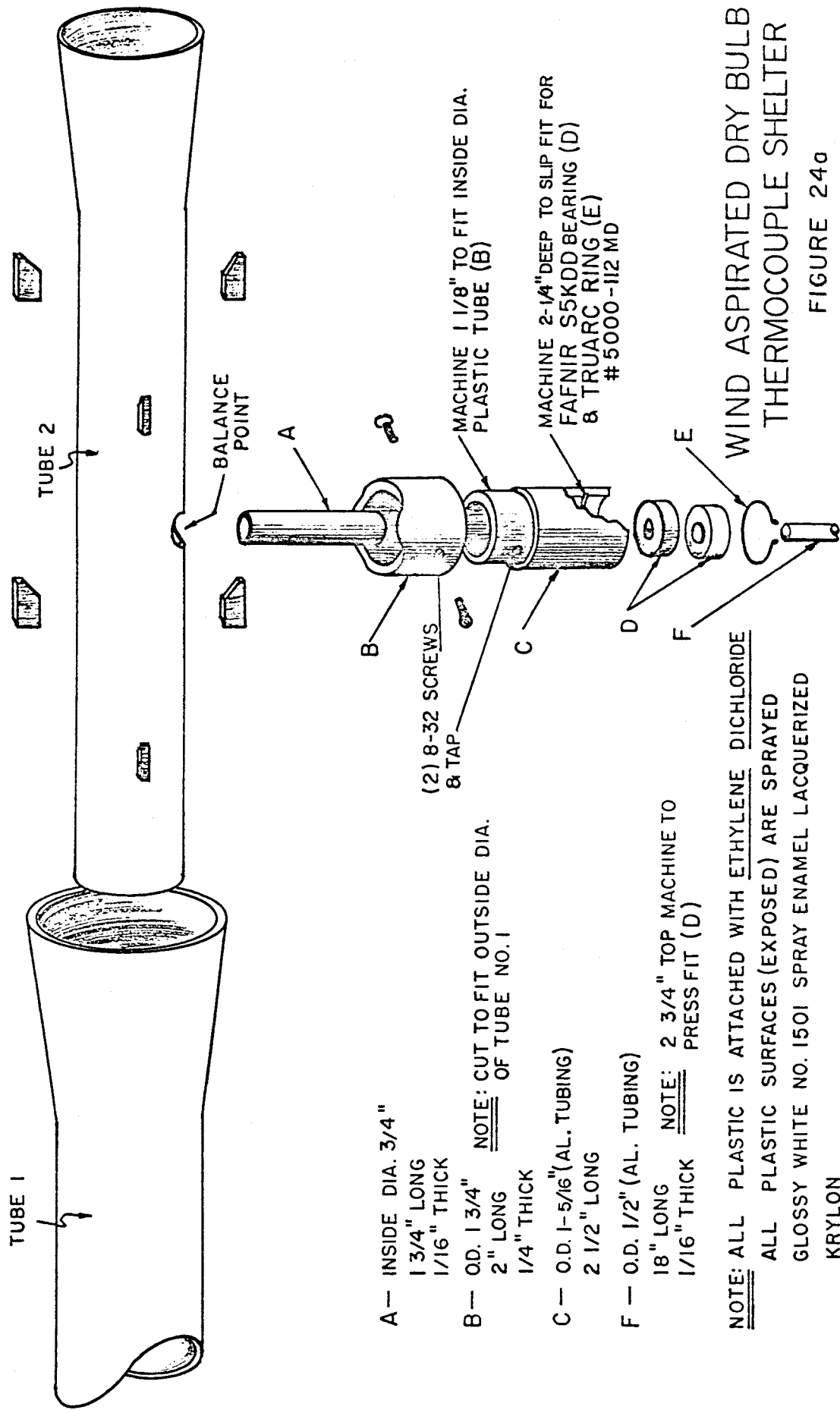


FIGURE 23



A — INSIDE DIA. 3/4" 1 3/4" LONG 1/16" THICK

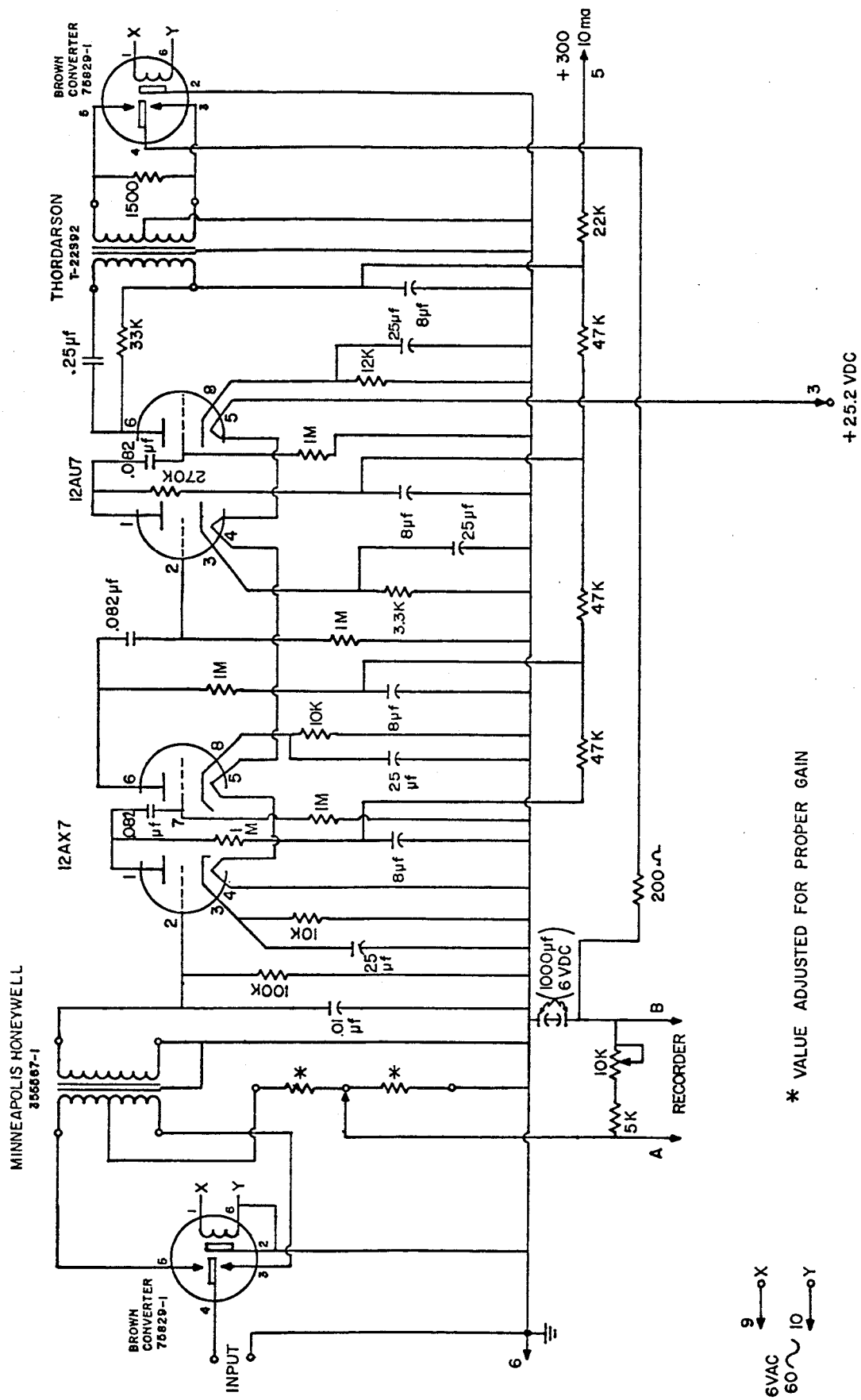
B — OD. 1 3/4" 2" LONG NOTE: CUT TO FIT OUTSIDE DIA. OF TUBE NO. 1 1/4" THICK

C — O.D. 1-5/16" (AL. TUBING) 2 1/2" LONG

F — O.D. 1/2" (AL. TUBING) 18" LONG NOTE: 2 3/4" TOP MACHINE TO 1/16" THICK PRESS FIT (D)

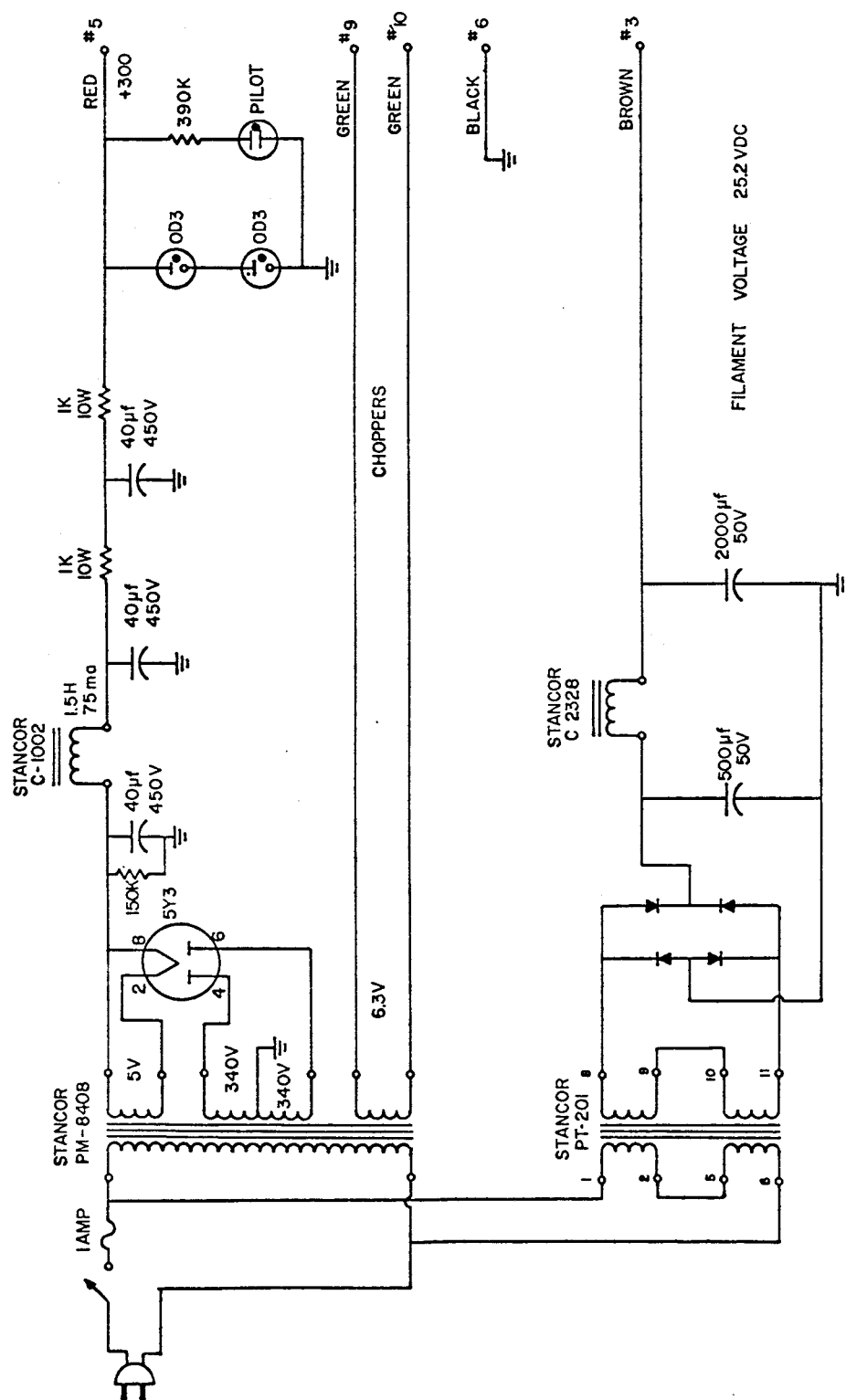
NOTE: ALL PLASTIC IS ATTACHED WITH ETHYLENE DICHLORIDE  
ALL PLASTIC SURFACES (EXPOSED) ARE SPRAYED  
GLOSSY WHITE NO. 1501 SPRAY ENAMEL LACQUERIZED  
KRYLON





TEMPERATURE DIFFERENCE AMPLIFIER

FIGURE 25



**CINCH — JONES**

$\frac{9}{7}$	$\frac{10}{6}$	$\frac{4}{3}$	$\frac{2}{1}$
---------------	----------------	---------------	---------------

POWER SUPPLY FOR TEMPERATURE DIFFERENCE AMPLIFIER

FIGURE 25a

consists of a Solion transducer (manufactured by Texas Research Electronics—now Self-Organizing Systems—of Dallas, Texas) designed to measure  $1/2 C_D u_1^2$  with a frequency-response capability of about one-half cycle per second as an upper limit. The sensor output is fed simultaneously and directly to a TI Servowriter recorder and the A-D sonic channel. To date, however, no success has been realized in obtaining satisfactory operation of this transducer and it is probable though not certain that this device will have to be abandoned. The basic purpose in making such a measurement is to provide a gross back-up check on the sonic outputs and if subsequent efforts should continue to be unsuccessful in operation of this device, its loss will not be significant in the research sense.

4. Flow Corporation Dynamic Wind Force Indicator ("bouncing ball"). This transducer was available to the project for only a short period through sponsor-loan and was intended as a check-device on the sonics. Measurement location was near the surface (due to mass) and at a point some six feet from the sonic mounting pole. However, the operational characteristics and requirements for calibration and recording are such that it did not appear feasible to retain this transducer, and it was returned to the manufacturer through the sponsor's representatives. Following manufacturer's modifications it may be reinstalled and, if so, recording for any two of the three coordinate components will be by a Dual-Channel TI Servowriter, with simultaneous input to the A-D sonic channel.

5. Instantaneous temperature. This system has yet to be designed and will not be so until further investigation as to necessity and feasibility is completed. If, however, such installation is made, two transducers will be employed, one at each of the sonic measuring levels, with recording on the dual-channel Servowriter and simultaneously on the A-D channel of the sonic system.

c. Cedar Hill Wind Speed Comparison Tests

In an attempt to provide answers to long-standing and significant questions concerning the relative capabilities of various wind-measuring devices in both the mean and instantaneous sense, to

evaluate the newly-developed sonic system, and to supply information concerning subsequent wind-measuring installations planned by the sponsor at other sites, the Principal Investigator invited the companies and agencies listed below to participate in a comparative evaluation test to be held at Cedar Hill, Texas on 26-27 July.

<u>Company and Sensor</u>	<u>Representative</u>
Beckman & Whitley, Inc. 993 E. San Carlos Avenue San Carlos, California  Hundred-hole chopper anemometer and comparable wind vane	Fred W. Stang Sales Manager, Meteorology Division Grant Goodwin Engineer
CLIMET 570 San Xavier Avenue Sunnyvale, California  Hundred-hole chopper anemometer and comparable wind vane	H. V. Thompson President E. F. Kingman Vice President
Flow Corporation 205 - 6th Street Cambridge, Massachusetts  Dynamic Wind Force Indicator ("bouncing ball")	Michael Wall President
Gelman Company Ann Arbor, Michigan  Bivane	Did not participate
Iowa State University Ames, Iowa  Sonic anemometer	Dr. Robert M. Stewart, Jr. Professor of Physics Dr. Robert E. Post Associate Professor of Electrical Engineering
Meteorology Research, Inc. 2420 Lake Avenue Altadena, California  Vector Vane (3-component bivane)	Maurice G. Amesbury Senior Electronic Engineer

NASA Marshall Space Flight Center  
Huntsville, Alabama

(Provided Bendix-Friez  
as well as recording  
facilities for all but  
sonic sensors)

Texas A&M University  
College Station, Texas

Mobile micrometeorologi-  
cal measuring station  
(Station A of Dallas  
Tower Network)

James R. Scoggins  
Deputy Chief, Aerophysics and  
Astrophysics Branch,  
Aeroballistics Division  
F. P. Herring  
Computation Division  
George Norwood  
Aerophysics and Astrophysics  
Branch

William H. Clayton  
Director of Micro-  
meteorological Research  
B. Jesse Eckelkamp  
Research Engineer III  
Joe H. Machetta, Capt., USAF  
Graduate Student  
James J. O'Brien  
Graduate Student (NASA Fellow)

In this test the individual sensors were installed and calibrated by the pertinent representatives and recording was done on magnetic tape—digital for the sonic system, and analog for all other instrumentation. Processing of the data from the tapes has not been completed at the close of the reporting period but is being performed by the Contracting Officer's technical representatives in Huntsville, Alabama, and the analyses will be performed by the Principal Investigator.

Unfortunately, initial processing at Huntsville indicates that the sonic data are not correct due to a component malfunction. If such should finally turn out to be the case, the loss of the sonic data though greatly reducing the efficacy of the intended goals of these tests, will not destroy them since the analog information apparently is in good shape and subsequent comparative runs can be made, though not of course with the full instrumentation complex that was available on these specific tests.

Figure 26 shows the schematic layout during the Cedar Hill tests and Fig. 27 is a photograph of the installation. In Fig. 27 it may be seen that the upper sonic level (8 meters) is located on the tower supporting the mean-measuring gear previously cited whereas the lower sonic level is on the pipe mast next to the bouncing ball. The reason for splitting the installation in this fashion was to see the effects



NOTE: \* ARE AT HEIGHT SHOWN  
ALL OTHERS ARE AT 2 METERS = 78 3/4"

MAIN  
TOWER

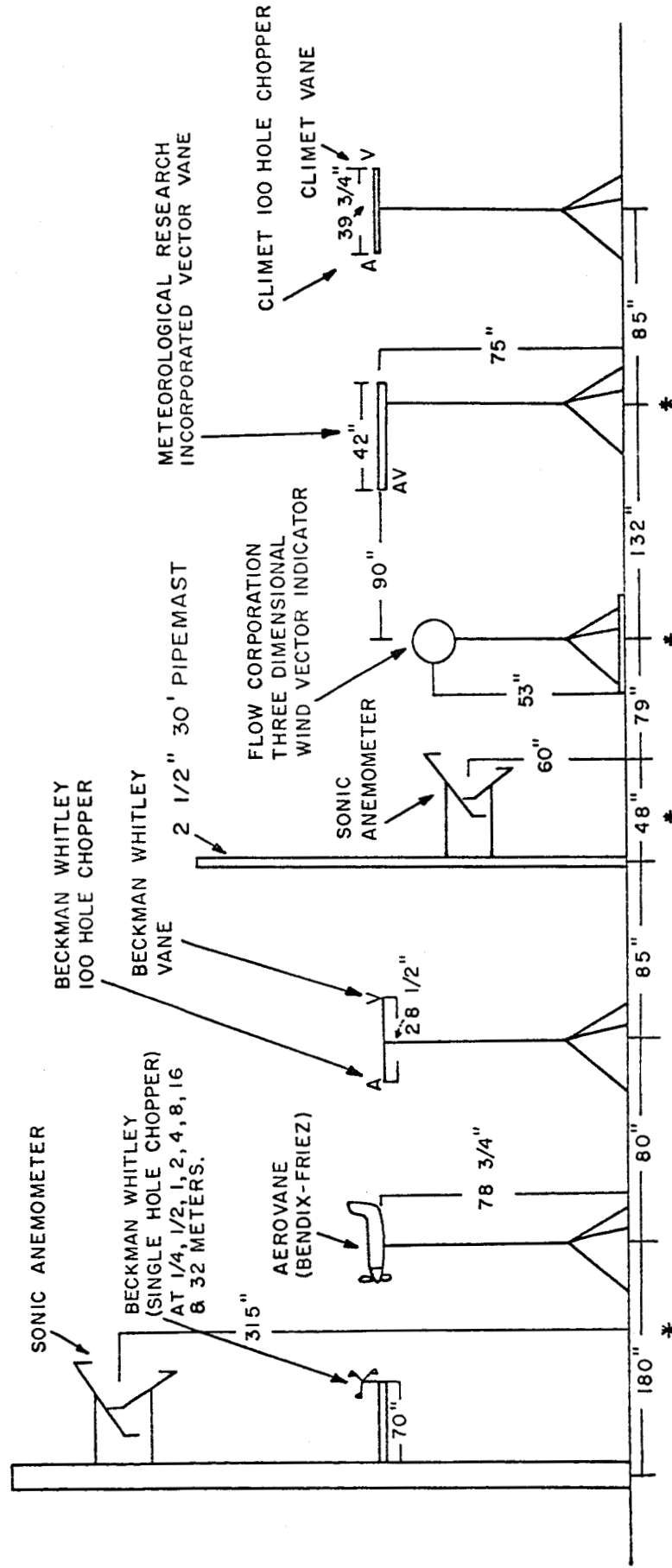


FIGURE 26: CEDAR HILL WIND SENSOR COMPARISON TEST, INSTRUMENT LOCATION

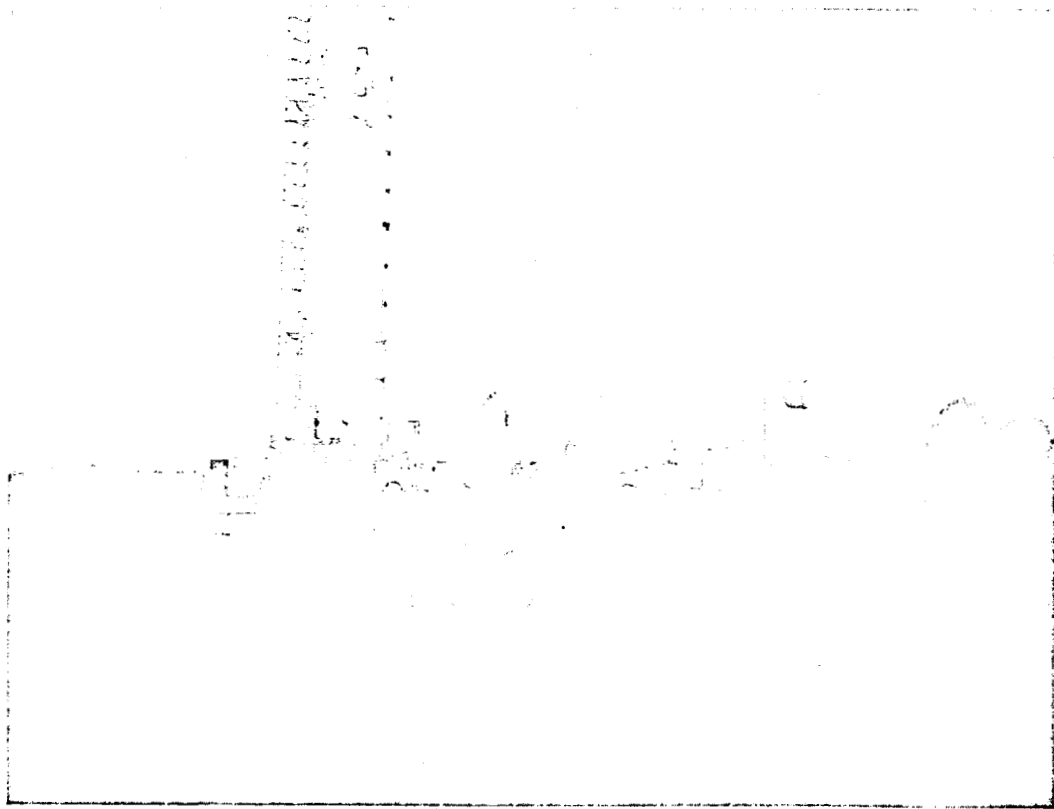


FIGURE 27: INSTRUMENTATION - CEDAR HILL COMPARISON TEST

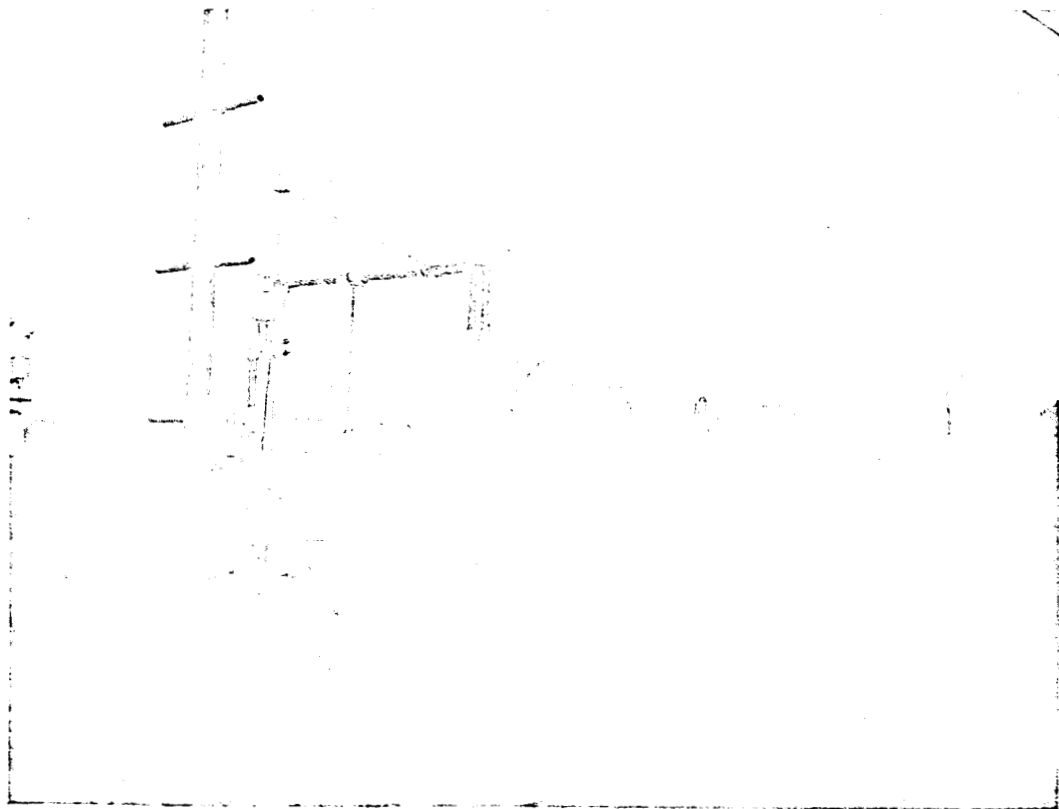


FIGURE 28: SONIC SENSOR INSTALLATION (CLOSE-UP VIEW)

of vibration on the sonics, which for the upper level is primarily caused by tower-vibration, as opposed to the lower level on the pipe mast where vibration is virtually limited to the sonic configuration itself. A close-up view of the lower sonic level is shown in Fig. 28.

Figure 29 shows both sonic levels mounted on the pipe mast at 2 and 8 meters as well as a 1500-foot television tower (KRLD-WFAA) which is usually noted in the literature as the Dallas Tower.

#### IV. Data Processing and Analyses

Inasmuch as a seven-channel magnetic tape is employed (six data channels, one parity), each 18-bit word is divided into three parts of 6-bits, such that a full data sequence consists of 36 bit characters. Thus the first step in the processing of the tape format is translation (by an IBM 709 with IBM 727 tape reader) into five standard IBM words of 36 bits for each complete sequence. In the recording of the 6-bit characters on the data tape, the recording is such that the least significant bit is in track 1 (the track closest to the operator on both the tape recorder and the 727 reader) and the most significant bit is in track 6 with the parity check track (7) being the track furthestest from the operator on both the recorder and the reader. Following proper computer assembly, then, the first half of IBM word 1 is the ident or analog signal and the second half is the cycle counter content; word 2 is the transit times for sonic paths 1 and 2, and so on.

The basic recording cycle employed is 60 seconds long with 59.9 seconds of sequence-recording and a .1-second record gap, with automatic repetition for basic intervals of 5, 10 or 15 minutes. Whatever operational mode may be subsequently employed, this recording pattern probably will be maintained in order to avoid additional computer time for intermediate data tapes, prior to the preparation of a secondary processed data tape on which the following data format is impressed:

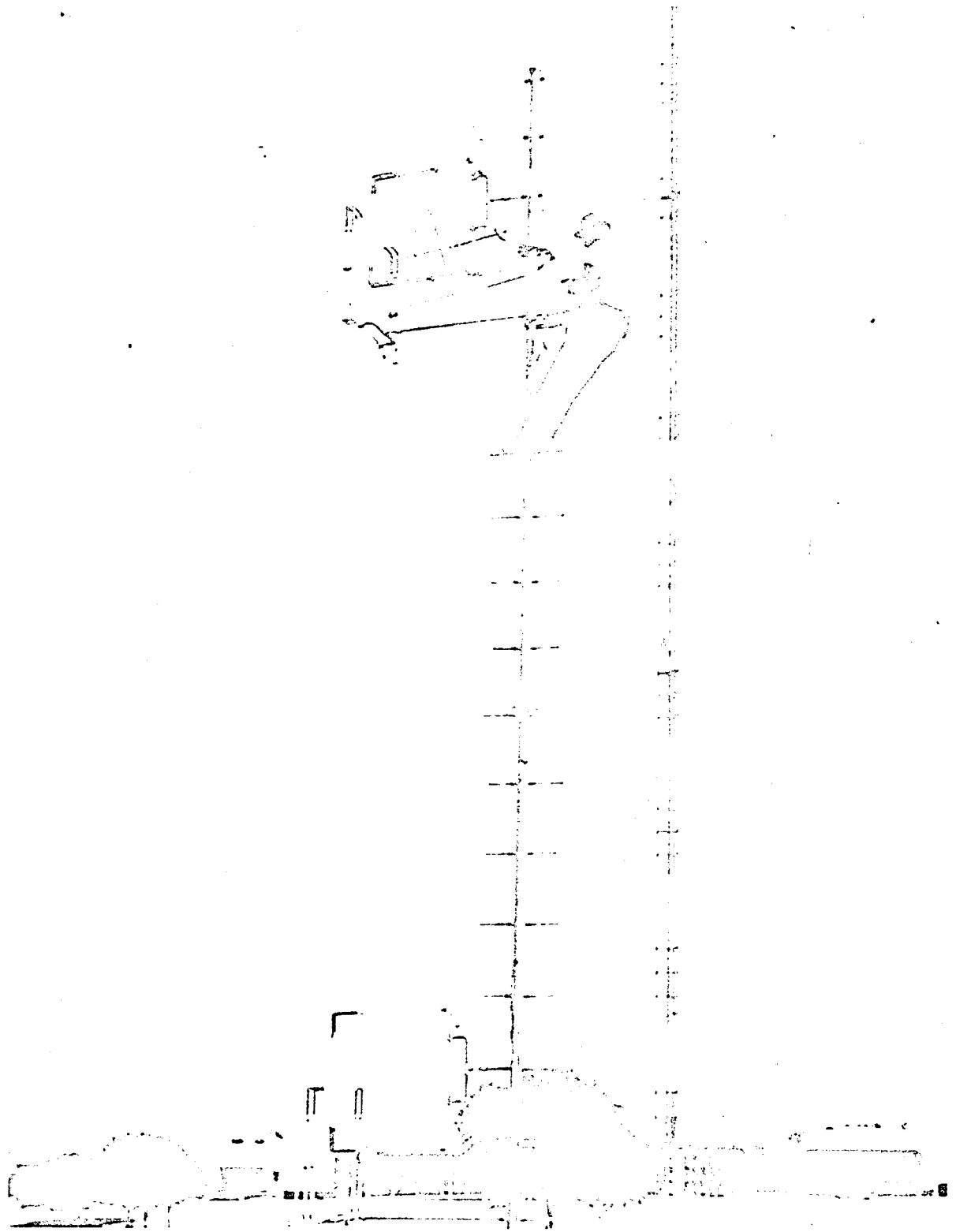


FIGURE 29: SONIC SENSOR INSTALLATION AT STATION A

Word 1	Cycle counter
2	Analog signal or fixed identification
3	$\Delta t_{zU}$
4	$\Sigma t_{zU}$
5	$w_U$
6	$\Delta t_{xU}$
7	$\Sigma t_{xU}$
8	$u_U$
9	$\Delta t_{zL}$
10	$\Sigma t_{zL}$
11	$w_L$
12	$\Delta t_{xL}$
13	$\Sigma t_{xL}$
14	$u_L$

where  $\Delta t_{zU}$  is the difference in transit times in the vertical direction at the upper sonic level,  $\Sigma t_{zU}$  is the sum of transit times for the upper vertical level, etc.

This basic pattern is repeated through a time interval of two seconds, that is, 100 samples, and at the end of each 100 samples, a supplementary data format, shown below, is recorded.

Word 1	$w_U$
2	$u_U$
3	$w_L$
4	$u_L$
5	$w_U'$
6	$u_U'$
7	$w_L'$
8	$u_L'$

and so on through the computation of all the primed quantities, thus yielding 100  $u'$  and  $w'$  values for each sonic level; this is followed by (1)  $\tau_U$ , (2)  $\tau_L$  where the  $\tau$  computations are equal to the averaged products of the corresponding  $u'$  and  $w'$  values times the air density. Following this the basic cycle begins again with the information contained in the second two-second interval, etc.

Presumably, at a later date when the program has been thoroughly checked out on both the A&M and the University of Hawaii computers,\* and necessary installation aids are completed, the individual time difference values will not be recorded on the secondary data tape nor will the time summation values, though the average of the latter with its standard deviation will be recorded at the end of each two-second interval as an additional check on the correct functioning of the sonic system. That is, the summation of  $\tau$  is nothing more than the ratio of twice the head separation divided by the velocity of sound, and this ratio should be constant for the interval considered, irrespective of the signal direction, that is,  $\Sigma \tau_z = \Sigma \tau_x$ .

Until then, the individual values will be retained inasmuch as the variations indicate logic errors or errors in head spacing either fixed or transitory due to vibration.

It is probable, though not yet certain, that the individual  $u'$  and  $w'$  values will be transferred to card format for subsequent spectrum analyses; however, it may later be found to be more feasible to run these analyses simultaneously with the  $\tau$  computation.

At the close of the current reporting period five sonic data runs had been made but only the last one is believed useful in the analytical sense, and the others were primarily intended to correct operational errors and procedures in the measuring system. Sample data from this last run is presented in the next section.

#### V. Experimental Data

The data presented herein are from a single sonic run (#1) made on 20 October 1963 since earlier runs, as previously noted, were primarily system checks rather than data runs.

---

\*The data analyses will be done at the University of Hawaii since the Principal Investigator will be a Visiting Professor of Meteorology and Oceanography during the period 1 September 1963 to 1 September 1964; however, as far as the aims of this contract are concerned this represents nothing more than a transfer of physical location of the Principal Investigator who retains full responsibility for the contract.

This presentation will begin with a description of zero testing which refers to measurement in the absence of any wind and which is accomplished through use of a tube that encloses the total sonic path. The zero velocity tube used to date is a cardboard tube approximately three inches in diameter and some 22 inches long which has been sliced in half, lined with a sound-absorbing material, and hinged on one side so that it may be clamped over a sonic path. The ends of the tube are closed such that no air motion can occur within the tube. As an example of its use, let us assume for the moment that we wish to test the zero condition of the upper vertical path. (For sonic run #1 the upper level was 8 meters, the lower level 2 meters.) The zero tube then is clamped over the four-head configuration comprising this vertical dual path with the ends of the tube closing just behind the sonic transducers. Referring to Fig. 28 it can be seen that as a consequence of the placing of this tube along the vertical path, the horizontal path will be blocked, that is, the transmit signal along the horizontal path, in either direction, will not be received and the resulting sum of transit times will be the total time permitted by the system. In a two-head system, zero testing would not be required except as a verification of the measuring system, but for the four-head system, it is possible to have a zero offset inasmuch as the "up" component and the "down" component paths employ different transducers; thus, the basic requirement for zero velocity under these conditions is exact identity of the head-spacing of the two paths. Since, as was noted in an earlier section, very small head-spacing differences can cause considerable errors (zero offset) this adjustment is rather critical and must be made by physical adjustment of the path lengths with the system in operation, using an oscilloscope as a zero indicator. This is a trial-and-error process which requires the technician making an adjustment to then move off the supporting structure in order that a check may be made since his mere presence will completely mask the adjustment.

Referring to Table 1, <sup>\*</sup> column 1, as indicated, is the cycle count;

---

<sup>\*</sup>In this and all other tables, all sonic time increments are given in microseconds and all sonic velocities in cm/sec.

Table 1. Upper Vertical Zero Test - Run 1A

Cycle	$\Delta T_o$	$\Delta t_{zU}$	$\Sigma t_{zU}$	$w_U$	$\Delta t_{xU}$	$\Sigma t_{xU}$	$u_U$
1	0.005	0.20	3299.40	1.84	0.	3813.60	0.
2	-0.	0.20	3299.40	1.84	0.	3813.60	0.
3	0.007	0.20	3299.40	1.84	0.	3813.60	0.
4	-0.	0.20	3299.00	1.84	0.	3813.60	0.
5	0.008	0.	3299.20	0.	0.	3813.60	0.
6	-0.	0.40	3299.20	3.67	0.	3813.60	0.
7	0.010	0.20	3299.40	1.84	0.	3813.60	0.
8	-0.	0.40	3299.20	3.67	0.	3813.60	0.
9	0.009	0.20	3299.40	1.84	0.	3813.60	0.
10	-0.	0.20	3299.40	1.84	0.	3813.60	0.
11	0.009	0.40	3299.20	3.67	0.	3813.60	0.
12	-0.	0.20	3299.40	1.84	0.	3813.60	0.
13	0.010	0.40	3299.20	3.67	-0.20	3813.80	-1.38
14	-0.	0.20	3299.40	1.84	0.	3813.60	0.
15	0.008	0.20	3299.40	1.84	0.	3813.60	0.
16	-0.	0.20	3299.40	1.84	0.	3813.60	0.
17	0.010	0.40	3299.60	3.67	0.	3813.60	0.
18	-0.	0.40	3299.20	3.67	0.20	3813.80	1.38
19	0.008	0.20	3299.40	1.84	0.	3813.60	0.
20	-0.	0.20	3299.40	1.84	-0.20	3813.80	-1.38
21	0.007	0.	3299.20	0.	0.	3813.60	0.
22	-0.	0.20	3299.40	1.84	0.	3813.60	0.
23	0.008	0.20	3299.40	1.84	0.	3813.60	0.
24	-0.	0.20	3299.40	1.84	0.	3813.60	0.
25	0.007	0.40	3299.20	3.67	0.20	3813.80	1.38
26	-0.	0.40	3299.60	3.67	0.	3813.60	0.
27	0.008	0.60	3299.40	5.51	-0.20	3813.80	-1.38
28	-0.	0.40	3299.60	3.67	0.	3813.60	0.
29	0.007	0.40	3299.60	3.67	0.	3813.60	0.
30	-0.	0.20	3299.40	1.84	0.	3813.60	0.
31	0.006	0.20	3299.40	1.84	0.	3813.60	0.
32	-0.	0.20	3299.00	1.84	0.20	3813.80	1.38
33	0.006	0.	3299.20	0.	0.	3813.60	0.
34	-0.	0.40	3299.20	3.67	-0.20	3813.80	-1.38
35	0.007	0.20	3299.40	1.84	0.	3813.60	0.
36	-0.	0.20	3299.40	1.84	0.	3813.60	0.
37	0.008	0.	3299.60	0.	0.	3813.60	0.
38	-0.	0.20	3299.40	1.84	0.	3813.60	0.
39	0.007	0.20	3299.40	1.84	0.20	3813.80	1.38
40	-0.	0.	3299.60	0.	0.	3813.60	0.
41	0.007	0.20	3299.40	1.84	0.	3813.60	0.
42	-0.	0.20	3299.40	1.84	0.	3813.60	0.
43	0.010	0.20	3299.40	1.84	0.	3813.60	0.
44	-0.	0.	3299.20	0.	0.	3813.60	0.
45	0.009	0.60	3299.40	5.51	0.	3813.60	0.
46	-0.	0.40	3299.20	3.67	0.20	3813.80	1.38
47	0.010	0.20	3299.40	1.84	0.	3813.60	0.
48	-0.	0.20	3299.40	1.84	0.	3813.60	0.
49	0.010	0.	3299.60	0.	0.	3813.60	0.
50	-0.	0.	3299.60	0.	0.	3813.60	0.

AVERAGE  $w(U)$  = 2.131



the second column, headed  $\Delta T_z$ , is the analog channel reading, which in this case is the output of the vertical gradient of temperature (between 2 and 8 meters) with the input terminals of the amplifier shorted; thus the signal recorded in this column is the amplifier offset of the system in  $^{\circ}\text{C}$  which, as can be seen, corresponds to  $.01^{\circ}$  or less. Note that every other reading in this column is zero which indicates that the digital voltmeter was blocked on every other reading in order to permit adequate time for settling. The third column is the difference in transit times along the vertical paths enclosed by the zero tube. As can be seen from a perusal of this column, an adjustment to precisely zero was not made. The fourth column, headed  $\Sigma t_{zu}$  is the summation of transit times along the same vertical paths within the zero tube which for a zero difference in transit times is equal to 3299.20 microseconds. There is no change of values within this column except those due to changes in the difference of transit times, thus indicating that no temperature or vapor change was present during this zero test-period illustrated which covers 50 cycles or one second. This column, as well as the preceding one, clearly demonstrates that the system resolution is  $.2$  microseconds or  $1.84$  cm/sec although the last digit is not significant.

The fifth column gives the vertical component of wind at the upper level in centimeters per second and at the bottom of the table it is shown that the average value of this component is  $2.131$  cm/sec, which represents then the zero offset. However, it should be noted that following this determination the zero tube was removed, and though this was done with great care, the possibility is always present that removal of the tube can cause a slight difference in head-spacing, thus changing the offset value. (The weight of the tube is not significant as tests made with and without weights strapped to the side of the tube showed no changes in offset.)

These details of zero adjustment should accent the fact that head-spacing error is a troublesome practical limitation of sonic anemometry that is easily underestimated when one considers principles of operation alone.

Columns 6, 7 and 8 are the difference in transit times, summation of transit times, and velocity determinations for the upper horizontal level, as indicated. Note here that the difference of transit times are all zero within .2 microsecond, the system resolution, which is as it should be since no signal is being received along this horizontal path inasmuch as the zero tube in the vertical path serves as a physical block. Also, the summation of the transit times, 3813.60 microseconds  $\pm$  .2 microsecond, is independent of head-spacing in this case since no signal was received and the summation indicated here is merely twice the maximum allowable transit time the system permits when operating at 50 cycles per second.

Tables 2, 3 and 4 are identical to Table 1 with the exception that the zero tube has been placed on different sonic paths. For instance, in Table 2 the zero tube is along the upper horizontal path, thus the blocked data columns are 3, 4 and 5, that is, those headed  $\Delta t_{2U}$ ,  $\Sigma t_{2U}$  and  $w_U$ . Note that in these four tables the velocity resolution is 1.38 cm/sec for the blocked paths, 1.87 cm/sec for the zero check of horizontal components and 1.84-1.85 cm/sec for the zero check of vertical components. The difference between 1.84 and 1.87 is due to lack of impractical precision within the system and the difference between blocked and zero path computations is due to the greatly increased effective path length for the blocked case.

Table 5, covering the first two seconds of Run 1F which was a 10-minute run (1431-1441 CST), corresponds to Table 8 except that the latter applies to Run 1L (1825-1835 CST, on the same date). As indicated in these two tables by the columnar headings, the format is the same except for the second column (analog inputs). In Table 5  $\Delta T$  indicates the temperature difference between the sonic levels (lower minus upper) in °C to within  $\pm .03^\circ$  as a maximum limit. In Table 8 the analog input  $V_6$  is the wind speed at 6 meters, in meters per second, as obtained from a modified Rett 100-hole chopper anemometer.

From the preceding section on instrumentation it will be recalled that the first reading in any analog signal column is not valid, and represents simply the contents of the DVM on the first cycle, and the

Table 2. Upper Horizontal Zero Test - Run 1B

Cycle	$\Delta T_o$	$\Delta t_{zU}$	$\Sigma t_{zU}$	$w_U$	$\Delta t_{xU}$	$\Sigma t_{xU}$	$u_U$
1	0.005	-0.20	3813.80	-1.38	0.20	3273.40	1.87
2	-0.	-0.20	3813.80	-1.38	0.40	3273.60	3.73
3	0.007	0.	3813.60	0.	0.20	3273.40	1.87
4	-0.	0.20	3813.80	1.38	0.20	3273.40	1.87
5	0.007	-0.20	3813.80	-1.38	0.	3273.60	0.
6	-0.	0.	3813.60	0.	-0.20	3273.40	-1.87
7	0.007	0.	3813.60	0.	0.	3273.20	0.
8	-0.	0.	3814.00	0.	0.20	3273.40	1.87
9	0.007	0.	3813.60	0.	0.20	3273.40	1.87
10	-0.	0.	3813.60	0.	0.20	3273.40	1.87
11	0.007	-0.20	3813.80	-1.38	0.20	3273.40	1.87
12	-0.	0.	3813.60	0.	0.20	3273.40	1.87
13	0.007	0.	3813.60	0.	0.20	3273.40	1.87
14	-0.	0.20	3813.80	1.38	0.	3273.20	0.
15	0.007	-0.20	3813.80	-1.38	0.20	3273.40	1.87
16	-0.	0.	3813.60	0.	-0.20	3273.40	-1.87
17	0.007	0.20	3813.80	1.38	0.	3273.20	0.
18	-0.	0.	3814.00	0.	0.	3273.20	0.
19	0.006	0.	3813.60	0.	0.	3273.60	0.
20	-0.	0.	3813.60	0.	0.	3273.20	0.
21	0.007	-0.20	3813.80	-1.38	-0.20	3273.40	-1.87
22	-0.	0.	3813.60	0.	-0.20	3273.40	-1.87
23	0.006	0.	3813.60	0.	-0.20	3273.40	-1.87
24	-0.	0.20	3813.80	1.38	-0.20	3273.40	-1.87
25	0.007	-0.20	3813.80	-1.38	-0.20	3273.40	-1.87
26	-0.	0.	3813.60	0.	-0.20	3273.40	-1.87
27	0.007	0.	3813.60	0.	0.20	3273.00	1.87
28	-0.	0.	3814.00	0.	0.20	3273.40	1.87
29	0.006	0.	3813.60	0.	0.	3273.20	0.
30	-0.	0.	3813.60	0.	0.40	3273.20	3.73
31	0.007	-0.20	3813.80	-1.38	0.60	3273.40	5.60
32	-0.	0.	3813.60	0.	0.60	3273.40	5.60
33	0.007	0.	3813.60	0.	0.60	3273.00	5.60
34	-0.	0.	3814.00	0.	0.40	3273.20	3.73
35	0.007	0.	3813.60	0.	0.20	3273.40	1.87
36	-0.	0.	3813.60	0.	-0.20	3273.40	-1.87
37	0.006	0.	3813.60	0.	0.	3273.20	0.
38	-0.	-0.20	3813.80	-1.38	0.20	3273.40	1.87
39	0.007	0.	3813.60	0.	-0.20	3273.40	-1.87
40	-0.	0.20	3813.80	1.38	0.	3273.20	0.
41	0.006	-0.20	3813.80	-1.38	-0.20	3273.40	-1.87
42	-0.	0.	3813.60	0.	-0.20	3273.40	-1.87
43	0.007	0.	3813.60	0.	0.	3273.20	0.
44	-0.	0.	3814.00	0.	-0.20	3273.40	-1.87
45	0.007	0.	3813.60	0.	-0.40	3273.60	-3.73
46	-0.	0.	3813.60	0.	-0.20	3273.40	-1.87
47	0.007	0.	3813.60	0.	-0.20	3273.40	-1.87
48	-0.	-0.20	3813.80	-1.38	-0.20	3273.40	-1.87
49	0.007	0.	3813.60	0.	-0.20	3273.40	-1.87
50	-0.	0.20	3813.80	1.38	0.	3273.20	0.

AVERAGE U(U) = 0.373

Table 3. Lower Vertical Zero Test - Run 1C

Cycle	$\Delta T_o$	$\Delta t_{zL}$	$\Sigma t_{zL}$	$w_L$	$\Delta t_{xL}$	$\Sigma t_{xL}$	$u_L$
1	0.010	0.20	3285.00	1.85	0.20	3813.80	1.38
2	-0.	0.20	3285.00	1.85	0.	3814.00	0.
3	0.013	0.	3285.20	0.	-0.20	3813.80	-1.38
4	-0.	0.	3285.20	0.	0.	3813.60	0.
5	0.012	0.	3285.20	0.	0.	3813.60	0.
6	-0.	0.20	3285.00	1.85	0.20	3813.80	1.38
7	0.013	0.20	3285.00	1.85	0.	3814.00	0.
8	-0.	0.20	3285.00	1.85	0.	3813.60	0.
9	0.012	0.20	3285.00	1.85	0.	3813.60	0.
10	-0.	0.40	3285.20	3.71	0.	3813.60	0.
11	0.012	0.40	3284.80	3.71	0.	3814.00	0.
12	-0.	0.40	3284.80	3.71	-0.20	3813.80	-1.38
13	0.013	0.	3285.20	0.	0.	3813.60	0.
14	-0.	0.	3285.20	0.	0.	3813.60	0.
15	0.012	0.	3285.20	0.	0.20	3813.80	1.38
16	-0.	0.40	3284.80	3.71	0.	3814.00	0.
17	0.012	0.20	3285.00	1.85	-0.20	3813.80	-1.38
18	-0.	0.20	3285.00	1.85	0.	3813.60	0.
19	0.012	0.20	3285.00	1.85	0.	3813.60	0.
20	-0.	0.20	3285.00	1.85	0.20	3813.80	1.38
21	0.012	0.40	3284.80	3.71	0.	3814.00	0.
22	-0.	0.20	3285.00	1.85	-0.20	3813.80	-1.38
23	0.012	0.	3285.20	0.	0.	3813.60	0.
24	-0.	0.	3285.20	0.	0.	3813.60	0.
25	0.014	-0.20	3285.00	-1.85	0.20	3813.80	1.38
26	-0.	0.20	3285.00	1.85	0.	3814.00	0.
27	0.013	0.40	3284.80	3.71	-0.20	3813.80	-1.38
28	-0.	0.60	3285.00	5.56	0.	3813.60	0.
29	0.012	0.20	3285.00	1.85	0.	3813.60	0.
30	-0.	0.	3284.80	0.	0.20	3813.80	1.38
31	0.012	0.40	3284.80	3.71	0.	3814.00	0.
32	-0.	0.	3284.80	0.	-0.20	3813.80	-1.38
33	0.012	-0.20	3285.00	-1.85	0.	3813.60	0.
34	-0.	0.	3285.20	0.	0.	3813.60	0.
35	0.012	-0.20	3285.00	-1.85	0.20	3813.80	1.38
36	-0.	0.	3284.80	0.	0.	3814.00	0.
37	0.012	0.40	3284.80	3.71	-0.20	3813.80	-1.38
38	-0.	0.40	3284.80	3.71	0.	3813.60	0.
39	0.011	0.20	3285.00	1.85	0.	3813.60	0.
40	-0.	0.	3284.80	0.	0.20	3813.80	1.38
41	0.011	0.20	3285.00	1.85	0.	3814.00	0.
42	-0.	0.	3284.80	0.	-0.20	3813.80	-1.38
43	0.012	0.20	3285.00	1.85	0.	3813.60	0.
44	-0.	0.20	3285.00	1.85	0.	3813.60	0.
45	0.011	0.	3284.80	0.	0.20	3813.80	1.38
46	-0.	0.40	3284.80	3.71	0.	3814.00	0.
47	0.012	0.40	3284.80	3.71	-0.20	3813.80	-1.38
48	-0.	0.40	3284.80	3.71	0.	3813.60	0.
49	0.012	0.40	3285.20	3.71	0.	3813.60	0.
50	-0.	0.20	3285.00	1.85	0.20	3813.80	1.38

AVERAGE  $w(L)$  = 1.631

Table 4. Lower Horizontal Zero Test - Run 1E

Cycle	$\Delta T_o$	$\Delta t_{zL}$	$\Sigma t_{zL}$	$w_L$	$\Delta t_{xL}$	$\Sigma t_{xL}$	$u_L$
1	0.011	0.	3813.60	0.	-0.60	3271.80	-5.61
2	-0.	0.20	3813.80	1.38	-0.60	3271.80	-5.61
3	0.010	0.20	3813.80	1.38	-0.40	3271.60	-3.74
4	-0.	0.	3814.00	0.	-0.40	3271.60	-3.74
5	0.010	0.	3814.00	0.	-0.20	3271.80	-1.87
6	-0.	0.	3814.00	0.	0.	3271.60	0.
7	0.010	-0.20	3813.80	-1.38	-0.20	3271.80	-1.87
8	-0.	-0.20	3813.80	-1.38	-0.20	3271.80	-1.87
9	0.010	-0.20	3813.80	-1.38	-0.20	3271.80	-1.87
10	-0.	0.	3813.60	0.	-0.60	3271.80	-5.61
11	0.010	0.	3813.60	0.	-0.60	3271.80	-5.61
12	-0.	0.	3813.60	0.	-0.80	3271.60	-7.47
13	0.010	0.	3813.60	0.	-0.60	3271.80	-5.61
14	-0.	0.20	3813.80	1.38	-0.40	3271.60	-3.74
15	0.010	0.20	3813.80	1.38	-0.40	3271.60	-3.74
16	-0.	0.	3814.00	0.	-0.40	3271.60	-3.74
17	0.010	0.	3814.00	0.	-0.40	3271.60	-3.74
18	-0.	0.	3814.00	0.	-0.20	3271.40	-1.87
19	0.010	-0.20	3813.80	-1.38	-0.20	3271.40	-1.87
20	-0.	-0.20	3813.80	-1.38	-0.20	3271.40	-1.87
21	0.010	0.	3813.60	0.	-0.40	3271.60	-3.74
22	-0.	0.	3813.60	0.	-0.40	3271.60	-3.74
23	0.010	0.	3813.60	0.	-0.60	3271.40	-5.61
24	-0.	0.	3813.60	0.	-0.60	3271.40	-5.61
25	0.010	0.20	3813.80	1.38	-0.20	3271.40	-1.87
26	-0.	0.20	3813.80	1.38	-0.20	3271.40	-1.87
27	0.010	0.	3814.00	0.	-0.20	3271.40	-1.87
28	-0.	0.	3814.00	0.	-0.20	3271.40	-1.87
29	0.010	0.	3814.00	0.	-0.20	3271.40	-1.87
30	-0.	-0.20	3813.80	-1.38	-0.20	3271.40	-1.87
31	0.010	-0.20	3813.80	-1.38	-0.20	3271.40	-1.87
32	-0.	0.	3813.60	0.	-0.20	3271.40	-1.87
33	0.010	0.	3813.60	0.	-0.20	3271.40	-1.87
34	-0.	0.	3813.60	0.	-0.20	3271.40	-1.87
35	0.010	0.	3813.60	0.	-0.20	3271.40	-1.87
36	-0.	0.20	3813.80	1.38	-0.40	3271.60	-3.74
37	0.010	0.20	3813.80	1.38	-0.20	3271.40	-1.87
38	-0.	0.	3814.00	0.	-0.20	3271.40	-1.87
39	0.010	0.	3814.00	0.	-0.20	3271.40	-1.87
40	-0.	0.	3814.00	0.	-0.20	3271.40	-1.87
41	0.010	-0.20	3813.80	-1.38	-0.20	3271.40	-1.87
42	-0.	-0.20	3813.80	-1.38	-0.40	3271.60	-3.74
43	0.010	-0.20	3813.80	-1.38	-0.20	3271.80	-1.87
44	-0.	0.	3813.60	0.	-0.20	3271.80	-1.87
45	0.010	0.	3813.60	0.	-0.20	3271.80	-1.87
46	-0.	0.	3813.60	0.	-0.40	3271.60	-3.74
47	0.010	0.	3813.60	0.	-0.40	3271.60	-3.74
48	-0.	0.20	3813.80	1.38	-0.20	3271.40	-1.87
49	0.010	0.20	3813.80	1.38	-0.20	3271.40	-1.87
50	-0.	0.	3814.00	0.	-0.20	3271.80	-1.87

AVERAGE  $U(L) = -2.915$

Table 5. First Two Seconds of Raw Data - Run 1F

Cycle	$\Delta T$	$\Delta T_{zu}$	$\Gamma_{t_{zu}}$	$w_u$	$\Delta T_{xu}$	$\Gamma_{t_{xu}}$	$w_u$	$\Delta T_{zL}$	$\Gamma_{t_{zL}}$	$w_L$	$\Delta T_{xL}$	$\Gamma_{t_{xL}}$	$w_L$
1	0.89	-4.40	3297.60	-40.46	54.60	3272.60	509.81	1.00	3295.00	9.21	50.60	3282.20	469.70
2	-0.	-3.60	3297.20	-33.11	53.00	3271.80	495.11	0.60	3295.40	5.53	50.60	3282.20	469.70
3	0.50	-2.20	3297.40	-20.23	53.60	3272.80	500.41	1.20	3295.20	11.05	49.80	3282.20	462.27
4	-0.	-3.40	3297.80	-31.26	52.60	3272.60	491.13	1.60	3295.20	14.74	49.20	3281.20	456.98
5	0.49	-2.00	3296.80	-18.40	51.80	3272.60	483.66	3.40	3295.00	31.32	49.60	3281.20	460.70
6	-0.	-1.40	3297.40	-12.88	50.60	3272.60	472.46	2.40	3295.20	22.10	50.80	3281.20	471.84
7	0.49	-1.60	3297.20	-14.72	51.40	3272.20	480.05	0.20	3295.40	1.84	51.60	3281.20	479.27
8	-0.	-4.40	3296.40	-40.49	52.00	3272.40	485.59	-0.40	3296.00	-3.68	52.00	3281.20	482.99
9	0.50	-4.20	3296.60	-38.65	51.80	3272.20	483.78	0.80	3295.20	7.37	52.00	3281.20	482.99
10	-0.	-3.60	3296.80	-33.12	53.00	3272.60	494.87	3.40	3294.60	31.32	51.60	3281.20	479.27
11	0.49	-3.60	3296.40	-33.13	54.00	3272.80	504.14	2.20	3295.00	20.26	51.20	3281.20	475.56
12	-0.	-5.60	3297.20	-51.51	54.40	3272.80	507.88	1.80	3295.40	16.58	50.40	3281.20	468.13
13	0.45	-7.60	3297.20	-69.91	54.60	3273.00	509.68	3.20	3295.60	29.46	49.40	3281.40	458.78
14	-0.	-6.80	3297.60	-62.53	53.80	3273.00	502.22	3.80	3295.00	35.00	48.20	3282.20	447.42
15	0.47	-7.20	3296.80	-66.24	52.60	3273.00	491.01	1.80	3295.00	16.58	48.40	3280.80	449.66
16	-0.	-8.40	3296.40	-77.30	51.80	3273.00	483.55	1.00	3295.00	9.21	49.40	3281.00	458.90
17	0.47	-7.00	3296.60	-64.41	50.60	3273.00	472.34	0.40	3295.20	3.68	51.40	3281.40	477.36
18	-0.	-7.00	3296.20	-64.43	50.60	3273.00	472.34	-1.20	3295.60	-11.05	53.60	3282.00	497.61
19	0.45	-6.40	3297.20	-58.87	51.40	3273.00	479.81	0.	3295.60	0.	54.80	3282.00	508.75
20	-0.	-7.60	3296.40	-69.94	51.40	3273.00	479.81	-0.60	3295.80	-5.52	54.40	3282.00	505.34
21	0.45	-7.00	3296.60	-64.41	51.80	3273.00	483.55	-0.60	3295.80	-5.52	53.20	3282.00	493.89
22	-0.	-6.80	3296.40	-62.58	50.60	3273.00	472.34	1.00	3295.40	9.21	52.40	3282.00	486.47
23	0.45	-5.40	3296.60	-49.69	50.60	3273.00	472.34	-0.40	3295.60	-3.68	52.40	3282.00	486.47
24	-0.	-6.00	3297.20	-55.19	50.20	3273.00	468.61	-0.20	3295.40	-1.84	52.80	3282.00	490.18
25	0.44	-7.20	3296.00	-66.28	49.80	3273.00	464.88	-2.60	3296.20	-23.93	52.80	3282.00	490.18
26	-0.	-6.80	3296.00	-62.59	50.60	3273.80	472.11	-2.00	3295.20	-18.42	52.00	3282.00	482.75
27	0.44	-7.20	3296.00	-66.28	50.00	3273.60	466.57	-1.40	3295.40	-12.89	51.20	3282.00	475.33
28	-0.	-6.80	3295.60	-62.61	49.80	3273.80	464.65	-3.00	3295.40	-27.63	50.80	3282.40	471.50
29	0.41	-6.60	3295.80	-60.76	49.40	3274.20	460.80	-1.60	3295.20	-14.74	51.00	3282.20	473.41
30	-0.	-5.60	3296.00	-51.55	50.00	3273.60	466.57	-1.60	3295.20	-14.74	51.00	3282.60	473.30
31	0.43	-6.00	3295.60	-55.24	50.20	3273.80	468.38	0.40	3295.20	3.68	49.80	3283.00	462.05
32	-0.	-6.00	3295.60	-55.24	50.00	3274.00	466.46	-1.00	3295.80	-9.21	50.40	3282.80	467.67
33	0.40	-6.40	3296.00	-58.91	50.40	3274.00	470.19	-1.20	3295.60	-11.05	49.60	3282.40	460.36
34	-0.	-6.60	3296.20	-60.75	49.20	3274.00	458.99	-1.20	3296.00	-11.05	49.60	3282.40	460.36
35	0.42	-6.60	3295.80	-60.76	50.00	3274.00	466.46	-2.20	3295.40	-20.26	48.80	3282.00	453.05
36	-0.	-7.60	3295.60	-69.98	49.20	3274.00	458.99	-0.80	3295.60	-7.37	48.60	3281.80	451.24
37	0.42	-8.00	3295.60	-73.66	50.40	3274.00	470.19	0.	3295.20	0.	48.80	3282.40	452.94
38	-0.	-8.20	3297.00	-75.44	51.60	3274.00	481.38	-0.60	3295.80	-5.52	48.20	3282.20	447.42
39	0.40	-9.80	3296.60	-90.18	52.00	3273.60	485.24	-2.00	3296.00	-18.41	48.60	3282.60	451.02
40	-0.	-9.60	3296.80	-88.33	52.00	3273.60	485.24	-1.00	3295.80	-9.21	49.40	3281.80	458.67
41	0.40	-8.80	3296.80	-80.96	51.60	3273.60	481.50	-0.80	3295.80	-7.36	49.60	3282.00	460.47
42	-0.	-8.80	3296.80	-80.96	52.40	3273.60	488.97	0.	3295.20	0.	50.00	3282.80	463.96
43	0.40	-7.00	3296.20	-64.43	53.40	3273.80	498.24	-0.40	3295.20	-3.68	49.80	3282.60	462.16
44	-0.	-7.60	3297.20	-69.91	53.00	3273.40	494.63	-2.20	3295.40	-20.26	50.60	3282.60	469.59
45	0.41	-7.40	3296.60	-68.09	51.80	3273.40	483.43	-1.80	3295.60	-18.41	49.80	3282.20	462.27
46	-0.	-10.00	3296.80	-92.01	50.40	3272.80	470.53	-1.80	3295.40	-16.58	49.20	3282.40	456.65
47	0.42	-9.80	3297.00	-90.15	50.40	3273.60	470.30	-1.00	3295.40	-9.21	49.40	3282.60	458.45
48	-0.	-9.60	3297.20	-88.30	51.20	3273.60	477.77	-1.60	3295.60	-14.73	49.60	3282.00	460.47
49	0.40	-10.60	3296.60	-97.54	51.60	3273.60	481.50	-1.80	3295.00	-16.58	49.00	3282.60	454.74
50	-0.	-10.20	3296.20	-93.88	51.60	3273.60	481.50	-1.40	3295.40	-12.89	48.20	3282.20	447.42

Table 5. First Two Seconds of Raw Data - Run 1F (Continued)

Cycle	$\Delta T$	$\Delta t_{zU}$	$\Sigma t_{zU}$	$v_U$	$\Delta t_{xU}$	$\Sigma t_{xU}$	$u_U$	$\Delta t_{zL}$	$\Sigma t_{zL}$	$v_L$	$\Delta t_{xL}$	$\Sigma t_{xL}$	$u_L$
51	0.40	-10.00	3296.40	-92.03	51.60	3273.60	481.50	-1.80	3294.60	-16.58	47.60	3282.40	441.80
52	-0.	-9.00	3295.80	-82.86	50.80	3273.60	474.04	-1.80	3295.00	-16.58	46.00	3281.20	427.26
53	0.40	-8.20	3296.20	-75.47	51.20	3273.60	477.77	-0.80	3294.80	-7.37	45.80	3281.80	425.25
54	-0.	-10.40	3296.40	-95.71	50.80	3273.60	474.04	0.40	3294.80	3.68	45.80	3281.80	425.25
55	0.39	-11.00	3296.20	-101.24	50.00	3273.60	466.57	0.20	3295.40	1.84	46.20	3282.20	428.86
56	-0.	-9.80	3296.60	-90.18	49.40	3273.80	460.92	-1.00	3295.40	-9.21	46.20	3282.60	432.46
57	0.39	-11.00	3296.20	-101.24	47.80	3273.80	445.99	-1.20	3295.60	-11.05	48.20	3282.20	447.42
58	-0.	-9.20	3296.00	-84.59	47.20	3274.00	440.34	-1.80	3295.40	-16.58	48.20	3282.20	447.42
59	0.37	-10.20	3295.80	-93.90	46.00	3274.00	429.14	-1.80	3295.40	-16.58	48.40	3281.60	449.44
60	-0.	-9.60	3296.00	-88.37	45.80	3273.80	427.33	-1.00	3295.40	-9.21	49.20	3282.80	456.54
61	0.40	-10.00	3296.00	-92.05	45.40	3274.20	423.49	-0.40	3295.20	-3.68	49.60	3282.00	460.47
62	-0.	-9.20	3295.60	-84.71	44.60	3273.80	416.13	-2.00	3295.60	-18.41	51.00	3281.80	473.53
63	0.39	-8.00	3295.20	-73.68	42.80	3273.20	399.48	-2.00	3295.20	-18.42	50.60	3281.80	469.88
64	-0.	-7.20	3295.20	-66.31	42.60	3273.00	397.67	-1.80	3295.40	-16.58	49.40	3281.40	458.74
65	0.38	-6.60	3295.40	-60.78	42.60	3273.40	397.57	-0.20	3295.00	-1.84	48.60	3281.80	451.24
66	-0.	-8.00	3295.20	-73.68	42.60	3273.40	397.57	-4.60	3295.40	-42.36	48.80	3282.00	453.05
67	0.39	-9.00	3295.40	-82.88	43.00	3273.80	401.20	-4.00	3294.80	-36.85	49.00	3282.20	454.85
68	-0.	-10.40	3295.60	-95.76	42.80	3273.20	399.48	-2.40	3295.20	-22.10	49.20	3281.60	456.87
69	0.36	-13.20	3296.00	-121.51	43.60	3272.80	407.05	-2.00	3294.80	-18.42	49.00	3281.40	455.07
70	-0.	-12.60	3295.00	-116.05	43.80	3272.60	408.97	-3.80	3294.60	-35.01	47.80	3281.40	443.93
71	0.38	-12.40	3294.80	-114.23	44.40	3272.40	414.62	-3.60	3295.20	-33.15	49.00	3281.40	455.07
72	-0.	-12.60	3296.20	-115.97	45.00	3273.40	419.97	-2.20	3295.00	-20.26	49.00	3281.80	454.96
73	0.36	-11.40	3295.40	-104.98	44.00	3272.80	410.78	-1.80	3295.40	-16.58	47.00	3281.80	436.39
74	-0.	-12.00	3295.60	-110.49	44.80	3273.20	418.15	-2.00	3294.80	-18.42	47.40	3282.20	440.00
75	0.37	-10.80	3295.60	-99.44	44.40	3273.20	414.42	-3.60	3295.20	-33.15	47.80	3282.60	443.60
76	-0.	-10.20	3295.80	-93.90	43.20	3272.80	403.32	-3.00	3295.00	-27.63	48.00	3282.40	445.51
77	0.37	-8.60	3295.80	-79.17	42.20	3272.60	394.03	-1.60	3295.20	-14.74	48.00	3282.00	445.62
78	-0.	-8.80	3295.60	-81.02	41.20	3272.40	384.74	-1.00	3294.60	-9.21	48.40	3282.00	449.33
79	0.35	-12.00	3295.60	-110.49	41.20	3272.00	384.83	-1.00	3295.40	-9.21	47.00	3281.80	436.39
80	-0.	-14.80	3295.20	-136.30	41.80	3271.80	390.48	-1.40	3294.60	-12.90	46.40	3282.00	430.77
81	0.38	-13.60	3295.60	-125.22	42.20	3271.80	394.22	-2.60	3294.20	-23.96	45.00	3282.20	417.72
82	-0.	-13.20	3295.20	-121.57	42.60	3272.20	397.86	-1.40	3294.60	-12.90	44.60	3281.80	414.11
83	0.35	-12.80	3296.00	-117.82	43.60	3272.00	407.25	-0.40	3294.40	-3.69	45.00	3282.20	417.72
84	-0.	-12.40	3294.80	-114.23	44.00	3272.40	410.88	0.60	3294.60	5.53	45.00	3281.80	417.82
85	0.35	-12.80	3296.00	-117.82	44.20	3271.80	412.90	-0.20	3295.00	-1.84	44.00	3281.60	408.58
86	-0.	-14.80	3295.60	-136.27	44.40	3271.60	414.82	-0.80	3294.80	-7.37	42.60	3282.20	395.44
87	0.36	-16.20	3295.40	-149.18	46.00	3272.40	429.56	0.	3294.40	0.	41.80	3281.80	388.11
88	-0.	-14.80	3295.60	-136.27	46.80	3271.60	437.25	-1.40	3294.60	-12.90	42.80	3282.00	397.34
89	0.34	-13.40	3296.20	-123.33	47.20	3272.00	440.87	-2.40	3294.80	-22.11	43.20	3281.60	401.16
90	-0.	-12.60	3295.80	-116.00	47.60	3271.60	444.72	-1.60	3294.80	-14.74	43.20	3281.60	401.16
91	0.37	-11.20	3296.00	-103.10	48.60	3272.20	453.90	-2.20	3294.60	-20.27	43.00	3281.80	399.25
92	-0.	-12.00	3296.40	-110.43	49.60	3271.60	463.41	-3.60	3294.80	-33.16	42.60	3281.80	395.54
93	0.35	-12.60	3297.00	-115.91	50.00	3271.60	467.14	-4.20	3295.00	-38.68	42.00	3281.60	390.01
94	-0.	-13.60	3296.00	-125.19	48.00	3271.20	448.57	-3.40	3294.60	-31.32	41.80	3281.80	388.11
95	0.34	-13.00	3296.20	-119.65	47.40	3271.80	442.80	-1.60	3294.40	-14.74	41.40	3281.80	384.39
96	-0.	-14.60	3296.20	-134.38	45.40	3271.40	424.22	1.20	3294.80	11.05	41.80	3281.80	388.11
97	0.35	-15.60	3295.60	-143.63	45.00	3271.80	420.38	1.60	3294.00	14.75	42.80	3281.60	397.44
98	-0.	-14.80	3295.60	-136.27	44.20	3271.80	412.90	2.20	3294.60	20.27	43.60	3281.60	404.87
99	0.35	-15.80	3295.80	-145.46	44.60	3271.80	416.64	2.60	3293.80	23.97	43.40	3281.00	403.16
100	-0.	-15.80	3295.80	-145.46	45.20	3272.00	422.19	3.80	3294.20	35.02	43.80	3280.60	406.97
AVERAGE													
-83.74													
0													
-7.11													
16													
448.61													

Table 6. Velocity Anomalies for First Two Seconds of Run 1F

Cycle	$w_U^i$	$w_L^i$	$w_U^i$	$w_L^i$	Cycle	$w_U^i$	$w_L^i$	$w_U^i$	$w_L^i$
1	43.28	16.32	57.25	21.09	51	-8.28	28.94	-9.47	-6.81
2	50.63	12.63	42.55	21.09	52	0.89	21.48	-9.47	-21.35
3	63.51	18.16	47.85	13.66	53	8.27	25.21	-0.26	-23.37
4	52.48	21.84	38.57	8.37	54	-11.96	21.48	10.79	-23.37
5	65.34	38.43	31.10	12.09	55	-17.50	14.01	8.95	-19.76
6	70.87	29.21	19.90	23.23	56	-6.43	8.36	-2.10	-16.15
7	69.03	8.95	27.49	30.66	57	-17.50	-6.57	-3.94	-1.19
8	43.25	3.43	33.03	34.38	58	-0.94	-12.22	-9.47	-1.19
9	45.10	14.48	31.22	34.38	59	-10.16	-23.42	-9.47	0.83
10	50.62	38.43	42.31	30.66	60	-4.62	-25.23	-2.10	7.92
11	50.61	27.37	51.58	26.95	61	-8.31	-29.07	3.43	11.86
12	32.23	55.32	55.32	19.52	62	-0.96	-36.43	-11.31	24.92
13	13.84	36.57	57.12	10.17	63	10.07	-53.08	-11.31	21.20
14	21.21	42.11	49.66	-1.19	64	17.44	-54.90	-9.47	10.17
15	17.50	23.69	38.45	1.05	65	22.97	-54.99	5.27	2.63
16	6.44	16.32	30.99	10.28	66	10.07	-54.99	-35.25	4.43
17	19.33	10.79	19.78	28.75	67	0.87	-51.36	-29.74	6.23
18	19.32	-3.94	19.78	49.00	68	-12.01	-53.08	-14.99	8.26
19	24.88	7.11	27.25	60.14	69	-37.76	-45.51	-11.31	6.46
20	13.80	1.59	27.25	56.42	70	-32.31	-43.59	-27.90	-4.69
21	19.33	1.59	30.99	45.28	71	-30.48	-37.94	-26.05	6.46
22	21.17	16.32	19.78	37.85	72	-32.22	-32.59	-13.15	6.35
23	34.06	3.43	19.78	37.85	73	-21.23	-41.78	-9.47	-12.22
24	28.55	5.27	16.05	41.57	74	-26.74	-34.41	-11.31	-8.62
25	17.47	-16.82	12.32	41.57	75	-15.69	-38.14	-26.05	-5.01
26	21.15	-11.31	19.55	34.14	76	-10.16	-49.24	-20.52	-3.10
27	17.47	-5.78	14.01	26.71	77	4.57	-58.53	-7.63	-2.99
28	21.14	-20.52	12.09	27.89	78	2.72	-67.82	-2.10	0.72
29	22.98	-7.63	8.24	24.80	79	-26.74	-67.73	-2.10	-12.22
30	32.20	-7.63	14.01	24.68	80	-52.56	-62.08	-5.79	-17.85
31	28.50	10.79	15.82	13.44	81	-41.47	-58.34	-16.85	-30.90
32	28.50	-2.10	13.90	19.06	82	-37.82	-54.70	-5.79	-34.51
33	24.83	-3.94	17.63	11.75	83	-34.08	-45.31	3.42	-30.90
34	23.00	-3.94	6.43	11.75	84	-30.48	-41.68	12.64	-30.79
35	22.98	-13.15	13.90	4.43	85	-34.08	-39.66	5.27	-40.03
36	13.77	-0.26	6.43	2.63	86	-52.52	-37.74	-0.26	-53.17
37	10.09	7.11	17.63	4.32	87	-65.43	-23.00	7.11	-60.51
38	8.31	1.59	28.82	-1.19	88	-52.52	-15.31	-5.79	-51.27
39	-6.43	-11.30	32.67	2.41	89	-39.59	-11.69	-15.00	-47.46
40	-4.58	-2.10	32.67	10.06	90	-32.25	-7.84	-7.63	-47.46
41	2.78	-0.25	28.94	11.86	91	-19.35	1.34	-13.16	-49.36
42	2.78	7.11	36.41	15.35	92	-26.69	10.85	-26.05	-53.08
43	19.32	3.43	45.68	13.55	93	-32.17	14.58	-31.58	-58.60
44	13.84	-13.15	42.07	20.97	94	-41.44	-3.99	-24.21	-60.51
45	15.65	-11.31	30.87	13.66	95	-35.91	-9.76	-7.63	-64.22
46	-8.26	-9.47	17.97	8.04	96	-50.63	-28.34	18.16	-60.51
47	-6.41	-2.10	17.74	9.84	97	-59.89	-32.18	21.86	-51.17
48	-4.56	-7.62	25.21	11.86	98	-52.52	-39.66	27.38	-43.74
49	-13.79	-9.47	28.94	6.12	99	-61.71	-35.92	31.07	-45.45
50	-10.14	-5.78	28.94	-1.19	100	-61.71	-30.37	42.13	-41.64

TAU(1) = 0.760

TAU(2) = 0.048



**Table 7. Average Wind Components and Flux of Momentum - Run 1F**

Time	$\bar{v}_U$		T.E.		$\bar{v}_L$		T.E.		$\bar{v}_U$		T.E.		$\bar{v}_L$	
	Upper	Lower	Upper	Lower	Upper	Lower	Upper	Lower	Upper	Lower	Upper	Lower	Upper	Lower
1431-1436	-25.133	0	363.690	1039	37.429	1	309.551	308	-0.301	251	-	300	-0.469	-
1436-1441	-28.537	0	411.443	631	43.399	0	331.759	283	-0.503	-	-	-	-0.437	-

Flux of Momentum - Two Second Values

$\bar{v}_U$		T.E.		$\bar{v}_L$		T.E.		$\bar{v}_U$		T.E.		$\bar{v}_L$	
Upper	Lower	Upper	Lower	Upper	Lower	Upper	Lower	Upper	Lower	Upper	Lower	Upper	Lower
001	051	-	100	101	150	151	200	201	250	-	300	-	300
0.760	0.048	-1.139	-0.291	-0.264	0.038	-0.712	-0.271	-0.407	-0.071	-0.407	0.269	-0.476	-0.476
0.233	0.052	-0.393	-0.421	-0.912	-0.001	0.438	-2.642	-1.132	-0.408	-1.132	-0.798	-0.951	-0.951
1.098	-0.619	-1.491	0.121	0.952	-0.042	-0.004	-0.841	-0.195	-0.018	-0.195	-0.286	-1.410	-1.410
0.056	-0.964	-3.079	0.455	-1.397	-0.162	-1.123	0.328	-0.181	-0.332	-0.181	0.012	-0.203	-0.203
-0.259	-0.789	-0.067	-0.348	1.079	-0.143	-1.091	-0.140	0.037	-0.447	0.037	-0.033	-0.036	-0.036
-1.346	-0.042	-2.380	-0.151	0.274	-0.583	-1.896	-0.791	-0.186	-0.080	-0.186	0.073	-0.615	-0.615
-0.030	0.030	-0.392	-2.164	0.066	-0.173	-1.467	1.459	-0.095	-0.343	-0.095	-0.312	-0.044	-0.044
-0.072	-0.124	-0.125	-0.474	1.835	-0.006	-0.305	0.298	-0.080	-0.108	-0.080	-3.063	-0.410	-0.410
-0.202	-0.724	-0.182	-0.309	0.083	-1.008	-0.315	-0.187	-0.333	-0.145	-0.333	0.314	-0.416	-0.416
-1.327	-0.464	-0.329	-3.015	-0.306	-0.404	-0.112	-0.084	-0.436	-0.248	-0.436	0.146	-0.126	-0.126
-0.059	-0.410	0.156	-0.225	0.079	-0.108	-0.939	-0.145	0.067	0.115	0.067	0.119	-0.555	-0.555
-0.536	-0.240	-0.171	0.091	0.463	-0.152	-0.281	0.006	-0.014	-0.131	-0.014	-0.132	-0.184	-0.184
-0.457	-0.311	-1.303	-0.535	-0.163	-0.630	-0.387	-0.335	-0.121	-0.134	-0.121	-0.140	-1.030	-1.030
-1.128	-0.418	0.622	-0.535	-0.033	-0.284	-0.073	-0.212	0.230	-0.127	0.230	0.521	-0.307	-0.307
-0.339	-0.339	-0.030	-0.343	-0.484	-0.077	-0.141	-0.010	-0.835	-0.110	-0.835	-0.377	-1.257	-1.257
-1.091	-0.730	-0.578	-0.730	0.005	-0.049	-0.035	-0.202	0.076	-0.391	0.076	-0.143	-0.629	-0.629
-0.302	-0.228	-0.529	-0.746	-0.004	-0.182	0.019	-0.374	2.369	-0.067	2.369	0.436	-0.462	-0.462
-0.233	-0.301	0.004	-0.111	-0.380	-0.013	-0.480	-0.037	0.223	-0.146	-0.480	-1.364	-0.931	-0.931
-0.034	-0.285	-0.412	-0.091	0.238	-0.107	0.262	-0.012	-1.283	-0.119	-1.283	1.180	-1.132	-1.132
-1.284	-0.112	-0.095	-0.112	0.028	-0.027	-0.016	-0.303	0.088	0.009	-14.294	1.246	-3.388	-3.388</

Table 8. First Two Seconds of Raw Data - Run 1L

Cycle	V <sub>6</sub>	$\Delta t_{2U}$	$t_{2U}$	W <sub>U</sub>	$\Delta t_{xU}$	$t_{xU}$	u <sub>U</sub>	$\Delta t_{zL}$	$t_{zL}$	W <sub>L</sub>	$\Delta t_{xL}$	$t_{xL}$	u <sub>L</sub>
1	1.10	0.60	3305.40	5.49	14.40	3285.60	133.39	2.60	3301.00	23.86	9.80	3298.20	90.09
2	-0.	1.00	3305.00	9.15	14.00	3285.60	129.69	2.20	3301.40	20.18	9.40	3298.20	86.41
3	1.03	1.20	3304.80	10.99	14.00	3285.60	129.69	2.40	3301.20	22.02	9.00	3298.20	82.73
4	-0.	1.00	3305.00	9.15	14.00	3285.60	129.69	2.20	3301.00	20.19	9.00	3298.20	82.73
5	1.05	1.20	3305.20	10.98	13.80	3285.80	127.82	1.60	3301.20	14.68	9.00	3298.20	82.73
6	-0.	1.20	3305.20	10.98	14.20	3285.80	131.52	1.40	3301.00	12.85	8.80	3298.40	80.89
7	1.04	1.20	3305.20	10.98	15.00	3285.80	138.93	2.00	3301.20	18.35	8.60	3298.20	79.06
8	-0.	0.80	3305.60	7.32	15.60	3285.60	144.51	3.00	3301.00	27.53	8.80	3298.00	80.91
9	1.01	0.80	3305.20	7.32	16.40	3285.60	151.92	3.00	3301.00	27.53	8.80	3298.00	80.91
10	-0.	0.40	3306.00	3.66	17.00	3285.40	157.50	3.00	3301.00	27.53	8.60	3298.20	79.06
11	1.00	0.80	3305.60	7.32	17.20	3285.60	159.33	3.00	3301.00	27.53	9.00	3298.20	82.73
12	-0.	0.20	3305.40	1.83	17.60	3285.60	163.04	3.20	3301.20	29.36	9.00	3298.20	82.73
13	1.01	0.	3305.60	0.	18.00	3285.60	166.74	3.40	3301.40	31.19	9.20	3298.40	84.56
14	-0.	0.40	3305.60	3.66	18.20	3285.40	168.61	3.20	3301.20	29.36	9.00	3298.60	82.71
15	1.01	0.20	3305.80	1.83	19.00	3285.00	176.07	3.00	3301.40	27.52	9.40	3298.60	86.39
16	-0.	-0.20	3305.80	-1.83	19.40	3285.00	179.78	2.80	3301.20	25.69	10.20	3299.00	93.72
17	1.00	-0.40	3305.60	-3.66	19.60	3285.20	181.61	2.20	3301.40	20.18	10.60	3299.00	97.40
18	-0.	-1.40	3305.80	-12.81	19.80	3285.40	183.44	2.00	3301.60	18.35	10.80	3298.80	99.25
19	0.98	-0.40	3305.60	-3.66	19.60	3285.20	181.61	1.80	3301.80	16.51	11.20	3298.80	102.92
20	-0.	-0.80	3305.60	-7.32	18.80	3285.40	174.19	1.80	3301.80	16.51	11.20	3298.80	102.92
21	0.98	-0.60	3305.80	-5.49	19.00	3285.40	176.03	1.40	3301.80	12.84	11.20	3298.80	102.92
22	-0.	-1.00	3305.40	-9.15	19.00	3285.60	175.98	1.20	3301.60	11.01	11.40	3299.00	104.75
23	0.99	-0.80	3305.60	-7.32	18.80	3286.00	174.11	1.60	3301.60	14.68	11.20	3298.80	102.92
24	-0.	-0.60	3305.80	-5.49	18.20	3285.80	168.57	1.40	3301.40	12.84	11.40	3299.60	104.77
25	1.00	-1.20	3305.60	-10.98	18.00	3285.60	166.74	1.20	3301.60	11.01	11.40	3298.60	104.77
26	-0.	-1.20	3306.00	-10.98	18.20	3285.40	166.61	1.20	3301.20	11.01	11.60	3298.40	106.62
27	1.00	-1.40	3305.40	-12.81	18.40	3286.00	170.41	0.80	3301.20	7.34	11.60	3298.40	106.62
28	-0.	-0.40	3305.60	-3.66	18.80	3286.00	174.11	0.80	3301.20	7.34	11.60	3298.00	106.65
29	0.98	0.20	3305.80	1.83	19.20	3286.00	177.81	1.00	3301.00	9.18	11.20	3298.40	102.95
30	-0.	-0.20	3305.80	-1.83	20.20	3285.80	187.10	1.20	3301.20	11.01	11.20	3298.40	102.95
31	0.98	0.	3306.40	0.	20.80	3285.60	192.68	1.40	3301.40	12.84	11.20	3298.40	102.95
32	-0.	-0.60	3306.20	-5.49	21.20	3285.60	196.38	1.00	3301.40	9.17	11.20	3298.40	102.95
33	1.00	-0.40	3306.00	-3.66	21.40	3285.40	198.26	0.80	3301.60	7.34	11.00	3298.20	101.12
34	-0.	-0.60	3305.80	-5.49	21.00	3285.40	194.56	1.20	3301.60	11.01	10.80	3298.00	99.29
35	1.00	-0.20	3305.80	-1.83	20.80	3285.60	192.68	1.40	3301.40	12.84	10.60	3298.20	97.44
36	-0.	-0.20	3305.80	-1.83	20.40	3285.60	188.97	1.20	3301.20	11.01	10.60	3298.20	97.44
37	0.98	-0.80	3306.00	-7.32	20.40	3285.60	188.97	1.40	3301.00	12.85	10.00	3298.00	91.94
38	-0.	-0.40	3306.00	-3.66	20.20	3285.80	187.10	1.80	3301.00	16.52	10.00	3298.00	91.94
39	0.96	-0.40	3306.40	-3.66	20.00	3285.60	185.27	1.60	3301.20	14.68	9.80	3297.80	90.11
40	-0.	-0.60	3306.60	-5.49	20.00	3286.00	185.22	1.80	3301.40	16.51	9.60	3298.00	88.26
41	0.95	-0.40	3306.00	-3.66	19.60	3286.00	181.52	2.00	3301.20	18.35	9.20	3298.00	84.58
42	-0.	0.20	3306.20	1.83	20.00	3286.00	185.22	2.60	3301.00	23.86	8.80	3298.00	80.91
43	0.95	0.	3306.00	0.	19.80	3285.80	183.39	2.80	3300.80	25.70	8.80	3298.00	80.91
44	-0.	0.20	3306.20	1.83	19.20	3285.60	177.86	2.80	3301.20	25.69	8.60	3298.20	79.06
45	0.95	-0.60	3306.20	-5.49	19.00	3285.40	176.03	2.80	3300.80	25.70	8.60	3298.20	79.06
46	-0.	0.20	3306.20	1.83	18.80	3285.20	174.19	3.00	3301.00	27.53	8.40	3298.40	77.21
47	0.96	1.00	3306.20	9.15	19.00	3285.40	176.03	2.80	3300.80	25.70	8.40	3298.40	77.21
48	-0.	0.60	3305.80	5.49	19.80	3285.40	183.44	2.40	3301.20	22.02	8.40	3298.40	77.21
49	0.94	0.20	3305.80	1.83	19.60	3285.20	181.61	2.60	3301.40	23.85	8.80	3298.40	80.89
50	-0.	-0.20	3306.20	-1.83	19.60	3285.20	181.61	2.00	3301.60	18.35	8.80	3298.40	80.89

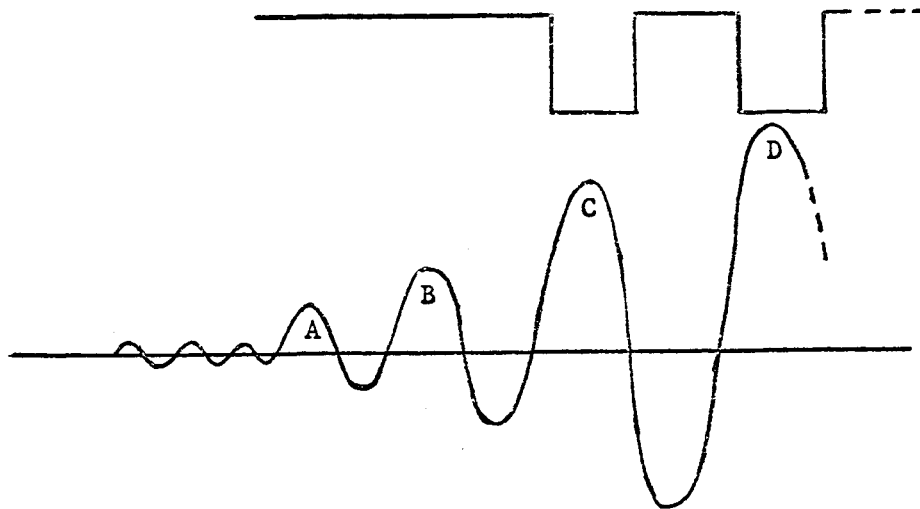
Table 8. First Two Seconds of Raw Data - Run 1L (Continued)

Cycle	V <sub>6</sub>	Δt <sub>zL</sub>	Σt <sub>zL</sub>	w <sub>U</sub>	Δt <sub>xU</sub>	Σt <sub>xU</sub>	u <sub>U</sub>	Δt <sub>zL</sub>	Σt <sub>zL</sub>	w <sub>L</sub>	Δt <sub>xL</sub>	Σt <sub>xL</sub>	u <sub>L</sub>
51	0.92	-0.60	3306.20	-5.49	20.20	3285.80	187.10	2.20	3301.40	20.18	9.20	3298.40	84.56
52	0.	-0.20	3305.80	-1.83	20.40	3286.00	188.93	2.20	3301.40	20.18	9.20	3298.40	84.56
53	0.93	-0.20	3306.20	-1.83	21.00	3285.80	194.51	2.20	3301.40	20.18	9.60	3298.40	88.24
54	0.	-1.40	3306.20	-12.81	21.40	3285.40	198.26	1.80	3301.40	16.51	10.00	3298.40	91.92
55	0.95	-1.60	3305.00	-14.64	21.80	3285.40	201.97	1.80	3301.40	16.51	10.20	3298.60	93.74
56	0.	-2.20	3306.60	-20.12	22.20	3285.80	205.62	1.20	3301.60	11.01	10.40	3298.80	95.57
57	0.95	-2.20	3306.20	-20.13	22.80	3286.00	211.15	0.40	3301.60	3.67	10.60	3298.60	97.42
58	0.	-1.80	3307.00	-16.46	22.60	3285.80	209.33	-0.20	3301.40	-1.83	10.60	3298.60	97.42
59	0.96	-1.40	3306.20	-12.81	22.40	3285.60	207.50	-0.20	3301.40	-1.83	10.60	3298.60	97.42
60	0.	-1.40	3306.60	-12.80	22.00	3285.60	203.79	-0.20	3301.40	-1.83	10.40	3298.40	95.59
61	0.95	-1.00	3306.60	-9.15	22.00	3286.00	203.75	-0.20	3301.40	-1.83	10.60	3298.60	97.42
62	0.	-1.40	3306.20	-12.81	21.80	3286.20	201.87	0.20	3301.40	1.83	10.60	3298.60	97.42
63	0.94	-0.80	3306.40	-7.32	21.40	3286.20	198.16	0.20	3301.80	1.83	10.40	3298.80	95.57
64	0.	-1.20	3306.00	-10.98	21.40	3285.20	198.16	0.40	3301.60	3.67	10.20	3298.60	93.74
65	0.95	-1.00	3306.20	-9.15	21.20	3286.00	196.34	0.40	3301.60	3.67	10.20	3298.60	93.74
66	0.	-1.80	3306.20	-16.47	20.60	3285.80	190.80	0.40	3301.60	3.67	10.20	3298.60	93.74
67	0.97	-2.20	3306.20	-20.13	20.20	3285.80	187.10	0.	3301.60	0.	10.20	3298.60	93.74
68	0.	-2.00	3306.00	-18.30	19.80	3286.20	183.35	0.	3301.60	0.	10.20	3298.60	93.74
69	0.96	-1.60	3306.80	-14.63	19.20	3286.00	177.81	0.	3301.60	0.	10.20	3298.60	93.74
70	0.	-1.20	3306.40	-10.98	18.60	3285.80	172.28	-0.40	3301.60	-3.67	10.40	3298.40	95.59
71	0.95	-1.20	3306.80	-10.97	18.60	3285.80	172.28	-0.40	3301.60	-3.67	10.40	3298.40	95.59
72	0.	-0.60	3307.00	-5.49	18.80	3286.00	174.11	-0.40	3301.60	-3.67	10.60	3298.20	97.44
73	0.92	-1.80	3307.00	-16.46	19.40	3286.20	179.64	-0.40	3301.60	-3.67	10.40	3298.00	95.62
74	0.	-1.40	3307.00	-12.80	19.40	3286.20	179.64	-0.60	3301.80	-5.50	10.40	3298.00	95.62
75	0.92	-1.20	3307.20	-10.97	20.00	3286.40	185.18	-0.60	3301.80	-5.50	10.20	3298.20	93.77
76	0.	-1.40	3307.40	-12.80	20.40	3286.40	188.88	-0.60	3301.80	-5.50	10.40	3298.40	95.59
77	0.90	-1.80	3307.00	-16.46	20.60	3286.20	190.76	0.	3301.60	0.	10.40	3298.40	95.59
78	0.	-1.80	3307.00	-16.46	20.60	3286.20	190.76	-0.40	3302.00	-3.67	10.40	3298.40	95.59
79	0.89	-2.60	3307.00	-23.77	20.60	3286.20	190.76	0.20	3302.20	1.83	10.40	3298.40	95.59
80	0.	-2.20	3307.00	-20.12	20.20	3286.20	187.05	0.60	3302.20	5.50	10.20	3298.60	93.74
81	0.87	-2.00	3306.80	-18.29	19.60	3286.40	181.47	0.20	3302.20	1.83	10.20	3298.60	93.74
82	0.	-1.80	3307.00	-16.46	19.20	3286.40	177.77	0.	3302.00	0.	10.20	3298.60	93.74
83	0.85	-2.00	3306.80	-18.29	19.40	3286.60	179.60	0.20	3301.80	1.83	9.80	3298.60	90.07
84	0.	-2.60	3307.00	-23.77	18.80	3286.40	174.07	0.	3302.00	0.	9.80	3298.60	90.07
85	0.83	-2.00	3306.80	-18.29	18.60	3286.60	172.19	0.40	3301.60	3.67	9.60	3298.40	88.24
86	0.	-2.00	3307.20	-18.29	18.20	3287.00	168.45	0.40	3301.60	3.67	9.20	3298.40	84.56
87	0.82	-2.00	3306.80	-18.29	18.00	3286.80	166.62	0.40	3301.20	3.67	9.20	3298.40	84.56
88	0.	-2.00	3307.20	-18.29	18.00	3286.80	166.62	0.40	3301.20	3.67	8.80	3298.40	80.89
89	0.82	-2.60	3307.00	-23.77	18.20	3286.60	168.49	0.40	3301.20	3.67	8.80	3298.40	80.89
90	0.	-2.60	3306.60	-23.78	18.40	3286.80	170.32	0.	3301.20	0.	8.60	3298.60	79.04
91	0.82	-2.80	3307.20	-25.60	18.20	3286.60	168.49	0.20	3301.00	1.84	8.60	3298.60	79.04
92	0.	-2.60	3306.60	-23.78	18.00	3286.40	166.66	0.60	3301.40	5.51	8.80	3298.80	80.87
93	0.81	-2.20	3307.00	-20.12	18.00	3286.40	166.66	1.40	3301.40	12.84	8.80	3298.40	80.89
94	0.	-1.80	3306.60	-16.46	17.60	3286.00	163.00	2.40	3301.20	22.02	9.00	3298.60	82.71
95	0.80	-1.60	3306.80	-14.63	17.60	3286.00	163.00	3.20	3301.60	29.36	9.00	3298.60	82.71
96	0.	-1.60	3306.80	-14.63	17.40	3286.20	161.12	3.60	3301.60	33.03	9.20	3298.40	84.56
97	0.79	-2.00	3306.80	-18.29	17.20	3286.40	159.25	3.80	3301.40	34.86	9.60	3298.40	88.24
98	0.	-1.80	3306.60	-16.46	17.60	3286.80	162.92	4.00	3301.20	36.70	10.20	3298.20	93.77
99	0.78	-1.80	3307.00	-16.46	17.80	3286.60	164.79	3.60	3300.80	33.04	10.40	3298.00	95.62
100	0.	-2.20	3307.00	-20.12	18.00	3286.40	166.66	2.80	3300.80	25.70	10.60	3297.80	97.47
AVERAGE				-8.01		176.85				12.72			91.09
ERRORS				0		0				0			0

third reading is the first significant analog signal. As in tables 1, 2, 3 and 4, every other analog reading is indicated as zero to show that the DVM was blocked in order to allow adequate stabilization time between readings.

The average wind components for the first two seconds of runs 1F and 1L are shown at the ends of tables 5 and 8, respectively, according to the following: For the vertical components, a minus sign indicates that the wind component is downward; for the horizontal components, a plus sign indicates a wind direction between  $90^\circ$  and  $270^\circ$  (through south) and a minus sign indicates a wind direction between  $270^\circ$  and  $90^\circ$  (through north). The line below the average wind components labeled "errors," represents the number of triggering errors that occurred during the two-second interval. Thus, from Table 5 it is seen that there were no triggering errors for the vertical, and 30 and 16, respectively, for the upper and lower horizontal components.

The following sketch will help demonstrate what is meant by triggering error.



The lower signal of the portrayed oscilloscope diagram represents the received sonic signal with the peaks marked A, B, C, D being the true received signal and the small perturbations prior to A

representing noise level due to reflection and internal system noise. Of the upper trace only the first pulse is significant and it may be thought of as the trigger that turns the transit time-counter off. The trigger can be adjusted to occur on A, B, C or D but should be on one of the first three, inasmuch as peaks after the fourth are not allowed to rise above a fixed level, and the third one, C, is usually employed since it represents the largest signal difference between successive amplitudes. Of course, the same triggering peak is chosen for all sonic levels. This adjustment is made with a potentiometer and an oscilloscope so that ideally the triggering always occurs on the selected peak and never on an adjacent one. If such an error does occur, a timing error on the order of 50 microseconds is automatically introduced since the frequency of the received signal is on the order of 20 kc. Such an error is very easily spotted in the  $\Delta T$ ,  $\Sigma t$  or the velocity computation column and since  $\Sigma t$  is very nearly constant, this parameter is used to detect such errors and to correct them.

In the machine processing of the raw-data tape,  $\Sigma t$  values per cycle reading are stored and compared with each successive reading, with reading number 2 being transferred to storage if correct, and so on. If there is a difference between readings in excess of 20 microseconds, it is known that a triggering error occurred, and processing logic determines whether it was an early or a late triggering error, and then replaces the erroneous value of  $\Sigma t$  with the preceding correct  $\Sigma t$  from storage. The error magnitude between the correct and the incorrect  $\Sigma t$  is applied to the corresponding erroneous  $\Delta t$  to correct it and, of course, to the velocity computation as well. The corrected  $\Sigma t$  value does not go into storage for comparison with the succeeding one; rather the last correct value is held until another correct value is available and so on.

This type of error was a rather severe limitation on earlier pulse-type sonics but is not significant in the current model of the Stewart-Post sonics and occurred in this run due to the fact that experimentation was being conducted to see whether a common triggering adjustment could be found for the sonic paths both with and without the zero tube in place. In Run 1L (Table 8), triggering was readjusted

following the zero tube check and, as will be seen later, no errors of this type occurred.

Tables 6 and 9, applicable to runs 1F and 1L, respectively, show the velocity anomalies for the first two seconds of the respective runs, as indicated by the columnar headings. The individual readings are the differences between the average velocity as shown at the bottom of tables 5 and 8 and the individual velocity components shown in the same tables. That is, reading number 1 in the second column of Table 6 (43.28) is the difference between the average  $w_U$  for the first two seconds (-83.74) and the first cycle value of  $w_U$  (-40.46). The sign of the difference is positive since the average value of  $w_U$  for the first two seconds represents a zero offset of -83.74 (downward direction) and the first cycle reading of  $w_U$  is less negative than this offset, hence the difference is positive as indicated in Table 6.

Thus, individual zero offset values of the sonic paths need not be of concern, at least in a theoretical sense, since they are subtracted out. However, practically speaking, it is necessary to reduce these as much as possible as was indicated in the discussion of tables 1, 2, 3 and 4.

At the end of tables 6 and 9 two individual shearing stresses or momentum flux values are shown. These values in dynes/cm<sup>2</sup> are computed from equation (26), assuming a constant density, and, of course, refer to the upper and lower levels for the first two seconds.

Tables 7 and 10 with applicability to runs 1F and 1L, respectively, show the mean wind and flux values based on five-minute intervals for the full run periods, as well as the momentum flux values for each two-second interval. Those columns of the first portions of tables 7 and 10, marked as  $\bar{w}_U$ ,  $\bar{u}_U$ , etc., show the mean wind components for the indicated five-minute intervals based on the individual two-second means which in turn were based on the 50 cycles per second measurements. Those columns headed T.E. are the number of triggering errors for the total run which, as noted previously, are numerous in Run 1F and absent completely in Run 1L. Those columns headed "upper" and "lower" are the flux computations for each two seconds of data with each column covering

Table 9. Velocity Anomalies for First Two Seconds of Run 11

Cycle	$w'_U$	$u'_U$	$w'_L$	$u'_L$	Cycle	$w'_U$	$u'_U$	$w'_L$	$u'_L$
1	13.50	-43.45	11.14	-1.00	51	2.52	10.25	7.47	-6.53
2	17.17	-47.16	7.47	-4.68	52	-4.18	12.08	7.47	-6.53
3	19.00	-47.16	9.30	-8.35	53	6.18	17.66	7.47	-2.85
4	17.17	-47.16	7.47	-8.35	54	-4.80	21.42	3.80	0.83
5	19.00	-49.03	1.96	-8.35	55	-6.63	25.12	3.80	2.65
6	19.00	-45.32	0.13	-10.20	56	-12.11	28.78	-1.71	4.48
7	19.00	-37.91	5.63	-12.03	57	-12.12	34.31	-9.65	6.33
8	15.33	-32.34	14.81	-10.18	58	-8.45	32.48	-14.55	6.33
9	15.33	-24.93	14.81	-10.18	59	-4.80	30.66	-14.55	6.33
10	11.67	-19.35	14.81	-12.03	60	-12.03	26.95	-14.55	4.50
11	15.33	-17.51	14.81	-8.35	61	-1.13	26.90	-14.55	6.33
12	9.84	-13.81	16.65	-8.35	62	-4.80	25.02	-10.88	6.33
13	8.01	-10.10	18.48	-6.53	63	0.69	21.32	-10.88	4.43
14	11.67	-8.23	16.65	-8.37	64	-2.97	21.32	-9.05	2.65
15	9.84	-0.78	14.81	-4.70	65	-1.14	19.49	-9.05	2.65
16	6.18	2.93	12.98	2.63	66	-8.46	13.96	-9.05	2.65
17	4.35	4.76	7.47	6.31	67	-12.12	1.25	-12.12	2.65
18	-4.80	6.59	5.63	8.16	68	-10.29	6.50	-12.12	2.65
19	4.35	4.76	3.79	11.83	69	-6.62	0.97	-12.12	2.65
20	0.69	-2.65	3.79	11.83	70	-2.97	-4.57	-16.39	4.50
21	2.52	-0.82	0.12	11.83	71	-2.96	-4.57	-16.39	4.50
22	-1.14	-0.86	-1.71	13.66	72	2.52	-2.74	-16.39	6.35
23	0.69	-2.74	1.96	11.83	73	-8.45	2.80	-16.39	4.53
24	2.52	-8.27	0.13	13.68	74	-4.79	2.80	-18.22	4.53
25	-2.97	-10.10	-1.71	13.68	75	-2.96	8.33	-18.22	2.68
26	-2.97	-8.23	-1.71	15.53	76	-4.79	12.04	-18.22	4.50
27	-4.80	-6.44	-5.38	15.53	77	-8.45	13.91	-12.12	4.50
28	4.35	-2.74	-5.38	15.56	78	-8.45	13.91	-16.39	4.50
29	9.84	0.97	-3.54	11.86	79	-15.76	13.91	-10.88	4.50
30	6.18	10.25	-1.71	11.86	80	-12.11	10.21	-7.22	2.65
31	8.01	15.83	0.13	11.86	81	-10.28	4.63	-10.88	2.65
32	2.52	19.54	-3.54	11.86	82	-8.45	0.93	-12.12	2.65
33	4.35	21.42	-5.38	10.03	83	-10.28	2.76	-10.88	-1.02
34	2.52	17.71	-1.71	8.21	84	-15.76	-2.78	-12.12	-1.02
35	6.18	15.83	0.13	6.35	85	-10.28	-4.65	-9.05	-2.85
36	6.18	12.13	-1.71	6.35	86	-10.27	-8.39	-9.05	-6.53
37	0.69	12.13	0.13	0.85	87	-10.28	-10.23	-9.05	-6.53
38	4.35	10.25	3.80	0.85	88	-10.27	-10.23	-9.05	-10.20
39	4.35	8.42	1.96	-0.98	89	-15.76	-8.35	-9.05	-10.20
40	2.52	8.38	3.80	-2.83	90	-15.77	-6.52	-12.12	-12.05
41	4.35	4.67	5.63	-6.51	91	-17.59	-8.35	-10.88	-12.05
42	9.84	8.38	11.14	-10.18	92	-15.77	-10.19	-7.21	-10.22
43	8.01	6.55	12.98	-10.18	93	-12.11	-10.19	0.13	-10.20
44	9.84	1.01	12.98	-12.03	94	-8.45	-13.85	9.30	-8.37
45	2.52	-0.82	12.98	-12.03	95	-6.62	-13.85	16.64	-8.37
46	9.84	-2.65	14.81	-13.88	96	-6.62	-15.72	20.31	-6.53
47	17.16	-0.82	12.98	-13.88	97	-10.28	-17.59	22.15	-2.85
48	13.50	6.59	9.30	-13.88	98	-8.45	-13.93	23.99	2.68
49	9.84	4.76	11.14	-10.20	99	-8.45	-12.06	20.32	4.53
50	6.18	4.76	5.63	-10.20	100	-12.11	-10.19	12.98	6.38

TAU(1) = -0.078

TAU(2) = -0.043

**Table 10. Average Wind Components and Flux of Momentum - Run 1L**

Time	Upper	Lower	$\bar{v}_U$	I.E.	$\bar{v}_L$	I.E.	$\bar{v}_U$	I.E.	Upper	Lower	$\bar{v}_U$	I.E.	Upper	Lower	$\bar{v}_U$	I.E.	Upper	Lower
1825-1830	-0.078	-0.043	-18.540	0	-5.292	0	218.423	0	-0.171	-0.032	-0.171	0	201	-0.131	-0.138	0	251	300
1830-1835	-0.028	-0.031	-25.033	0	-8.124	0	243.197	0	-0.808	-0.519	-0.808	0	0.069	-0.131	-0.167	0	-	-
	-0.237	-0.134						0.055	0.067	0.055	0	0.057	-0.067	-0.138				
	-0.041	0.005						-0.147	-0.058	-0.147	0	-0.055	-0.111	-0.077				
	-0.109	-0.001						-0.083	-0.575	-0.039	0	-0.026	-0.074	-0.067				
	-0.328	-0.093						-0.046	-0.019	-0.178	0	-0.134	-0.011	-0.027				
	-0.506	-0.009						-0.058	-0.120	0.009	0	0.005	-0.330	-0.308				
	-0.057	0.071						-0.165	-0.011	-0.247	0	-0.133	-0.490	-0.308				
	-0.032	-0.044						0.303	-0.002	-0.068	0	-0.135	-0.790	-0.050				
	-0.184	-0.018						0.009	0.057	-0.104	0	-0.477	-0.048	-0.103				
	-0.161	-0.032						-0.127	-0.111	-0.257	0	-0.145	-0.230	-0.047				
	-0.103	0.031						-0.974	-0.034	-0.043	0	-0.905	-0.260	-0.203				
	-0.068	-0.075						0.143	-0.401	0.260	0	-0.173	-0.096	-0.002				
	-0.073	-0.091						0.059	-0.152	0.101	0	-0.173	-0.585	-0.110				
	-0.335	-0.335						-0.037	-0.210	0.177	0	-0.270	-0.226	-0.246				
	-0.164	-0.025						-0.072	-0.180	-0.004	0	0.072	-0.144	-0.451				
	-0.114	-0.092						-0.164	0.051	-0.606	0	-0.034	-0.012	-0.158				
	-0.138	-0.213						-0.387	0.039	0.121	0	-0.048	0.116	-0.116				
	-0.010	-0.082						-0.255	-0.260	-0.111	0	-0.594	0.083	-0.189				
	-0.001	-0.080						0.004	0.010	-0.345	0	-0.091	0.189	-0.153				
	-0.361	-0.163						-0.108	-0.059	-1.152	0	0.005	-0.016	-0.588				
	-0.094	-0.094						-0.302	-0.214	-0.156	0	-0.436	-0.224	-0.158				
	-1.296	-0.010						-0.095	-0.032	-0.474	0	-0.113	-0.113	-0.163				
	-0.331	-0.038						-0.039	0.021	-0.495	0	-0.270	-0.424	-0.129				
	-0.385	-0.033						-0.089	0.001	0.078	0	-0.170	-0.064	-0.289				
	-0.071	-0.033						-0.385	-0.080	-0.016	0	-0.575	-0.126	-0.093				
	-0.014	-0.012						-0.200	-0.011	-0.021	0	-0.488	-0.081	-0.094				
	-0.050	-0.050						-0.480	-0.006	-0.127	0	-0.064	0.057	-0.573				
	-0.098	0.019						-0.533	-0.062	-0.249	0	-0.108	-0.172	-1.170				
	-0.038	0.038						-0.196	-0.012	-0.086	0	-0.143	-0.130	-0.320				
	-0.423	-0.084						0.053	0.005	-0.279	0	-0.066	-0.067	-0.482				
	-0.029	-0.011						-0.725	-0.066	-0.207	0	-0.240	-0.165	-0.976				
	-0.129	-0.129						-0.496	-0.388	-1.205	0	-0.001	-0.027	-0.034				
	-0.082	-0.111						0.312	-0.912	-0.240	0	-0.055	-0.121	-0.487				
	-0.088	-0.031						-0.586	-0.149	-0.222	0	-0.145	-0.145	-0.487				
	-1.283	-0.209						0.044	-0.368	-0.131	0	-0.223	-0.174	-0.320				
	-0.050	-0.113						-0.210	-0.194	-0.025	0	-0.119	0.023	-0.233				
	-0.417	-0.267						-0.312	-0.108	0.073	0	-0.191	-0.109	-0.322				
	-0.497	0.059						-0.301	-0.163	-0.104	0	-0.566	-0.665	-0.364				
	-0.079	0.079						-0.026	-0.418	0.041	0	-0.429	-0.227	-0.378				
	-0.474	-0.094						-0.146	0.006	-0.002	0	-0.002	0.004	-0.428				
	-0.085	-0.160						-0.100	-0.311	-0.075	0	-0.511	0.004	-0.237				
	0.268	-0.434						0.047	-0.309	-0.121	0	-0.023	-0.285	-0.049				
	-0.313	-0.008						-0.037	-0.152	0.067	0	-0.384	-0.112	-0.028				
	-0.393	-0.323						-0.112	-0.465	-0.091	0	-0.035	-0.068	-0.164				
	-0.836	-0.025						-1.031	-0.273	-0.018	0	-0.622	-0.247	-0.197				
	-0.113	-0.113						-0.162	-0.422	-0.295	0	-0.181	-0.101	-0.729				
	-0.381	-0.133						-0.142	-0.490	-0.011	0	-0.241	-0.080	-0.090				
	-0.186	-0.086						-0.219	-0.185	-0.097	0	-0.357	-0.181	-0.282				
	-0.944	0.054						-0.051	-0.055	-0.598	0	-0.050	-0.321	-0.155				



100 seconds. That is, the first value in column 1 is the shearing stress based on the first two seconds of the run and is identical to the value shown for Tau 1 at the bottom of Table 6. The  $\bar{\tau}_U$  and  $\bar{\tau}_L$  values shown in the first part of tables 7 and 10 are based on the individual flux values shown in the lower portion of the tables.

From these tables it is possible to make some estimates concerning data quality. Looking at the summations of transit times given in the various tables, it can be seen that the summation of transit times applicable to a given sonic path are indeed essentially constant. However, this constancy is not invariant between individual sonic paths, as may be seen in the following table covering runs 1F, 1L and the zero tests.

Table 11.  $\Sigma t$  Comparative Summary

Run	$\Sigma t_{zU}$	$\Sigma t_{xU}$	$\Sigma t_{zL}$	$\Sigma t_{xL}$
1F	3297	3272	3295	3282
1L	3305	3285	3301	3298
ZERO TESTS	3299	3273	3285	3271

It can be seen in Table 11 that a definite pattern is present and while one could expect some variation in sound velocity, and thus in  $\Sigma t$ , at a given level during a given run, that pattern should not be present in different runs separated by large time increments. Thus, there seems little question that static spacing errors for the individual paths are present as well as some vibration error, though the latter is small inasmuch as the individual four-head sonic configurations are so mounted that the whole system must vibrate as a unit. Error calculations based on the equations defining wind component, difference in transit times and summation of transit times will show that a .1% error in spacing or a .1% change in sound velocity will result in a  $\Sigma t$  change of 3 and 30 microseconds, respectively. Also, it will be found that the percentage change in sonic velocity components is twice the percentage change in  $\Sigma t$  which will be on the order of 1% or 2% for sound velocity changes and a tenth of that for vibration errors. This

is not to say that vibrations are not present, only that, comparatively speaking, they are minor compared to the head-spacing error.

There is, of course, no way to utilize the data of Table 11 to analyze the absolute nature (or even existence) of the spacing error, yet it seems reasonable to assume that the averages of the individual columns of Table 11 would be representative of spacing differences between the individual sonic paths in view of the pattern present. This assumption, plus the error calculations cited, would show, for example, that between the horizontal and vertical paths of the upper level there were path differences on the order of .04 cm and between the vertical paths at the upper and lower levels a difference on the order of .01 cm. These head-spacing errors are not large in the magnitude sense, but introduce corresponding percentage errors in  $\Sigma t$  and  $\Delta t$  and in velocity components, as well as in mean computations based on these parameters and are thus significant quality limitations. Practical difficulties have so far prevented elimination of spacing errors of these magnitudes and it is not likely that the head configuration and mounting of the current system will ever permit such correction without introducing worse complications through obstruction of the air flow. Certainly it can be said that until such time as the spacing errors can be reduced there is little point in utilizing a head-spacing less than one-half meter with these sonic anemometers.

Table 12, below, compares the five-minute average winds from the sonics with simultaneous measurements of the analog wind (Run 1L) and simultaneous horizontal wind measurements made with Station A instrumentation during these runs.

Table 12. Mean Horizontal Wind Summary

<u>Time</u>	<u>Sonic (2m)</u>	<u>Sta. A (2m)</u>	<u>Sonic (8m)</u>	<u>Sta. A (8m)</u>	<u>Analog (6m)</u>
1431-1436	309	507	364	575	-
1436-1441	332	577	411	672	-
1825-1830	186	313	218	377	332
1830-1835	213	330	243	400	370

In this table columns 2 and 4 are the same mean values found in tables 7 and 10 whereas columns 3 and 5 are the winds as measured at Station A (at the same levels, some 20 feet west of the sonic installations) utilizing Beckman-Whitley single-hole chopper anemometers, and the final column is the wind determinations made with the Rett 100-hole chopper anemometer mounted between the sonic levels at 6 meters. As can be seen, the sonic analog wind fits the Station A data, but the sonic values themselves are consistently lower. Inasmuch as sonic run #1 was the last one made prior to the preparation of this report, it is not possible to state with certainty why the mean sonic wind values should be lower than those obtained with standard anemometers. However, it is probable that this is a result of an orientation error of the sonic system. That is, prior to making a run with the sonics, the mounting staff on which the sonics are fixed is so located that the u component is as nearly coincident with the prevailing wind as possible. It would not be too surprising to find the sonic means running somewhat lower in magnitude than the three-cup anemometers for this short time-interval but not as much as shown in Table 12, and it seems almost certain that a significant v component is present due to sonic orientation.

Looking at Table 7 it can be seen that there are quite a few instances where the stresses at the upper and lower levels are oppositely directed and although the majority of these are past the point of meteorological or mathematical significance, many of them are not. Also, in this same table there are some odd values beyond reasonable physical possibility and it is likely that this is a factor of the large number of triggering errors present in this run since in Table 10 for Run 1L there are only a few opposing sign conditions and no wild jump values.

Inasmuch as this is a rather limited data set and comparable data from other sources do not exist, it is rather difficult to be conclusive concerning the quality of the data presently obtainable from the sonic system at Cedar Hill. In general, however, it would appear that with the exclusion of the wild values in Run 1F these are good data in the usual sense of the word and representative of the sampled

atmospheric structure. This is mainly applicable to those data that are independent, or nearly so, of spacing error (anomalies and flux values) and, of course, none of these data are good in an absolute sense, this not only because of known errors, but because of uncertainties regarding implied assumptions of eddy structure.

Some of the measurement system limitations apparent from these data can be corrected in the existing system and some cannot. An example of the latter is the inclusion of another orthogonal component path to eliminate orientation error. Some modifications of a feasible nature are discussed in the final section of this report which follows.

## CONCLUSIONS AND RECOMMENDATIONS

Inasmuch as any research task necessarily proceeds on the basis of unproved concepts, it is never possible to answer, prior to successful completion of the research, whether the methods of attack being employed are correct or even adequate. However, on the basis of related knowledge and past efforts, it is possible to make a reasonable assessment of the techniques that have been, are, and will be used toward attainment of the research goals. In the present case this assessment can largely be shown through three questions whose answers, though in part based on postulates, can nevertheless be reasonably conclusive.

1. Do the planned research goals actually exist, or, does the instantaneous wind profile bear any relationship to the mean wind profile? The answer is obviously "yes," although not as a simple one-to-one parameter correspondence. That is, the fact that the mean value of any parameter is nothing more than the average of the instantaneous values over the interval for which the mean is computed provides the affirmation itself but not the nature of it.

2. Are the proposed parameters adequate to afford functional definition of the instantaneous profile? The answer here is "probably not," in the ultimate sense, and a qualified "yes," in the practical sense, since it is known from related work, both theoretical and empirical, that these parameters can cause significant variation in fluid flow. While the degree of qualification cannot be known until testing with collected data is made, it is important to note that it is the primary indicator as to how much time and effort will have to be expended in reaching an acceptable level of usefulness of the sought-for definition.

3. Are the methods of measurement being employed sufficient to provide the necessary data for determination of the functional definition that is sought? Considering the employed instrumentation as

well as past and current data programs, this question can be reduced without serious loss to "Are sonic anemometers the best tool for the job and if so, do the sonics in use on the contract represent the best capability in this type of sensor?" On the basis of the Phase 1 activities of this study, it may be unequivocally stated that of all known existing instrumentation, sonic anemometry offers the most potential for field measurement of the turbulent properties of wind flow, that is, instantaneous wind within the definition of instantaneous previously given. Further, it may be stated that at this time, and considering all factors of operation, the Stewart-Post sonics constructed for the project represent the most capability within the scale of motion in which we are interested. It is also reasonable to assume that these sonics are capable of providing the necessary information for the analytical procedures that are contemplated; however, more definitive evaluation depends on as yet unknown factors, such as what is an eddy, and what is the upper limit of significant atmospheric frequency variations.

Thus, in general, the research under way and planned, which is reviewed herein and in previous reports, is considered necessary and sufficient and is recommended for continuation. This does not say, however, that there are no problems and that modification of details are not in order.

To date, five sonic runs have been made and each of these has revealed difficulties in part resolved or capable of resolution and in part outstanding. An example of the latter is the present sensor-mounting configuration which is cumbersome, unwieldy, and more of a flow-disturbance than it should be. Resolution here is outside the scope of the present effort, and it is suggested that the sponsor's technical representatives look into the feasibility of supporting transducer studies that would provide reduction of head size and improvement of acoustic properties which would lead to instrumentation utilizing two-head sonic paths with closer head-spacing and less modification of wind flow. In short, sonic anemometer deficiencies today are primarily in the transducer assemblies rather than in the principles of operation which appear adequate though some debugging is in order.

From these five runs a primary deficiency which has been noted is the difficulty in determining in the field the difference between useful operation and mere operation. An example of this is the Cedar Hill comparison tests discussed in a previous section. Here all possible field checks were performed but useful data were not collected and this was not known until the recording tapes were put on the computer.\* However, other failures that have occurred could have been avoided through acquisition of better test-equipment and, in some cases, through performance of tests that were not possible because of simple lack of equipment. Specifics in this vein include

1. Installation of scanning switches to permit rapid checking of transmitter-receiver operation on all channels;
2. Installation of read-cards and necessary logic check circuitry for all channels of the magnetic tape recorder;
3. Acquisition of a suitable cathode ray oscilloscope for permanent use at the measuring site as opposed to the current practice of carrying a scope back and forth between College Station and Dallas with resulting discrepancies in calibration and operation;
4. Acquisition of an adequate spare-part complement, particularly in printed circuit boards utilized exclusively in the logic circuitry of the recording system;
5. Construction of a precise head-spacing tool that can be readily used on the transducer assemblies in their tower-mounted positions;
6. Construction of zero wind facilities for the transducer assemblies in their mounted positions (more simply, construction of tubes of proper acoustic material that will fit over a complete sonic path, thus providing a zero wind condition for check purposes); and

---

\* Subsequent investigation has shown that this type of failure cannot in general be detected by present field test procedure, and studies are in progress to improve this situation.

7. Installation of additional logic check circuitry in order to permit more thorough pre-run testing of less-than-obvious malfunctioning.

The seven items listed above are all obtainable with only reasonable expenditures in an economic and time sense and, where necessary, documentation for authorization will be submitted to the Contracting Officer within the immediate future.

Summarizing, within the limitations listed above, no necessity or desire has been found for the realignment of research procedures; no problem with magnitude sufficient to doubt the capabilities of acquisition of the research goals has been met nor is it anticipated that such problems will arise, and it is recommended that already proposed extension of the contract activities at Texas A&M University be favorably acted upon.



# PERSONNEL

## Terminated

Clayton, William H.	Principal Investigator	
Eckelkamp, B. Jesse	Research Scientist III	
Alexander, Linda C.	Steno-Computer	
Andrzejewski, Stanley	Senior Technician	
Brady, Helen J.	Secretary	
Brent, Mary Anne	Computer I	9/6/63
Burris, Charles E.	Technician I	7/2/63
Chaffin, Judy	Computer I	8/31/63
Darr, Barbara	Computer I	9/15/63
Jackson, Wilbur M.	Engineering Aide II	
Johnson, Robert W.	Engineering Aide II	5/31/63
LaMotte, Lynn Roy	Technical Assistant	
Latham, Judith C.	Computer I	
McMath, Ruth Ann	Computer II	
Polaski, Maxine	Engineering Aide I	
Post, Robert E.	Senior Research Scientist	7/15/63
Skola, Natalie	Stenographer	5/31/63
Stewart, Jr., Robert M.	Senior Research Scientist	7/15/63
Thomas, Donald Lee	Student Assistant	
Vitols, Visvaldis A.	Senior Technician	5/31/63
Wessels, Carolyn J.	Computer I	8/30/63
Wilson, Tony E.	Technician I	
York, H. Andrew	Senior Technician	5/15/63

## REFERENCES

1. Clayton, William H. and Jerry D. Merryman, 1957: The Design of Micrometeorological Experiments. Texas A&M Research Foundation Project 121, Final Report, USASRDL Contract DA 36-039 SC-70138.
2. Deacon, E. L., 1953: Vertical Profiles of Mean Wind in the Surface Layer of the Atmosphere. Geophys. Memoirs, No. 91.
3. Elliott, Wm. P., 1957: A Comparison of Some Approaches to the Diabatic Wind Profile. Trans., Amer. Geophys. Union, 38(1), 21-24.
4. Ellison, T. H., 1957: Turbulent Transfer of Heat and Momentum from an Infinite Rough Plane. J. Fluid Mech., 2, 456-466.
5. Halstead, M. H., 1954: The Fluxes of Momentum, Heat and Water Vapor in Micrometeorology. Johns Hopkins Univ., Lab. of Climatology, Seabrook, N. J., 7(2), 326-61.
6. Monin, A. S. and Obukhov, A. M., 1954: Basic Regularity in Turbulent Mixing in Surface Layer of the Atmosphere. U.S.S.R. Acad. Sci.; Geophys. Inst., No. 24.
7. Panofsky, H. A., A. K. Blackadar and G. E. McVehil, 1960: The Diabatic Wind Profile. Q. J. R. Met. Soc., 86(369), 390-98.
8. Monin, A. S., 1958: The Structure of Atmospheric Turbulence (Translated by R. A. Silverman). Theory of Probability and Its Applications, III, 1: 266-96 (publisher unknown).
9. Armstrong, Ralph W., 1962: Derivation of Equations for Sonic Anemometry. USAERDL Technical Report 2289, U. S. Army Electronics Research and Development Laboratory, Fort Monmouth, N. J.
10. Kaimal, J. Chandran, 1962: A Sonic Anemometer for the Study of Turbulent Wind Loading on Missiles. AFCRL-62-1064, Meteorological Research Laboratory Project 7655, L. G. Hanscom Field, Mass.
11. Suomi, V. E. and Businger, J. A., 1959: Sonic Anemometer-thermometer. Project Prairie Grass, A Field Program in Diffusion. Geophysical Research Papers #59, III. ASTIA Document AD-217076:1-27.
12. Stewart, Robert M., Jr., Robert E. Post, Terry A. Smay and James E. Carson, 1962: Sonic Anemometer Data Acquisition and Analysis System and Calculation of Eulerian Scale of Turbulence from Bivane Data. Iowa State University Engineering